Myxobacterial P450s as drug metabolizers: derivatization and metabolite production of drugs

Kumulative Dissertation
zur Erlangung des akademischen Grades des
Doktors der Naturwissenschaften
der Naturwissenschaftlich-Technischen Fakultät III
Chemie, Pharmazie, Bio- und Werkstoffwissenschaften
der Universität des Saarlandes

von

Fredy Kern
(Dipl. Chem.)

Saarbrücken
2016

Tag des Kolloquiums:	18.07.2016
Dekan:	Prof. Dr.-Ing. Dirk Bähre
Berichterstatter:	Prof. Dr. R. Bernhardt
	Prof. Dr. A. Speicher
	....
Vorsitz:	Prof. Dr. G. Jung
Akad. Mitarbeiter:	Dr.-Ing. M. Kohlstedt

Abstract

Since many years, myxobacterial cytochrome P450 enzymes from *Sorangium cellulosum* gained attention as biocatalysts for different compounds. However, their application in the pharmaceutical and biotechnological industry, especially for the derivatization and metabolite production of drugs, remained unclear. Investigations on EpoK, a P450 responsible for the epoxidation of epothilone C/D from *S. cellulosum* So ce90, resulted in the establishment of the most efficient redox system to date with potential biotechnological application. Additionally, three P450s of *S. cellulosum* So ce56, CYP265A1, CYP266A1 and CYP267B1, were found to hydroxylate epothilone D. The latter one was also able to form a novel epothilone derivative, 7-ketone epothilone D, with potential antitumor activity. With respect to the production of human drug metabolites, the CYP267 family was found to contain versatile drug metabolizers. Especially CYP267B1 showed the ability to convert structurally diverse drug compounds with high selectivity. In combination with the established co-expression of the autologous redox partners Fdx8 and FdR_B in *E. coli*, a multi-milligram production of the human drug metabolites chlorpromazine sulfoxide, 4'-hydroxydiclofenac, 2-hydroxyibuprofen, omeprazole sulfone and thioridazine-5-sulfoxide was achieved. In addition, CYP267B1 was characterized as a bacterial P450s with an uncommon broad substrate range and displays a great potential for a diverse biotechnological applicability.

Zusammenfassung

Seit einigen Jahren sind myxobakterielle Cytochrom P450 Enzyme aus *Sorangium cellulosum* als Biokatalysatoren für verschiedenste Verbindungen bekannt. Allerdings blieb deren Einsatz für eine biotechnologische Herstellung von Arzneimittelderivaten und -metaboliten ungeklärt. Im Rahmen dieser Arbeit wurde für CYP167A1 (EpoK) aus *S. cellulosum* So ce90, verantwortlich für die Epoxidierung von Epothilon C/D, das zurzeit effizienteste Redoxsystem mit großem biotechnologischen Potenzial etabliert. Zusätzlich wurden CYP265A1, CYP266A1 und CYP267B1 aus *S. cellulosum* So ce56 als Hydroxylasen von Epothilone D identifiziert und das neue Derivat 7-Keton-Epothilon D mit potenzieller Antitumoraktivität als Produkt von CYP267B1 charakterisiert. Des Weiteren konnte die CYP267 Familie, bestehend aus CYP267A1 und CYP267B1, als vielseitige und selektive Biokatalysatoren für die Produktion von Arzneimittelmetaboliten etabliert werden. Im Speziellen konnte mit CYP267B1 und der Co-expression der autologen Redoxpartner Fdx8 und FdR_B die Produktion der humanen Arzneimittelmetabolite Chlorpromazin-Sulfoxid, 4'-Hydroxydiclofenac, 2-Hydroxyibuprofen, Omeprazol-Sulfon und Thioridazine-5-Sulfoxid im multi-Milligramm Maßstab erzielt werden. Mit CYP267B1 wurde ein bakterielles P450 Enzym mit einem außergewöhnlich großen Substratspektrum entdeckt, das ein großes Potenzial für diverse biotechnologische Anwendungsmöglichkeiten bereithält.

Danksagungen

Ich möchte mich recht herzlich bei Frau Prof. Dr. Rita Bernhardt für die Möglichkeit bedanken, dass ich meine Doktorarbeit in ihrem Arbeitskreis anfertigen und dieses interessante Thema nach meinen Wünschen gestalten konnte. Ferner möchte ich ihr für die wertvollen Anregungen und konstruktiven Diskussionen danken.

Im Speziellen möchte ich mich bei Dr. Yogan Khatri und Martin Litzenburger für die langjährige und ausgezeichnete Zusammenarbeit bedanken. Mein Dank gilt Tobias Dier und Prof. Dr. Dietrich A. Volmer für die unkomplizierte Kooperation und Hilfe bei den LC-MS/MS Experimenten sowie auch für die wertvollen Anregungen und Verbesserungen der entstandenen Publikation. Prof. Dr. Jean-Pierre Jacquot möchte ich nochmal herzlich für die Einladung nach Nancy und der Bereitstellung von SynFdx und FNR danken, sowie für seine Verbesserungsvorschläge beim Erstellen der entstandenen Publikation. Für das Überlassen der gereinigten FdR_B und ihre durchgehende Hilfsbereitschaft möchte ich mich auch bei Dr. Kerstin M. Ewen bedanken.

Ich bedanke mich bei allen Mitgliedern der Arbeitsgruppe für das angenehme Arbeitsklima und die hervorragende Zusammenarbeit. Vielen Dank an Birgit Heider-Lips, Alexander Schifrin und Tanja Sagadin für die gereinigten Redoxproteine. Für ihre Hilfe bei allen bürokratischen Angelegenheiten möchte ich mich auch bei Gabi Schon bedanken.

Ich möchte mich im Besonderen bei meiner Frau Heike Kern bedanken. Mit ihrer Hilfe und Unterstützung konnte ich mich ganz auf meine Ziele fokussieren. Dieser Rückhalt bedeutet mir sehr viel und ich freue mich alle zukünftigen Herausforderungen mit ihr zusammen zu meistern.

Mein größter Dank gilt meinen Eltern Werner und Brigitte Kern, ohne deren Unterstützung und bedingungsloser Aufopferung mein Studium nicht möglich gewesen wäre.

Contents

Scientific contributions

Kern *et al.* (2015)

Highly Efficient CYP167A1 (EpoK) dependent Epothilone B Formation and Production of 7-Ketone Epothilone D as a New Epothilone Derivative

Fredy Kern expressed and purified EpoK, CYP265A1, Fdx2 and Fdx8 and performed all *in vitro* conversions and the bioinformatics studies. He established the analytical methods for the HPLC and drafted the manuscript. Tobias K.F. Dier performed and evaluated all LC-MS/MS experiments, elucidated the structures of the products and participated in writing the manuscript. Dr. Yogan Khatri expressed and purified the members of the CYP109, CYP260, CYP264 and CYP267 family. Additionally, he supported the bioinformatics studies and participated in writing the manuscript. Dr. Kerstin M. Ewen expressed and purified FdR_B and participated in writing the manuscript. Prof. Dr. Jean-Pierre Jacquot expressed and purified SynFdx and FNR and participated in writing the manuscript. Prof. Dr. Dietrich A. Volmer supervised the LC-MS/MS experiments and participated in writing the manuscript. Prof. Dr. Rita Bernhardt supervised the project and participated in writing the manuscript.

Kern *et al.* (2016)

CYP267A1 and CYP267B1 from *Sorangium cellulosum* So ce56 are highly versatile drug metabolizers

Fredy Kern expressed and purified CYP267A1 and performed all *in vitro* and whole-cell conversions with CYP267A1 and CYP267B1. He established the analytical methods, purified and analyzed the products, and drafted the manuscript. Martin Litzenburger participated in the establishment of the analytical methods, expressed and purified CYP267B1, performed the inhibition experiments and participated in writing the manuscript. Dr. Yogan Khatri performed all bioinformatics studies and the characterization of the CYP267 family members. Additionally, he participated in writing the manuscript. Prof. Dr. Rita Bernhardt supervised the project and participated in writing the manuscript.

Litzenburger *et al.* (2015)

Conversions of tricyclic antidepressants and antipsychotics with selected P450s from *Sorangium cellulosum* So ce56

Fredy Kern performed all experiments with CYP267A1 and CYP267B1 (*in vitro* conversions, whole-cell conversions, product purification and analyses of the NMR spectra) and participated in writing the manuscript. Martin Litzenburger performed all experiments with the enzymes CYP109C1, CYP109C2, CYP109D1, CYP260A1, CYP260B1, CYP264A1 and CYP264B1 (*in vitro* conversions, whole-cell conversions, product purification and analyses of the NMR spectra) and drafted the manuscript. Dr. Yogan Khatri provided the plasmids encoding the corresponding P450s as well as purified CYP109C1, CYP109C2, CYP109D1 and CYP264B1. Additionally, he participated in writing the manuscript. Prof. Dr. Rita Bernhardt supervised the project and participated in writing the manuscript.

List of abbreviations

AdR	Adrenodoxin reductase
Adx	Adrenodoxin
Adx_{4-108}	Truncated adrenodoxin
Arh1	Adrenodoxin reductase homologue 1 from *S. pombe*
CO	Carbon monoxide
CPR	Cytochrome P450 reductase
CYPome	Cytochrome P450 complement
DME	Drug metabolizing enzyme
DMSO	Dimethylsulfoxide
E. coli	*Escherichia coli*
$Etp1^{fd}$	Electron-transfer protein 1 from *S. pombe*
EpoK	Cytochrome P450 167A1
FAD	Flavin adenine dinucleotide
FDA	Food and Drug Administration
Fdx2	Ferredoxin 2 from *S. cellulosum* So ce56
Fdx8	Ferredoxin 8 from *S. cellulosum* So ce56
FdR_B	Ferredoxin NADP+ reductase B from *S. cellulosum* So ce56
FMN	Flavin mononucleotide
FNR	Ferredoxin $NADP^+$ reductase from *Chlamydomonas reinhardtii*
FpR	Ferredoxin reductase
HPLC	High Performance Liquid Chromatography
HTS	High-throughput screening
IC_{50}	Drug concentration that inhibits cell growth by 50%
ICH	International Conference on Harmonization of Technical Requirements for Registration of Pharmaceuticals for Human Use
k_{cat}	Catalytic rate constant
K_D	Dissociation constant
kDa	Kilo Dalton
K_m	Michaelis-Menten constant
KPP	Potassium phosphate buffer
LC-MS/MS	Liquid chromatography coupled to Mass spectrometry
NADP+	Nicotinamide adenine dinucleotide phosphate (oxidized form)
NADPH	Nicotinamide adenine dinucleotide phosphate (reduced form)
NMR	Nuclear magnetic resonance
n_H	Hill coefficient
P450	Cytochrome P450
SynFdx	Ferredoxin from *Synechocystis* sp PCC6803
v_{max}	Maximum reaction rate

List of tables and schemes

List of figures

1 Introduction

1.1 Pharmaceutical drugs

The usage of plants, parts of plants and isolated phytochemicals to treat, ease or prevent various health diseases is highly linked to the evolution of mankind (Sahoo *et al.*, 2010). Coming from the use of this natural sources as therapeutic means, the very first pharmaceutical drugs were herbs already used for thousands of years (Jones, 1996; Butler and Newman, 2008) and described in encyclopedias like *Naturalis historia*. Apart from vegetable drugs, also minerals, beverages, certain fats or oils, honey and milk were used medicinally (Kremers, 1976). The fast discoveries in natural sciences in the beginning of the 18th century played a huge role in forming the specific and related scientific fields investigating medicine and how they effect the human body (Müller-Jahncke and Friedrich, 1996). With the increasing knowledge and state of the art, more and more pharmaceutical effects were linked to a responsible specific chemical structure. Already described in 1955, the chemical structure of morphine and its derivatives is attributed to their analgesic effect, respectively (Braenden *et al.*, 1955). Another example are diverse flavonoids, which are common secondary metabolites in the plant kingdom participating in their anti-inflammatory and antioxidant activity (Odontuya *et al.*, 2005). However, humans have been subjected to disease, illness and accident since the beginning of time (Anderson, 2005). To fight these concomitants of life, medicine and drugs have always been highly valuable elements for health and healthcare.

1.2 Drug discovery cycle

To constantly improve known traditional or natural medicine toward a more effective treatment of diseases, drug research and discovery aroused as an intersectional field of medicine, biotechnology and pharmacology. Every new drug candidate in modern medicine, regardless of its source or manufacture procedure, is generally bound to a screening process. The classical way of pharmacological screening involved sequential testing of new chemical entities or extracts in isolated organs followed by pharmacological tests in animals (Vogel and Vogel, 1995). With the development of high-throughput screening (HTS) and ultra-HTS models, drug research shifted from animal studies to target-oriented research (Kubinyi, 2003). However, because drug metabolism is a highly complex system involving simultaneous cooperation of multiple organs and cellular processes (Staudinger, 2013), nowadays, drug candidates have to pass different tests and clinical trials in drug development (Figure 1).

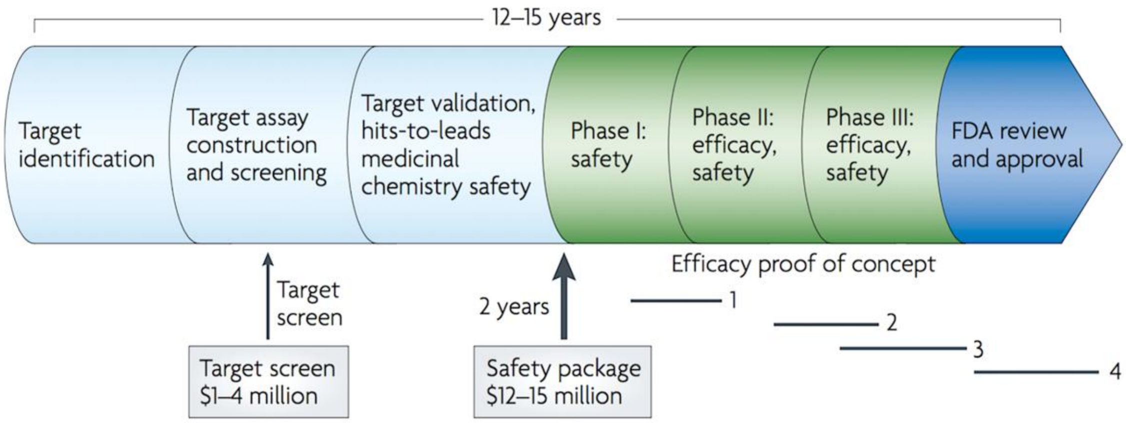

Figure 1. Drug discovery and development pipeline (taken from (Roses, 2008)). The timeframe of 12-15 years is representative for the most common period.

1.3 Guidelines for metabolite detection

The pharmaceutical industry traditionally invests a high sum of money in drug research and development. On one side, the profit margin obtained from patented drugs or new drug derivatives is significantly higher and more lucrative. On the other hand, the emergence of new diseases, rising concerns of drug resistance for pathogenic agents and the decreased efficacy of the existing drugs are of great pharmaceutical concerns (Drews, 2000). However, the number of new drugs reaching the market has settled down in the past few years (Figure 2). One of the main reasons for the failure of drug candidates is the detection of emerging toxicity and resulting side effects (Kim and Kang, 2011). To encounter potential negative effects of drugs, the International Conference on Harmonization of Technical Requirements for Registration of Pharmaceuticals for Human Use (ICH) dictated guidelines for the qualification and the analysis of drug metabolites during clinical trials (ICH, 2009, 2012). In detail, the Food and Drug Administration (FDA) published instructions for safety testing of human drug metabolites which are representing >10% of the parent drug exposure at steady state (FDA, 2008). Indeed, several drugs are reported to be metabolized in the human body into toxic and/or chemically more reactive compounds (Macherey and Dansette, 2008). The early detection of such metabolites during the drug discovery and development phases will timely reveal unsuitable candidates (Cavero, 2009) and prevent a damaging cause of withdrawal during clinical trials and post-marketing (Tamimi and Ellis, 2009).

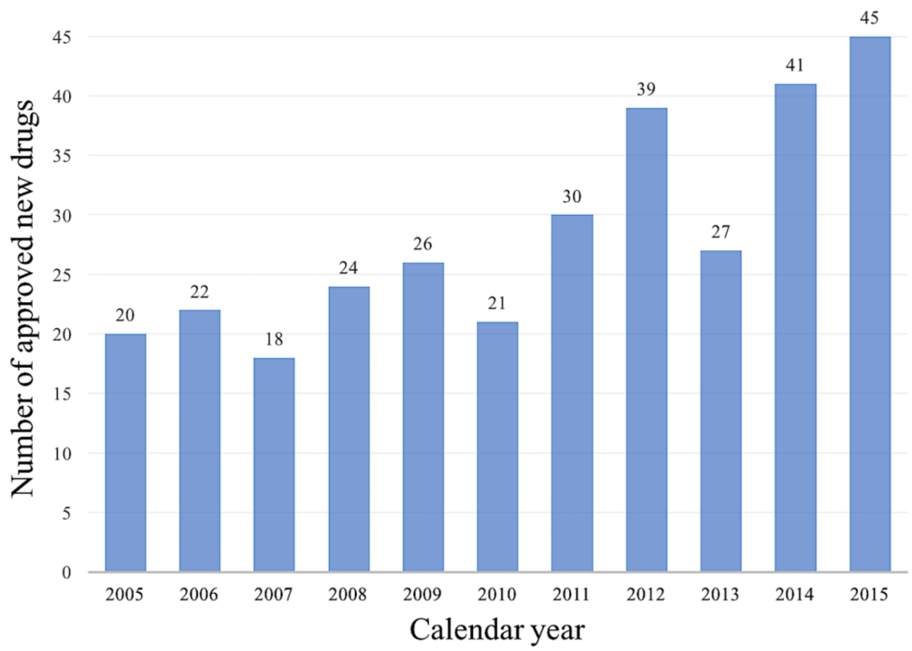

Figure 2. Number of new pharmaceutical drugs approved for the market (data taken from FDA drug report 2015).

1.4 Drug metabolizing enzymes (DMEs)

The field of drug metabolism research arose during the first half of the 19th century, when hippuric acid was detected in horse urine after benzoate administration (Delprat and Whipple, 1921). At about the same time, the responsible mechanism for the biotransformation of drugs or xenobiotics became the focus of attention. Since then, drug metabolism evolved in one headstone of the discovery and development process of drugs. Responsible for the biotransformation are drug metabolizing enzymes (DMEs), which play essential roles for the elimination and detoxification of drugs and xenobiotics (Meyer, 1996). The exposure with these compounds leads to an adaptive response of the human body to produce the suitable DME for their degradation (Xu *et al.*, 2005). The majority of DMEs participating in phase I metabolism are oxidoreductases and the percentages of their participation in drug metabolism is presented in Figure 3.

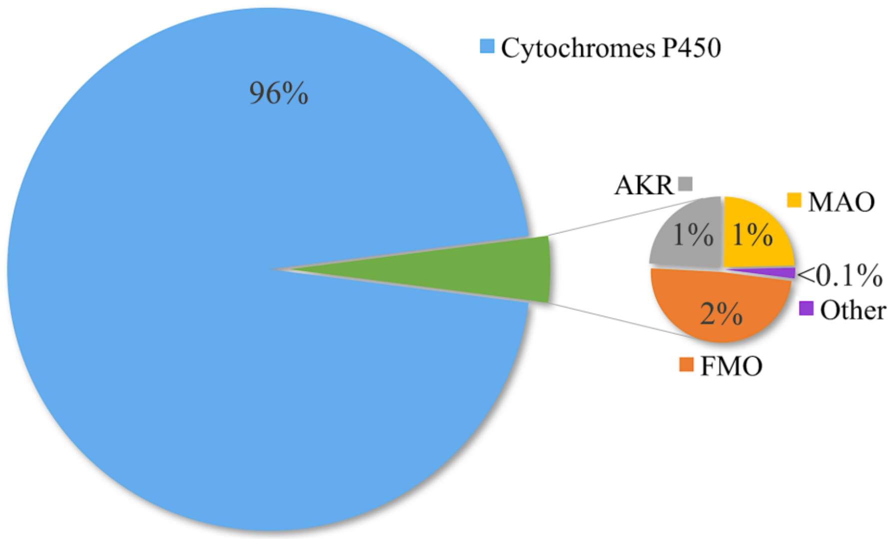

Figure 3. Human oxidoreductases participating in drug metabolism with cytochrome P450s, aldo-keto reductases (AKR), monoamine oxidase (MAO) and microsomal flavin-containing monooxygenase (FMO). The values were calculated from 860 drugs (taken from (Rendic and Guengerich, 2015)).

Flavin-containing monooxygenases (FMOs) are characterized by their ability to catalyze the oxidation of heteroatoms in xenobiotics, in particular soft nucleophiles such as amines, sulfides and phosphites (Geier *et al.*, 2015). Specialized for the oxidation of monoamines, the family of monoamine oxidases (MAOs) is responsible for the deamination of neurotransmitters and biogenic amines (Edmondson *et al.*, 2004). The enzyme family of aldo-keto reductases (AKRs), including aldehyde and aldose reductases, own a wide substrate specifity for carbonyl compounds (Bohren *et al.*, 1989). The enzyme families FMO and AKR are both NADPH-dependent enzymes whereas MAOs only need FAD as cofactor. However, all three enzyme families catalyze important reactions to induce the excretion of xenobiotics (Scheme 1). But taken together, FMOs, AKRs and MAOs are only responsible for 4% of drug metabolism (Figure 3).

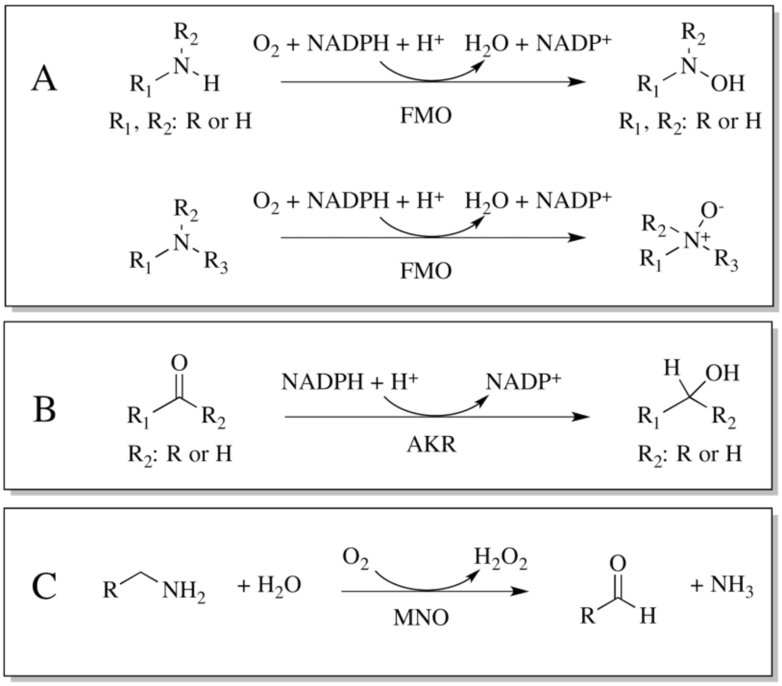

Scheme 1. Overview of exemplary reactions catalyzed by flavin-containing monooxygenases (A), aldo-keto reductases (B) and monoamine oxidases (C).

1.5 Cytochrome P450 enzymes (P450s)

As presented in Figure 3, the remaining 96% of phase I drug metabolism is catalyzed by cytochrome P450 enzymes (P450s). These enzymes can be found throughout the three domains of life, highlighting their special purpose in living organisms, in particular for eukaryotes. These enzymes belong to one of the largest superfamilies of enzyme proteins (Nelson, 2011) and play a crucial role in the metabolic pathways of drugs and xenobiotics in the human body. Furthermore, they are involved in the metabolism of various endogenous and exogenous compounds like bile acids, fatty acids, retinoids, steroids, hormones, lipids and antibiotics (Bernhardt, 2006; Monostory and Dvorak, 2011).

The origin of the P450 superfamily lies in prokaryotes, however, P450s were first found in rat liver microsomes (Klingenberg, 1958). For over 55 years, a large number of P450s were found and characterized in the genome of different organisms. The gram-negative bacterium *Escherichia coli* is one of those organisms which lack any P450 genes. In contrast, in the genome of higher plant species like *Arabidopsis thaliana* up to 244 P450s can be found (Bak *et al.*, 2011). For nomenclature purposes, the P450 superfamily genes are subdivided and classified on the basis of amino acid identity, phylogenetic criteria and gene organization (Nelson *et al.*, 1996). The root symbol CYP is followed by a number for the P450 family, a letter for the subfamily and a number for the respective gene. Thereby, genes with an amino acid sequence identity of more than 40% are classified in the same family. If the identity is higher than 55%, the genes are arranged to the same subfamily (Figure 4). Furthermore, the family numbers are assigned according to a P450 numbering scheme, which assigns the numbers 1-49 and 300-499 to animal P450s, 71-99 and 701-999 to plant P450s and the family numbers 101-299 to bacterial P450s (Nelson, 2009).

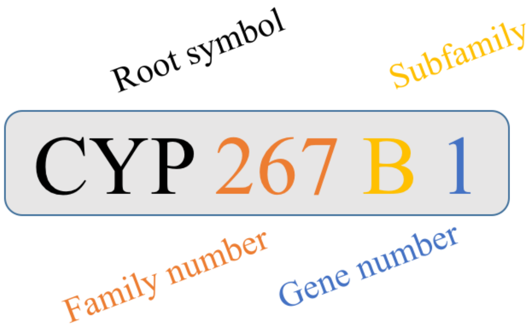

Figure 4. Nomenclature of cytochrome P450s.

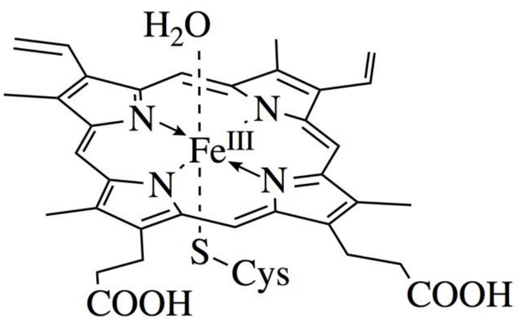

Figure 5. Schematic illustration of the heme cofactor in P450s. In general, the proximal side is coordinated by the thiol group of cysteine and the distal side is occupied by water (H_2O) or substrate.

Cytochrome P450 enzymes are heme-containing monooxygenases able to catalyze a large number of reactions including carbon hydroxylation, heteroatom oxygenation, dealkylation and epoxidation (Scheme 2) (Guengerich, 1990; Bernhardt and Urlacher, 2014). In the prosthetic group heme *b*, an iron ion is coordinated by four nitrogen atoms of porphyrin, which is proximally linked to the apoprotein via a conserved cysteine (Figure 5, (Urlacher and Girhard, 2012)). Within the structural fold of P450s there are highly conserved single amino acids and regions, which can be assigned to the special characteristics of this superfamily. As shown in Figure 5, the most important conserved amino acid, the proximal cysteine, is found in all P450s and plays a crucial role for their function. The result of this unique arrangement is the characteristic 450 nm peak in the reduced CO-bound absorption spectrum as well as a characteristic maximum at 420 nm in the oxidized form including two Q-bands at approximately 530 nm (α) and 570 nm (β) (Figure 6).

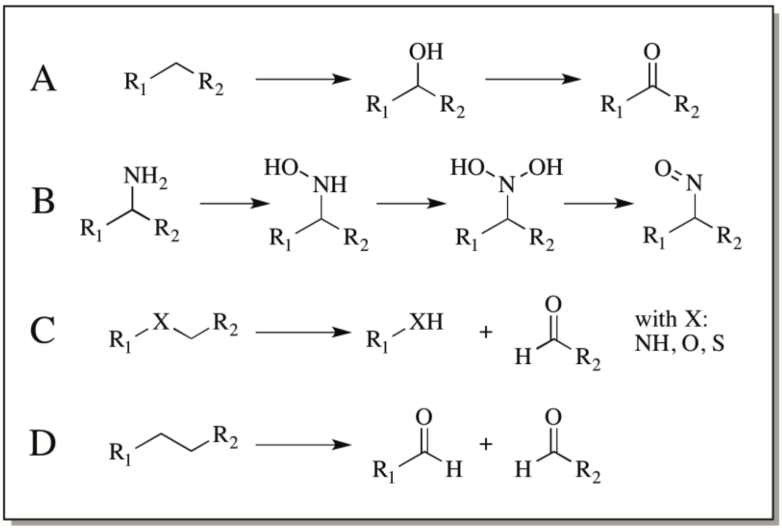

Scheme 2. Overview of notable reactions catalyzed by P450s with C-H hydroxylation and oxidation (A), N-oxidation (B), N, O, S-dealkylation (C) and C-C bond cleavage (D). The R_2 group can either be H or a random carbon chain.

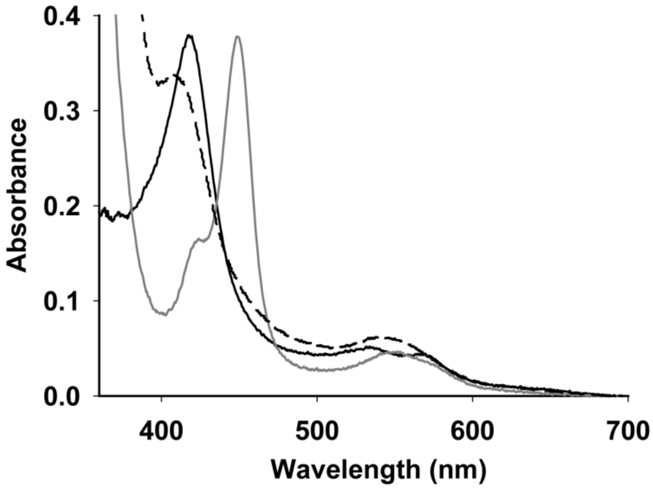

Figure 6. Spectroscopic characterization of CYP267B1 from *S. cellulosum* So ce56. The UV-visible spectra of oxidized, dithionite reduced and CO-bound CYP267B1 are shown as black, dotted and gray line (taken from (Kern *et al.*, 2016)).

In addition to the invariantly conserved proximal cysteine, P450s share a common fold and topology (Denisov *et al.*, 2005). The active site of P450s contains highly conversed regions which consist of a four-helix bundle (three parallel helices labeled D, L, I and an antiparallel helix E) and several important single amino acids. The latter ones are responsible for the correct orientation of the substrates (substrate recognition sites (SRS)) or indispensable for the catalytic activity of P450s, respectively (Sirim *et al.*, 2010)). Among others, it has been established that all P450 sequences contain a 10-residue signature motif FxxGx(H/R)xCxG which includes the cysteine ligand for heme-binding, the important (A/G)Gx(E/D)T-(T/S) region for creating an oxygen binding pocket and activate it (Werck-Reichhart *et al.*, 2002; Denisov *et al.*, 2005), and the totally conserved ERR triad motif, which is involved in stabilizing the core and heme-binding (Hasemann *et al.*, 1995). Another important aspect is the characteristic secondary and tertiary structure resulting from the amino acid sequence and its responsibility for a similar overall topology of P450s as well as the shape and size of their active site (Figure 7).

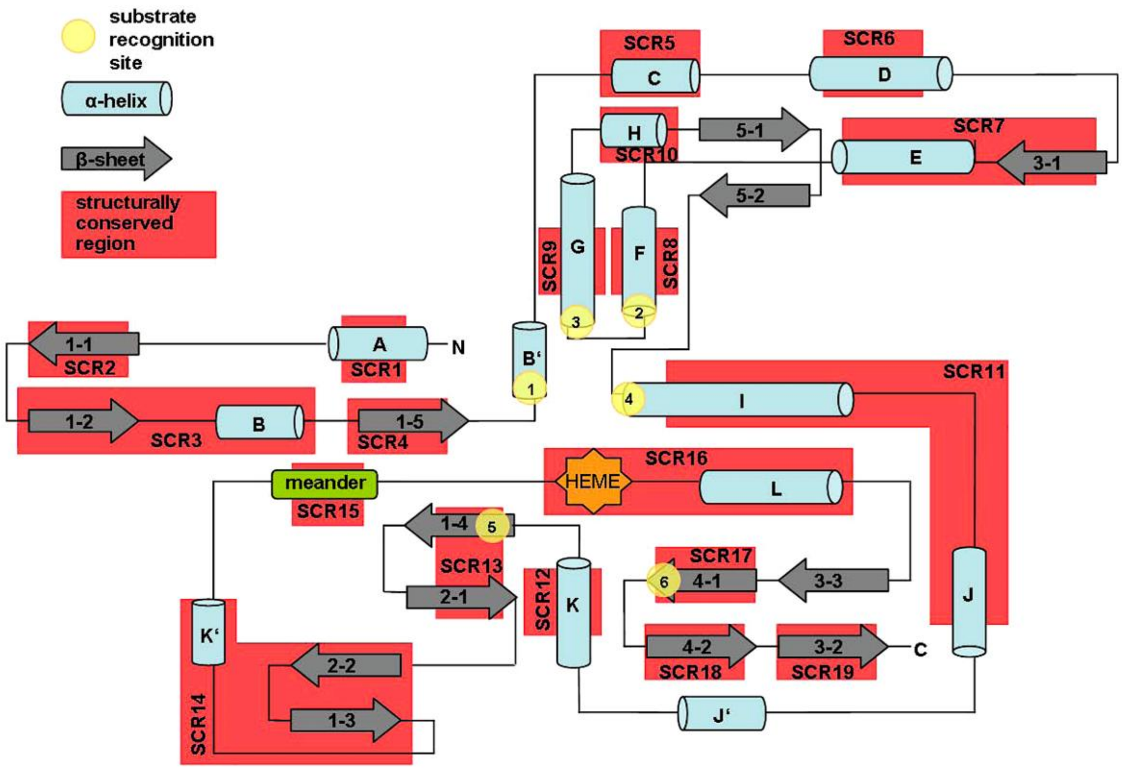

Figure 7. Topological illustration of P450s (taken from (Sirim *et al.*, 2010)). Substrate recognition sites are marked in yellow, all α-helices and β-sheets are highlighted as light blue tubes and grey arrows, respectively. The structurally conserved regions are framed in red.

Since P450s belong to the group of external monooxygenases, they require a two-electron reduction. However, a low number of P450s is known, which do not require an external protein component as reduction equivalent like CYP55 from *F. oxysporum* (Degtyarenko and Kulikova, 2001). The vast majority of P450s are in need of redox equivalents supplied by one or more redox partners. The diversity of these redox systems are in no way inferior to the diversity of P450s and are, therefore, classified by number, type and topology of the respective redox proteins. Most of the bacterial electron transfer systems belong to the class I P450 system, which consists of a soluble three protein arrangement with a FAD-containing ferredoxin reductase (FdR), a ferredoxin (Fdx) and the P450 (Hannemann *et al.*, 2007). As illustrated in Figure 8, the reductase transfers reduction equivalents from NAD(P)H to the ferredoxin, which in turn reduces the P450 itself.

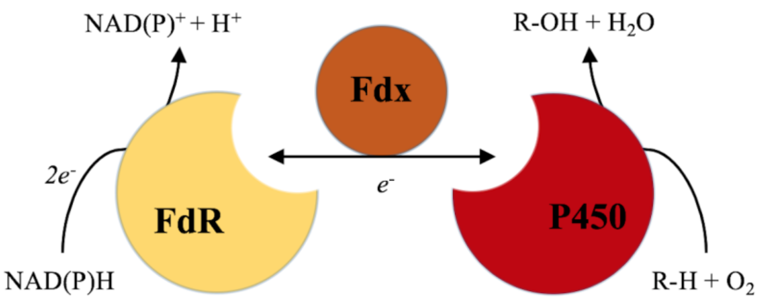

Figure 8. Schematic organization of class I P450 system with soluble ferredoxin reductase (FdR), ferredoxin (Fdx) and cytochrome P450 enzyme (P450).

As implied in Figure 8, the ferredoxin actually performs an one electron transfer from the reductase to the P450. Considered overall, the catalytic cycle of P450s successively requires two electrons for the oxygen activation and cleavage as well as the transfer into a substrate (Figure 9). Beginning with the resting state and Fe^{III} (**I**), the distal coordinated water molecule is replaced by the substrate (**II**) and, in the next step, the heme iron is reduced to Fe^{II} (ferrous state, **III**). After the binding of oxygen (**IV**), and its reduction to the ferric peroxy complex (**V**), the protonation of the terminal oxygen atom results in “Compound 0” (**VI**). A second protonation forms water and “Compound I” (**VII**), the active entity in most P450 oxidations. The superoxide (**IV-II**), peroxide (**VI-II**) or the oxidase (**VII-II**) uncoupling are side reactions within this pathway. Following the abstraction of a hydrogen atom from the substrate (**VIII**) and the subsequent combination to the oxidized product (**IX**), the coordination of a new substrate molecule initiates a new catalytic cycle (Whitehouse *et al.*, 2012).

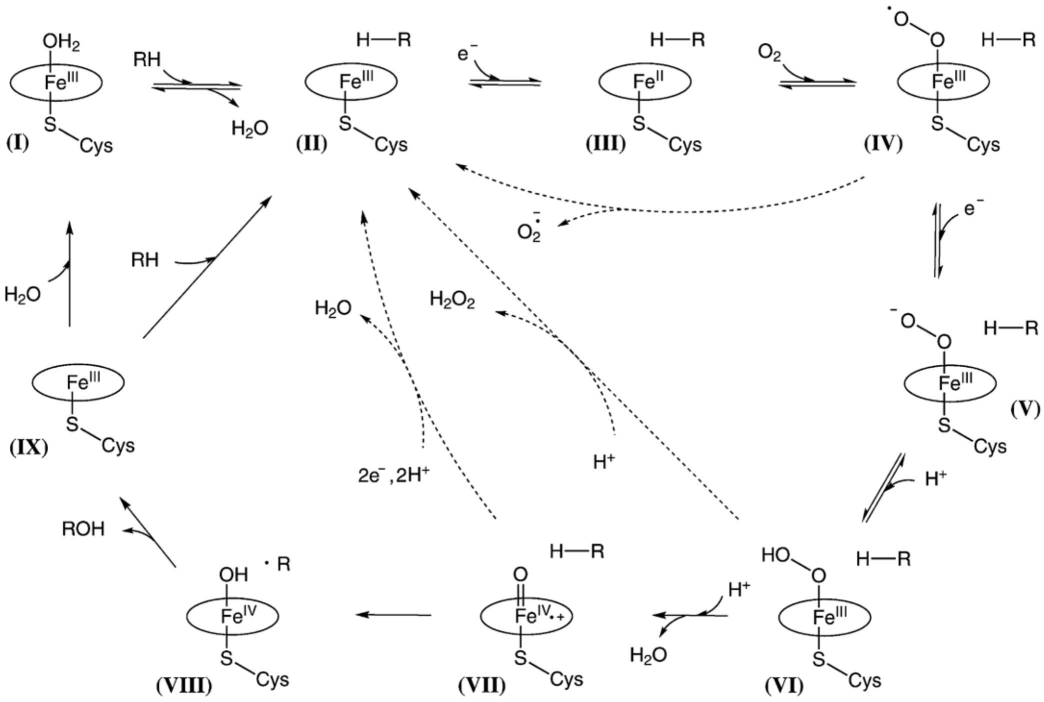

Figure 9. Catalytic cycle of P450s (taken from (Whitehouse *et al.*, 2012)).

1.6 Human P450s involved in the metabolism of drugs

Especially in the human body, P450s are indispensable biocatalysts in the metabolism of drug molecules (Figure 3). They are 57 human P450s known of which some are abundantly expressed in the liver, gastrointestinal tract, lung and kidney. Some of these P450s catalyze important steps in steroid and fatty acid metabolism, respectively (Bernhardt, 2006). Five P450 gene families, such as CYP1, CYP2, CYP3, CYP4 and CYP7, are believed to play a crucial role in the capability of dealing with drugs and chemicals (Zanger and Schwab, 2013). In fact, the CYP1, CYP2 and CYP3 families are responsible for 94% of the P450-dependent drug metabolism in the human body (Figure 10).

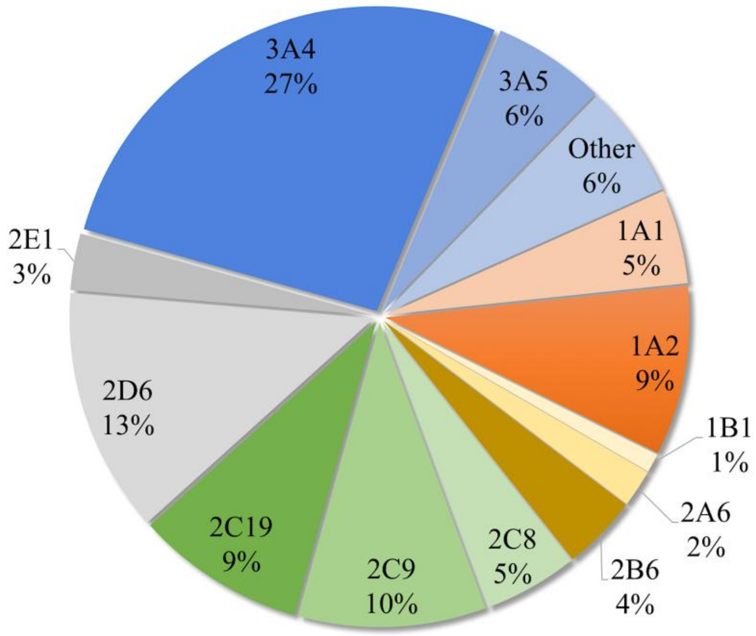

Figure 10. Human P450s responsible for the metabolism of drugs (data taken from (Rendic and Guengerich, 2015)).

The analysis of literature data (Rendic and Guengerich, 2015) revealed the participation of five major P450s in drug metabolism (Figure 10): CYP3A4 (27%), CYP2D6 (13%), CYP2C9 (10%), CYP2C19 (9%) and CYP1A2 (9%). Minor contributions were assigned for CYP3A5 (6%), CYP1A1 and CYP2C8 (both 5%), CYP2B6 (4%), CYP2A6 (2%) and CYP1B1 (1%). Taken together, the remaining 46 P450s are responsible for only 6% of metabolic reactions in the human body. The high number of accepted substrates by CYP3A4 and the resulting important role in drug metabolism is a product of its large and flexible active site (Scott and Halpert, 2005). Despite an amino acid sequence identity of 85% between CYP3A4 and CYP3A5, some limiting structural differences can be observed which lead to significantly lower substrate acceptance by CYP3A5 (Andrew Williams *et al.*, 2002).

1.7 Application of DMEs and microorganism as biocatalysts

Although the chemical synthesis is an option to produce metabolites of novel drugs and drug candidates, the implementation of costly multi-step chemical syntheses may not be sufficient enough to overcome the demand of the respective metabolites for toxicological tests or as authentic reference standards (Rushmore *et al.*, 2000). Besides the purification of major metabolites from urine (Gao *et al.*, 2012), alternative approaches without the need of subjects is needed. Although the *in vitro* application of oxidative enzymes is feasible, significant operational barriers are hindering a corresponding large-scale drug metabolite production (Cabana *et al.*, 2007). This led to the application of DMEs in biotechnological approaches and, furthermore, the screening for microorganisms able to metabolize drugs and derivatives. Since the late 1960s, microbial transformations of drugs were originally performed as 'microbial models of mammalian metabolism' (Smith and Rosazza, 1975). The use of microorganisms for drug metabolism is well documented and the microbial production of drug metabolites by biotransformation is known for decades (Clark and Hufford, 1991). Several microorganisms like *Cunninghamella* and *Streptomyces* strains showed the ability to metabolize drugs and xenobiotics to the respective human metabolites (Zhang *et al.*, 1996; Asha and Vidyavathi, 2009; Bright *et al.*, 2011; Murphy and Sandford, 2012). This opens a potential application of these strains for a large-scale production of these metabolites. Furthermore, the direct application of DMEs is also of interest to overcome the demand of drug metabolites. One promising option is the use of the Gram-negative bacterium *E. coli*, which is predominantly used as a host system for the production of enzymes. This bacterium is the most studied microorganism to date and easy to handle and modify toward the expression of heterologous enzymes (Rosano and Ceccarelli, 2014). It has been previously shown, that the expression of several DMEs like FMOs in *E. coli* results in the capability for the respective drug compound conversion *in vivo* (Geier *et al.*, 2015).

As a consequence of the participation of the human CYP1, CYP2 and CYP3 families in 94% of drug metabolism in the body (chapter 1.6), the P450 superfamily remains the means of choice. The human CYP3A4, CYP2C9 and CYP1A2 enzymes were successfully employed in such biotechnological approaches to directly produce the desired human metabolites in *E. coli* (Vail *et al.*, 2005). However, since it is not mandatory to employ associated human P450s to synthesize human drug metabolites (Schroer *et al.*, 2010; Geier *et al.*, 2015), microbial, especially bacterial, P450s became the focus of attention. Apart from the usage of engineered CYP102A1 (BM3) from *B. megaterium* (Reinen *et al.*, 2011; Di Nardo and Gilardi, 2012) or recently found bacterial P450s (Xu *et al.*, 2014; Kiss *et al.*, 2015; Kulig *et al.*, 2015) with drug metabolism activity, further suitable P450s are desired for such an application in the biotechnological production of drug metabolites.

1.8 Myxobacterial P450s from *Sorangium cellulosum* So ce56

Sequenced in 2007 (Schneiker *et al.*, 2007), the Gram-negative soil bacterium *Sorangium cellulosum* So ce56 caught the attention of the scientific community. For a timeframe of several years, the genome of *S. cellulosum* So ce56 was acknowledged as the largest bacterial genome ever sequenced. Even more interesting, the genus *Sorangium* is regarded as the most promising resource for novel and important compounds (Gerth *et al.*, 2003) including antimicrobial and antitumor macrolides (Bollag *et al.*, 1995; Mulzer *et al.*, 2008; Wenzel and Müller, 2009). After the bioinformatics analysis of the genome, 21 P450s (Khatri, Hannemann, *et al.*, 2010) as well as eight ferredoxins and two ferredoxin reductases were found and characterized (Ewen *et al.*, 2009). A schematic overview of the gene distribution in the genome of *S. cellulosum* So ce56 is presented in Figure 11.

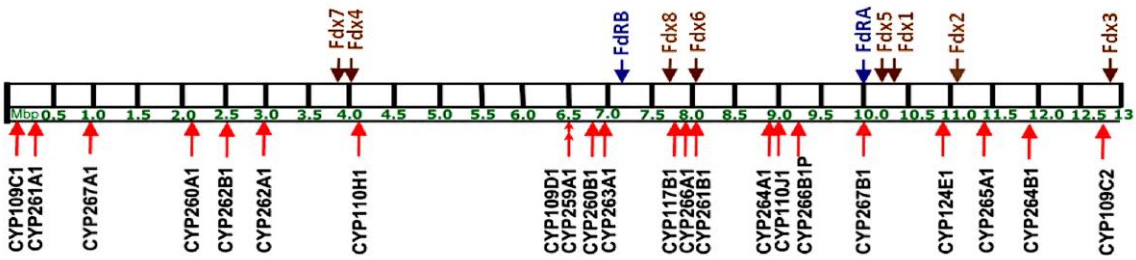

Figure 11. Schematic overview of the genome of *S. cellulosum* So ce56 and the localization of its CYPome and redox proteins (Khatri, 2009). Ferredoxins are presented in brown and reductases in blue letters.

Followed by this, several P450s from *S. cellulosum* So ce56 revealed promising and interesting characteristics. The first P450s from *S. cellulosum* So ce56 characterized were CYP109D1 and CYP260A1. The former revealed interesting fatty acid hydroxylase activity (Khatri, Hannemann, *et al.*, 2010) followed by the characterization of the remaining CYP109 family members, CYP109C1 and CYP109C2 (Khatri *et al.*, 2013; Shumyantseva *et al.*, 2016). The detailed characterization of the members of the CYP260 and CYP264 families led to new and interesting discoveries in norisoprenoid and sesquiterpene hydroxylations (Ly *et al.*, 2012; Schifrin, Litzenburger, *et al.*, 2015a; b; Schifrin, Ly, *et al.*, 2015; Khatri *et al.*, 2016; Litzenburger and Bernhardt, 2016). Several other P450s of *S. cellulosum* So ce56 remain so far unexplored and might ex-hibit potential activity toward other type of substrates and chemical compounds like drugs, xenobiotics and therapeutics.

1.9 Myxobacterial CYP167A1 (EpoK) from *S. cellulosum* So ce90

Several strains of *S. cellulosum* were found to contain epothilones, which feature cytotoxic activity against a number of tumor lines (Bollag *et al.*, 1995). This substance class is of great interest for the treatment of breast cancer up to Alzheimer's and Parkinson's disease (Zhang *et al.*, 2012; Cartelli *et al.*, 2013; Hirsch *et al.*, 2013). In *S. cellulosum* So ce90, the P450 CYP167A1 (EpoK) is responsible for the last step of the biosynthesis of epothilones (Ogura *et al.*, 2004). Thereby, EpoK catalyzes the epoxidation of a double bond resulting in epothilone A/B. However, even thought the complete biosynthesis of epothilones was clarified before (Molnár *et al.*, 2000; Tang, 2000), this last step was not clarified with respect to EpoK and its required natural redox partners. Additionally, no efficient redox system for further characterization of EpoK is known. This lack of knowledge hinders a potential application of a large-scale production of epothilones both in a biosynthetic and biotechnological manner. Furthermore, a derivatization of these epothilones is also of great pharmaceutical interest to improve or find more potent derivatives and metabolites of epothilone (Brogdon *et al.*, 2014). Several studies aiming for such a modification are covering this demand (Tang *et al.*, 2003; Basch and Chiang, 2007; Mulzer *et al.*, 2008; Zhang *et al.*, 2014), highlighting the need for new approaches to make new and more active epothilone compounds available.

2 Scope and objectives

With the focus on myxobacterial P450s from *S. cellulosum*, the main objective to clarify within this work is their potential application as drug derivatizer and metabolizer. Concerning this, the first part of this Thesis should be the characterization of EpoK from *S. cellulosum* So ce90 and the investigation of different hetero- and homologous redox partners to find an efficient electron transfer system for a potential application of EpoK in the biotechnological production of epothilone A/B. For this purpose, the established bovine Adx_{4-108}/AdR, the redox proteins Etp1/Arh1 from *S. pombe*, and Fdx2/FdR_B and Fdx8/FdR_B from *S. cellulosum* So ce56 are supposed to be investigated within the *in vitro* reaction of epothilone D to B by EpoK. While testing the homologous redox partners from So ce56, first indications for the natural redox partners of EpoK in *S. cellulosum* So ce90 might arise and could give insights into the biosynthesis of epothilones. Furthermore, a novel redox system for P450s, consisting of SynFdx from *Synechocystis* and FNR from *C. reinhardtii*, should also be tested in order to find a new efficient electron transfer system for EpoK.

In the second part of this Thesis, the myxobacterial P450s of *S. cellulosum* So ce56 should be characterized in terms of their substrate range, activity and their potential biotechnological applicability. Concerning this, a library of widely used drugs should be tested with respect to optimized reaction and extraction conditions and detection of metabolites by HPLC. Afterwards, the substrates should be tested in corresponding *in vitro* experiments in order to investigate the activity of myxobacterial P450s toward those drug compounds. To ensure and evaluate an application of the selected myxobacterial P450s in a biotechnological process, the positive hits from the *in vitro* experiments should be implemented in a whole-cell system for an up-scaled production of the drug metabolites. Based on the published whole-cell system in *E. coli* with the redox partners Adx_{4-108} and Fpr (Ringle *et al.*, 2013), the substitution of the former genes with the autologous redox partners Fdx8/FdR_B from *S. cellulosum* So ce56 will be performed and investigated in the following whole-cell experiments. The evaluation of the potential and the applicability of this whole-cell system for a large-scale production of drug metabolites is of great interest to produce desired and sufficient amounts of human metabolites as a reference standard or for toxicological testing during drug development.

3 Publications

3.1 Kern et al. 2015

Highly Efficient CYP167A1 (EpoK) dependent Epothilone B Formation and Production of 7-Ketone Epothilone D as a New Epothilone Derivative.

Fredy Kern, Tobias K. F. Dier, Yogan Khatri, Kerstin M. Ewen, Jean-Pierre Jacquot, Dietrich A. Volmer and Rita Bernhardt

Scientific Reports, 2015, 5:14881

www.nature.com/scientificreports

SCIENTIFIC REPORTS

OPEN

Received: 30 May 2015
Accepted: 11 September 2015
Published: 08 October 2015

Highly Efficient CYP167A1 (EpoK) dependent Epothilone B Formation and Production of 7-Ketone Epothilone D as a New Epothilone Derivative

Fredy Kern[1], Tobias K. F. Dier[2], Yogan Khatri[1], Kerstin M. Ewen[1], Jean-Pierre Jacquot[3], Dietrich A. Volmer[2] & Rita Bernhardt[1]

Since their discovery in the soil bacterium *Sorangium cellulosum*, epothilones have emerged as a valuable substance class with promising anti-tumor activity. Because of their benefits in the treatment of cancer and neurodegenerative diseases, epothilones are targets for drug design and pharmaceutical research. The final step of their biosynthesis – a cytochrome P450 mediated epoxidation of epothilone C/D to A/B by CYP167A1 (EpoK) – needs significant improvement, in particular regarding the efficiency of its redox partners. Therefore, we have investigated the ability of various hetero- and homologous redox partners to transfer electrons to EpoK. Hereby, a new hybrid system was established with conversion rates eleven times higher and V_{max} of more than seven orders of magnitudes higher as compared with the previously described spinach redox chain. This hybrid system is the most efficient redox chain for EpoK described to date. Furthermore, P450s from So ce56 were identified which are able to convert epothilone D to 14-OH, 21-OH, 26-OH epothilone D and 7-ketone epothilone D. The latter one represents a novel epothilone derivative and is a suitable candidate for pharmacological tests. The results revealed myxobacterial P450s from *S. cellulosum* So ce56 as promising candidates for protein engineering for biotechnological production of epothilone derivatives.

In 2012, the World Human Organization's global target of reducing premature mortality from non-communicable diseases (e.g. cancer) by 25% was set to be achieved by 2025[1]. To reach this ambitious target, population-based cancer registries and surveillance systems[2] as well as fundamental cancer research are essential. For decades, chemotherapy has been the leading therapeutic approach in the treatment of cancer. Interestingly, more than 60% of anticancer agents currently in use are derived from natural sources, including plants, marine organisms and microorganisms[3]. Among these compounds, agents blocking mitosis rate by targeting microtubules belong to the most efficient anti-cancer drugs identified to date[4]. One member of the group of microtubule-stabilizing agents are epothilones, which were first discovered in 1987 by Gerth and coworkers as antifungal compounds naturally produced by the soil bacterium *Sorangium cellulosum*[5,6]. After the discovery of the cytotoxic activity of epothilones against a number of tumor cell lines in 1995[7], many studies and clinical trials with epothilones were published, with epothilone D and B emerging as the most promising candidates for treatment of cancer.

[1]Department of Biochemistry, Saarland University, 66123 Saarbrücken, Germany. [2]Institute of Bioanalytical Chemistry, Saarland University, 66123 Saarbrücken, Germany. [3]Unité Mixte de Recherches, 1136 Interaction arbres microorganismes INRA, Nancy University, 54506 Vandoeuvre-lès-Nancy cedex, France. Correspondence and requests for materials should be addressed to R.B. (email: ritabern@mx.uni-saarland.de)

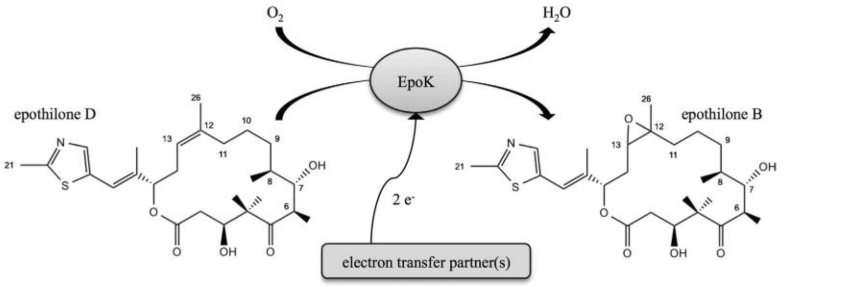

Figure 1. Conversion of epothilone D to B catalyzed by EpoK in *S. cellulosum* So ce90; electron transfer partners are unknown.

With respect to favorable characteristics as anticancer drugs, only derivatives of epothilone D and B have reached the stage of clinical investigation. Among those, Ixabepilone (an epothilone B analogue) is the only approved drug in cancer therapy to date[8]. Moreover, further studies have recently revealed additional benefits for treatment of Alzheimer's and Parkinson's disease with epothilone D[9,10]. Because of the variety of possible medical applications, epothilone D and its derivatives are most interesting targets for pharmaceutical and medical investigations.

The biosynthesis of epothilone D was first proposed by sequence determination of the biosynthetic gene cluster in *S. cellulosum* So ce90[11] and evaluated with the cloning of the complete gene cluster from *S. cellulosum* SMP44 into *S. coelicolor*[12]. It was demonstrated that the myxobacterial CYP167A1 (EpoK) is responsible for the final step of epothilone biosynthesis (epoxidation of epothilone D to B (Fig. 1), and epothilone C to A, respectively). In general, cytochrome P450 enzymes (P450) are versatile enzymes catalyzing a variety of reactions[13], a characteristic that makes them essential components of biotechnological and pharmaceutical research[14]. But P450s belong to the external monooxygenases and thus require electron supply from external redox partners[15]. Because neither the natural nor an efficient heterologous redox system supporting EpoK are known, the establishment of a whole-cell system in *E. coli* could not be achieved to date.

Although it was reported early on that an artificial redox chain consisting of spinach ferredoxin and ferredoxin reductase can support EpoK activity, the efficiency of the reaction was rather low. For the C-terminal his-tagged EpoK (1.5 μM), only 60% yields were observed after one hour at 30 °C when 100 μM epothilone D was used as substrate[12]. Putidaredoxin and putidaredoxin reductase from *Pseudomonas putida* also turned out not to be efficient enough to be a good alternative for the spinach system[16]. Therefore, it is paramount to establish an efficient redox chain to unlock the biotechnological potential of EpoK.

In this study, we first investigated homo- and heterologous electron transfer systems for an *in vitro* conversion of epothilone D by EpoK. Therefore, we studied *bovine* adrenodoxin (Adx_{4-108}) and adrenodoxin reductase (AdR), electron-transfer-protein 1 ($Etp1^{fd}$) and its autologous adrenodoxin reductase homologue 1 (Arh1) from *Schizosaccharomyces pombe*, and myxobacterial ferredoxins and ferredoxin reductase from *S. cellulosum* So ce56 (Fdx2/FdR_B and Fdx8/FdR_B), as well as a novel hybrid electron transfer system for P450s, ferredoxin (SynFdx) from *Synechocystis* and ferredoxin $NADP^+$ reductase (FNR) from *Chlamydomonas reinhardtii*.

In addition, we examined selected P450s from the related strain *S. cellulosum* So ce56 for a conversion of epothilone D. P450s of this strain were recently investigated by our group and exhibited novel functionalities and a broad substrate range[17–20]. Bioinformatics study revealed some of these P450s to be closely related to EpoK. As a result, the members of the CYP109, CYP260, CYP264 and CYP267 families as well as CYP265A1 and CYP266A1 from So ce56 were selected and implemented for *in vitro* conversions. The resulting products were subsequently analyzed via HPLC and LC-MS/MS. All structure proposals were tentatively assigned by LC-MS/MS and proposed collision-induced dissociation spectra are presented.

Results

Investigated electron transfer proteins: important characteristics. During our studies, several homologous and heterologous electron transfer systems were investigated. The general characteristics of the respective components are listed in Table 1 for ferredoxins and Table 2 for reductases, respectively. It is noteworthy that the redox potential of ferredoxins is decreasing from −344 mV for Adx_{4-108} to −353 mV for $Etp1^{fd}$ and to a redox potential of −380 mV for ferredoxin (SynFdx) from *Synechocystis*. The ferredoxins Adx_{4-108}, $Etp1^{fd}$ and SynFdx belong to the [2Fe-2S]-type and Fdx2 and Fdx8 from So ce56 to the [3Fe-4S]-type ferredoxins. Moreover, both eukaryotic reductases, AdR and Arh1, have a molecular

Name	Organism	Amino acids	Molecular weight [kDa]	Redox potential [mV]	Fe-S cluster type	Literature
$Adx_{4\text{-}108}$	*Bos taurus*	104	11.8	−344	[2Fe-2S]	[62,66]
$Etp1^{fd}$	*S. pombe*	127	14.1	−353	[2Fe-2S]	[67]
Fdx2	*S. cellulosum* So ce56	101	11.2	/	[3Fe-4S]	[31]
Fdx8	*S. cellulosum* So ce56	107	11.9	/	[3Fe-4S]	[31]
SynFdx	*Synechocystis*	96	10.3	−380	[2Fe-2S]	[35,68]

Table 1. Origins and properties of selected ferredoxins. (/: not described).

Name	Organism	Amino acids	Molecular weight [kDa]	Literature
AdR	*Bos taurus*	492	50.3	[69]
Arh1	*S. pombe*	469	51.4	[29]
FdR_B	*S. cellulosum* So ce56	244	26.7	[31]
FNR	*C. reinhardtii*	320	36.5	[38,70–72]

Table 2. Origins and properties of investigated reductases. The listed reductases contain flavin adenine dinucleotide and use both NADPH and NADH as a cofactor (Arh1 and FdR_B) with the preference for NADPH for FdR_B[31], while AdR and FNR use NADPH only.

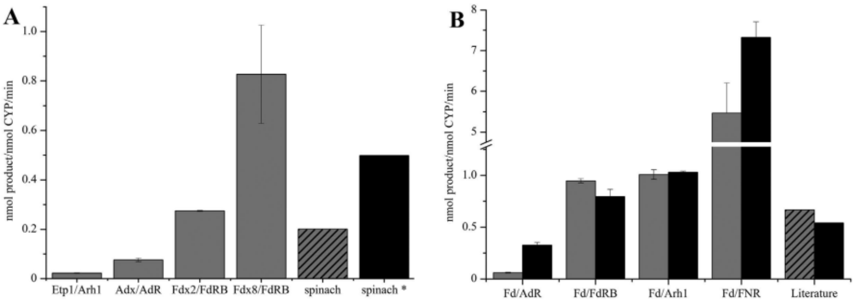

Figure 2. (**A**) Epothilone D conversions by EpoK with different electron transfer partners (spinach: ratio 1:100:0.025U; spinach*: ratio 1:100:0.125U for P450:Fdx:FdR; reductase in units); (**B**) Epothilone D conversions with EpoK, ferredoxin SynFdx (Fd) from *Synechocystis* and selected reductases (ratio 1:10:1 in grey bars and ratio 1:20:3 in black bars); bars designated as "Literature" were calculated from published data using spinach redox system: dashed[12] and black bar[21]

weight of around 50 kDa, almost twice the values for the comparatively small reductase FdR_B from *S. cellulosum* So ce56.

***In vitro* conversions of epothilone D by EpoK.** EpoK was tested with a variety of electron transfer partners as shown in Fig. 2A. The redox systems $Etp1^{fd}$/Arh1 from *S. pombe* and $Adx_{4\text{-}108}$/AdR from *Bos taurus* showed conversion rates below 0.1 nmol product per nmol P450 per min. The ferredoxins Fdx2 and Fdx8 with their autologous reductase FdR_B showed conversion rates of 0.3 and 0.8 nmol product per nmol P450 per min, respectively. Investigations with spinach redox partners analogous to Tang *et al.*[12] lead to conversion rates of 0.2 nmol product per nmol P450 per min for the described ratio (1.5:100:0.025U for P450:Fdx:FdR). Using optimized reaction conditions (five times higher reductase amount), 0.5 nmol product per nmol P450 per min were observed. Summarizing the results, the utilization of the homologous redox partners Fdx2/FdR_B and Fdx8/FdR_B resulted in an up to 4 times higher conversion rate compared to our results with the spinach redox system, thus presenting a more efficient redox chain for EpoK compared to published results.

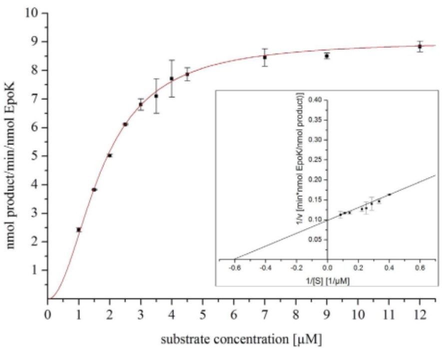

Figure 3. Kinetic studies on epothilone B formation supported by EpoK/SynFdx/FNR hybrid system (ratio 1:20:3 for EpoK:SynFdx:FNR). The Hill model with $n_H = 2$ resulted in a sigmoidal fit for EpoK kinetics with a coefficient of determination (R^2) of 0.99. The inset shows the Lineweaver-Burk plot of the data with $R^2 = 0.99$.

To evaluate the suitability of SynFdx as electron mediator for EpoK, different combinations and ratios of SynFdx with selected reductases were investigated. SynFdx was combined with different heterologous reductases in two different ratios (1:10:1 and 1:20:3 for P450:SynFdx:reductase). To compare the efficiency of the spinach redox system with our results, we calculated conversion rates [nmol product per min per nmol P450] from published data of epothilone D conversion by EpoK[12,21] to include them into Fig. 2B. All tested combinations, except SynFdx with *bovine* AdR, resulted in higher conversion rates than described in previous publications. When FdR_B from *S. cellulosum* So ce56 and Arh1 from *S. pombe* were used as electron donor for SynFdx, slightly higher rates compared to the spinach system were observed. However, the hybrid redox system containing ferredoxin from *Synechocystis* and FNR from *C. reinhardtii* yielded eight to eleven times (depending on component ratio) higher conversion rates *in vitro*, compared with the values calculated for spinach Fdx/FNR. Additionally, kinetic studies of the epoxidation of epothilone D were performed using the ratio 1:20:3 for the EpoK/SynFdx/FNR system. A v_{max} value of 9.03 ± 0.17 nmol product min^{-1} $nmol^{-1}$ EpoK and $K_{1/2} = 1.73 \pm 0.05\,\mu M$ were obtained by using the Hill-equation (Fig. 3). The replotted Lineweaver-Burk plot of the data (Fig. 3 inset) also showed the similar values of v_{max} and K_m of 10.10 nmol product min^{-1} $nmol^{-1}$ EpoK and 1.63 μM, respectively. Compared with literature data ($v_{max} = 5.6 \cdot 10^{-7}$ nmol product min^{-1} $nmol^{-1}$ EpoK and $K_m = 1.6\,\mu M$[16]), the v_{max} value was increased by seven orders of magnitude (10^7) with a similar K_m value. Thus, a highly efficient redox chain was established for EpoK.

Bioinformatics identification of potent epothilone D monooxygenases in *S. cellulosum* So ce56. To find additional P450s able to convert epothilones, we investigated the CYPome of So ce56. The phylogenetic comparison of EpoK with the CYPome of So ce56 revealed several P450s of So ce56 closely related to EpoK from So ce90 (Fig. 4A). Among the CYPome of So ce56, the greatest protein sequence homology (approximately 50%) and identity (≥30%) to EpoK was found for CYP124E1, CYP266A1, CYP267A1 and CYP267B1.

***In vitro* conversions of epothilone D with selected P450s from *S. cellulosum* So ce56.** CYP266A1, CYP267A1 and CYP267B1 of *S. cellulosum* So ce56 were tested with respect to their ability to convert epothilone D. Due to low expression levels[22], CYP124E1 was not studied. But, in addition to the P450 members with the greatest homologies to EpoK, also CYP109, CYP260 and CYP264 families as well as CYP265A1 were further investigated regarding a potential conversion of epothilone D. For this, reconstituted *in vitro* systems analogous to the ones used for EpoK-dependent epothilone D conversion were used. Interestingly, in contrast to EpoK from So ce90, efforts to apply the hybrid system SynFdx/FNR as an electron transfer system for P450s from So ce56 were unsuccessful. As a result, *bovine* Adx_{4-108}/AdR as well as the autologous Fdx2/FdR_B and Fdx8/FdR_B redox chains were used as described previously[22,23].

As shown in Table 3, CYP265A1 and CYP266A1 are able to convert epothilone D, with this compound representing the first presently identified substrate for each of these P450s. Interestingly, from the CYP267 family, only CYP267B1 showed activity towards epothilone D. Thus, all of the tested P450s closely related to EpoK, with the exception of CYP267A1, are able to convert epothilone D. In contrast, for the respective CYP109, CYP260 and CYP264 family members, no conversion of epothilone D was observed neither with the heterologous redox partners Adx_{4-108}/AdR nor with the autologous electron transfer proteins Fdx2/FdR_B and Fdx8/FdR_B.

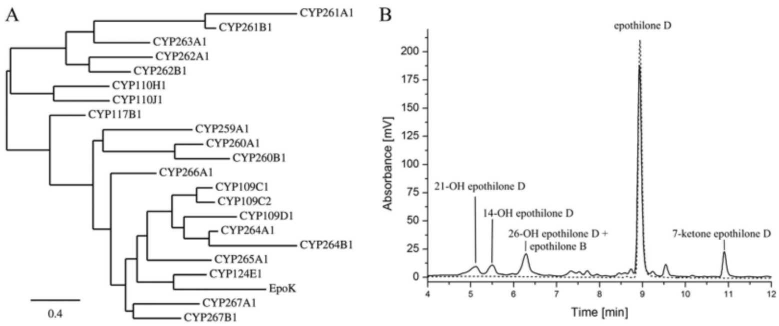

Figure 4. (**A**) Phylogenetic tree of EpoK and CYPome of So ce56. The tree was constructed by using protein sequences and the "One Click" mode of the online phylogenetic analysis tool from Information Génomique et Structurale, Marseille, France. The bar in the left corner indicates 0.4 amino acid substitutions per amino acid for the branch length[65]. (**B**) HPLC chromatogram of epothilone D (dashed line) and its conversion by CYP267B1/Fdx8/FdR_B (solid line).

P450	Product	Retention time [min]	Conversion of epothilone D [%] with		
			Adx_{4-108}/AdR	Fdx2/FdR_B	Fdx8/FdR_B
EpoK	Epothilone B	6.3	6.8	24.7	74.4
CYP265A1	14 OH-epothilone D	5.5	3.2	5.5	6.0
CYP266A1	14 OH-epothilone D	5.5	/	6.9	2.6
CYP267B1	21-OH epothilone D	5.1	3.5	3.2	5.5
	14-OH epothilone D	5.5	3.5	3.4	4.8
	26-OH epothilone D/ epothilone B	6.3	11.6*	4.0*	11.7*
	Not further characterized product	9.5	3.9	2.0	4.8
	7-ketone epothilone D	10.9	6.6	9.3	8.7

Table 3. Epothilone D conversion with selected P450s of *S. cellulosum* So ce56 (/: no conversion; *: combined yields of 26-OH epothilone D and epothilone B).

Both, CYP265A1 and CYP266A1 were able to catalyze a hydroxylation of epothilone D in position 14 (Table 3, details on identification and characterization of the products via LC-MS/MS see below). Three of the tested redox systems (Adx_{4-108}/AdR, Fdx2/FdR_B and Fdx8/FdR_B) were able to transfer electrons to CYP265A1, with CYP265A1/Fdx8/FdR_B showing the highest conversion yield (6% 14-OH epothilone D). CYP266A1 converts epothilone D to 14-OH epothilone D most efficiently when supported by Fdx2/FdR_B (6.9% conversion), whereas *bovine* Adx_{4-108}/AdR was not able to transfer electrons to CYP266A1. The system yielding the highest total conversion of epothilone D was found to be the autologous CYP267B1/Fdx8/FdR_B system. Most remarkably, the product pattern of CYP267B1 revealed five products of epothilone D conversion (Fig. 4B). Besides 14-OH epothilone D (4.8% conversion) and 21-OH epothilone D (5.5% conversion), 26-OH epothilone D and epothilone B were observed and gave a combined conversion of 11.4%. Due to their chemical similarity, 26-OH epothilone and epothilone B display the same retention time of 6.3 min (Table 3 and Fig. 4B). However, only small amounts of epothilone B were formed (supplemental Figure S2). Among the apolar products, only the product at 10.9 min has been characterized and revealed 7-ketone epothilone D (8.7% conversion). These products have not been characterized for P450-derived catalysis to date and thus represent novel products. The chemical structures of the identified products are shown in supplemental Figure S1.

LC-MS/MS identification of products formed during *in vitro* conversion of epothilone D by CYP265A1, CYP266A1 and CYP267B1. Product identification for the *in vitro* conversion of epothilone D by CYP265A1, CYP266A1 and CYP267B1 was performed by LC-MS/MS analysis. As shown in supplemental Table S1, five epothilone derivatives were obtained and characterized during this study. To elucidate the structures of conversion products and to identify sites of hydroxylation or

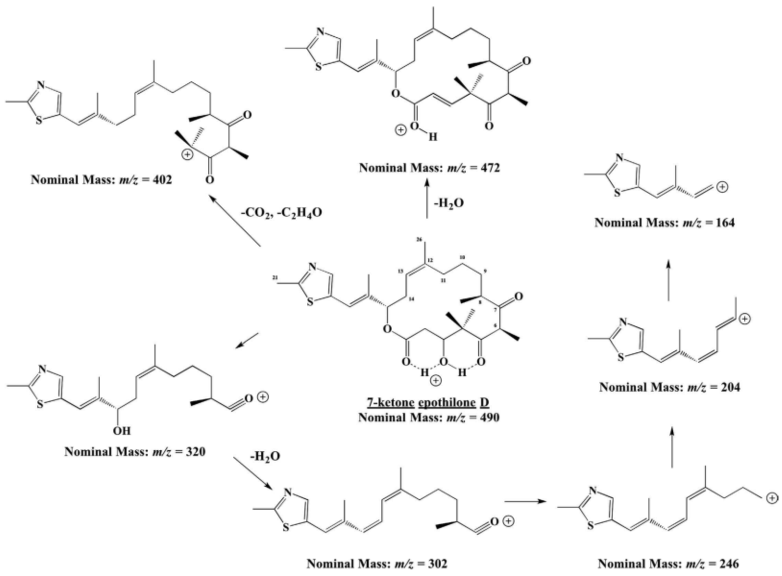

Figure 5. Proposed collision-induced dissociation spectrum of 7-ketone epothilone D (*m/z* 490). Loss of water at position C-3 results in a fragment with *m/z* 472. The fragment ion at *m/z* 402 appears after the loss of CO_2 and C_2H_4O. Step-wise fragmentation of the precursor ion is proposed and presented counterclockwise.

oxidation, CID of the analogous epothilone B compound was performed for comparison purposes. Blum *et al.* have shown that single or multiple losses of small molecules such as water (18 Da) dominated the CID spectra of epothilone B[24]. Losses of water originated at positions C-2 and C-3 and/or C-6 and C-7 from the precursor ion or as final step in serial dissociations. Further cleavages occurred at the carbon-oxygen bond at position 15 with formal loss of CO_2 (44 Da). Subsequent C-C cleavages at various positions in addition to C-O dissociation led to a number of characteristic ions (supplemental Table S1) in our experiments. Several of these product ions (marked with *) were also present in the CID spectra of the other products of epothilone D conversion. Tentative structure assignments of the conversion products A to D to the general epothilone substance class were therefore readily possible. Substance-specific ions such as *m/z* 168, 206 and 220 permitted identification of hydroxylation reactions. In addition, the presence of these ions as well as the precursor ion at *m/z* 508 pointed to a single hydroxylation site located directly at or near the thiazole ring. The proposed structures of the product ions listed in the supplemental Table S1 allowed us to tentatively assign the products A and B as 21-OH epothilone D, product C as 14-OH epothilone D, and product D as 26-OH epothilone D (supplemental Figure S2). Conversion product E corresponded to an oxidation product of epothilone B with a specific fragmentation scheme (supplemental Figure S3), which was assigned to the general epothilone substance class. Product E was identified as 7-ketone epothilone D and the proposed collision-induced scheme is illustrated in Fig. 5.

Discussion

Epothilones belong to a family of novel microtubule-stabilizing agents, which inhibit mitosis. Therefore they are interesting compounds for cancer research and treatment[25]. Their benefits over e.g. paclitaxel as anti-tumor agents are numerous. For example, some studies revealed higher water solubility[6] and inhibition of cancer cells resistant to various other chemotherapeutic agents[7]. During further studies, additional benefits of a treatment with epothilone D were described. Low-dose epothilone D treatment of aged PS19 mice with tau protein malformation in brain neurons (characteristic for Alzheimer disease) led to promising reduction of axonal dysfunction and neurotoxicity[10]. For Parkinson's disease, studies with epothilone D showed a rescue of chemically induced microtubule defects[9].

CYP167A1 (EpoK) is a P450 enzyme located downstream of the polyketide synthase (PKS) system of *S. cellulosum* So ce90. It is responsible for the last step in epothilone biosynthesis in this organism, resulting in epoxidation of epothilone D to epothilone B[21]. However, detailed information on the redox partners of EpoK, necessary for epothilone A/B formation in *S. cellulosum* So ce90, are not available. Generally, the P450 systems are classified (class I-X) according to the number, structure and topology of the protein components involved in the electron transfer to the P450 enzyme[15]. Most bacterial P450 systems belong to class I, in which the systems are composed of three separate proteins. Currently, the only electron transfer system described to support EpoK consists of spinach ferredoxin and spinach ferredoxin NADP$^+$ reductase. In 2000, Tang *et al.* observed a 60% conversion of epothilone D to B within one hour, using the redox chain from spinach. Attempts to replicate these results during our study resulted in considerably lower yields and conversions rates than described[12]. To find new efficient redox partners for EpoK, different homo- and heterologous class I electron transfer proteins were investigated in the present study.

Several investigations by our group have revealed the *bovine* Adx_{4-108}/AdR electron system as high-profile partner for efficient P450 *in vitro* and whole-cell experiments with a broad spectrum of P450s of prokaryotic origins supported[23,26,27]. Here, we found that *bovine* Adx_{4-108}/AdR is also able to transfer electrons to the heterologous EpoK from *S. cellulosum* So ce90. However, conversion of epothilone D by the EpoK/Adx_{4-108}/AdR system led to conversion rates significantly below the described and replicated results with the spinach system. For the electron transfer proteins $Etp1^{fd}$ and Arh1 from *S. pombe*, yields and conversion rates for the investigated EpoK/$Etp1^{fd}$/Arh1 system were even lower. Despite their ability to provide mammalian P450s with reduction equivalents[28,29], the application of $Etp1^{fd}$/Arh1 (or Adx_{4-108}/AdR) as electron donor system for EpoK thus remains limited.

After Schneiker *et al.* sequenced the genome of *S. cellulosum* So ce56 in 2007[30], our group characterized not only 21 P450s[22] but also 8 ferredoxins and 2 ferredoxin reductases[31]. It was revealed that the combination of Fdx2 and Fdx8 with FdR_B offers suitable electron transfer activities to many myxobacterial P450s, making the So ce56 redox pairs Fdx2/FdR_B and Fdx8/FdR_B interesting targets for *in vitro* studies with EpoK from So ce90. During this study, it was shown that the utilization of myxobacterial ferredoxin and ferredoxin reductase leads to higher yields and conversion rates compared with bovine Adx_{4-108}/AdR or $Etp1^{fd}$/Arh1 from *S. pombe*. With regard to the yields described by Tang *et al.* and Julien *et al.*[12,21] and conversion rates calculated based on these data, the homologous EpoK/Fdx8/FdR_B system revealed an efficiency to convert epothilone D comparable with the results published for the spinach redox chain. Bioinformatics study on the genes of Fdx2, Fdx8 and FdR_B from So ce56 revealed high identity (93.1%, 78.2% and 92.7%) to putative ferredoxin and ferredoxin reductase genes of *S. cellulosum* So0157-2 (supplemental Table S2). Sequenced in 2013 by Han *et al.*[32], the So0157-2 strain of *S. cellulosum* is an alkaline-adaptive producer of glycosylated epothilone A and B derivatives with high relationship to the not yet sequenced So ce90 strain[33]. Thus, the detection of ferredoxin and ferredoxin reductase genes, which are highly similar to the respective genes from So ce56, whose gene products were shown to support EpoK activity, is the first step to identify and ultimately purify the natural redox partners of EpoK from *S. cellulosum* So ce90.

In order to further optimize *in vitro* conversions catalyzed by EpoK, novel electron transfer proteins were also tested. We selected ferredoxin (SynFdx) from the unicellular cyanobacterium *Synechocystis* sp PCC6803 as electron mediator. *Synechocystis* is a photoautotrophic organism capable of oxygen-producing photosynthesis[34] and is able to synthesize two different Photosystem-I electron acceptors, a [2Fe-2S] ferredoxin and flavodoxin, both first purified and characterized by Bottin *et al.* in 1992[35]. There are eight other ferredoxins in *Synechocystis*, but the ferredoxin (SynFdx) chosen for this study presently received the most attention as a result of its diversified involvement in redox processes, such as cyclic photophosphorylation, nitrogen assimilation, biosynthesis of glutamate and chlorophyll, sulfite reduction and fatty acid metabolism[36]. As an additional novel member for an *in vitro* P450 electron transport chain, ferredoxin NADP$^+$ reductase (FNR) from the unicellular green alga *C. reinhardtii* was included in our studies. The selected FNR, a protein naturally involved in the NADP$^+$ reduction in the chloroplast stroma[37], was first isolated and characterized by Decottignies *et al.* in 1995[38]. A comparison of plant and bacterial ferredoxin-NAD(P)$^+$ reductases led to the conclusion that plant ferredoxin-NAD(P)$^+$ reductases evolved higher efficiency and turnover rates to operate in rapid metabolic pathways such as oxygenic photosynthesis[39], recommending FNR from *C. reinhardtii* as an interesting partner for *in vitro* investigations.

The SynFdx/FNR/NADPH hybrid system was recently tested for cytochrome c reduction[40]. However, the combination of the SynFdx/FNR system with P450s in *in vitro* experiments remained unexplored. Therefore, we employed two different ratios of the P450 and redox partners (1:10:1 or 1:20:3 for EpoK:SynFdx:FNR) and found that the latter ratio of the hybrid system revealed a significant increase of conversion rates and a complete conversion of 100 μM epothilone D to B within one hour. A change in the ratio of EpoK:SynFdx:FNR did not alter the regioselectivity of epothilone D epoxidation. For an efficient electron transfer chain, the formation of short-lived complexes is essential, dictated and controlled by the details of non-covalent interactions[41]. Optimal redox partners can be advantageous to increase the activities of recombinant P450 systems[14]. Therefore, it is noteworthy that although a reconstituted system with components originating from very different organisms (a myxobacterial P450, a cyanobacterial ferredoxin from *Synechocystis* and a plant ferredoxin NADP$^+$ reductase from *C. reinhardtii*) was studied, a high efficiency for *in vitro* conversions was detected.

As shown in Fig. 3, kinetic studies of the EpoK/SynFdx/FNR system resulted in sigmoidal kinetics. It can be assumed that allosteric effects are responsible for the Hill coefficient $n_H = 2$. Two substrate molecules in the active site, as known for CYP3A4 or CYP2C9[42] and already proposed for EpoK[16], and the special feature of EpoK to be renaturated by its natural substrate epothilone D[16], support this assumption. Our regenerated Lineweaver-Burk plot showed that the observed K_m value is similar to the one reported in the literature[16]. However, the observed v_{max} value is remarkably more than seven orders of magnitude

(10^7) higher than the one described for EpoK supported by the spinach redox partners[16], thus rendering the EpoK/SynFdx/FNR system much more attractive for biotechnological application. With possible further improvements of the system in mind, it is also interesting to consider the characteristics of the tested electron transfer partners and their implications for the system: spinach ferredoxin, the first and - until this study - only ferredoxin reportedly supporting EpoK, has a low redox potential of $-415\,mV$[43]. Interestingly, SynFdx, which exhibited the best conversion rates in this study (Fig. 2B), shows the most negative redox potential compared with Adx_{4-108} and $Etp1^{fd}$ (Table 1). It is assumed that EpoK generally requires an electron mediator with a rather low redox potential. However, the redox potential is clearly not the only determinant for efficient electron transfer to EpoK since spinach ferredoxin is characterized by a yet lower redox potential than SynFdx.

Moreover, with SynFdx from the phototrophic *Synechocystis* acting as electron mediator for EpoK, a new way of epothilone B synthesis is imaginable. Recently, Jensen and co-workers described a light-driven hydroxylation of hydrocarbons using mycobacterial CYP124 in combination with spinach Fdx and photosystem I from *Hordeum vulgare*[44]. Applying SynFdx and photosystem I from *Synechocystis* as a redox chain for EpoK, a new interesting possibility of a light-driven, NADPH-independent epoxidation of epothilone D might be accessible.

Besides investigation of redox partners for EpoK and conversion of epothilone D to B, we investigated further opportunities for derivatization of epothilone D during this study. As mentioned before, the broad range of applications highlights epothilones as interesting targets for drug design, cancer therapy and pharmaceutical research. The availability and production of epothilones is therefore of great interest to the pharmaceutical industry. In addition to the recently improved extraction methods for epothilones from *S. cellulosum* fermentation broth[45], total chemical synthesis of epothilones[46], precursor-directed biosynthesis[47] and heterologous production of epothilones in microorganisms[48,49] are fields of research. Furthermore, also novel derivatives of epothilones are desirable compounds[8]. Investigations towards epothilone derivatives were described using chemical modifications[50], extraction of derivatives from different *S. cellulosum* strains[51], biotransformations with *Amycolata autotrophica*[52] or selective conversion of epothilone B to epothilone F with a P450 hydroxylase from *Amycolatopsis orientalis*[53]. During the past few years, P450s of *S. cellulosum* So ce56 have revealed a great potential for industrial and biotechnological applications[17,20,22,23,54]. In order to produce potentially useful epothilone derivatives, we selected the members of CYP109, CYP260, CYP264 and CYP267 families as well as CYP265A1 and CYP266A1 from *S. cellulosum* So ce56 to test their ability to convert epothilone D. For the study described here, three different redox systems (P450/Adx_{4-108}/AdR, P450/Fdx2/FdR_B and P450/Fdx8/FdR_B) were tested with the P450s mentioned above.

For the members of CYP109, CYP260 and CYP264 families and for CYP267A1, no conversions of epothilone D with any of the redox systems were observed. In contrast, CYP265A1, CYP266A1 and CYP267B1, which were showing high similarity to EpoK (Fig. 4A), were found to be able to convert epothilone D, in which CYP265A1 showed almost similar preference for Fdx2/FdR_B and Fdx8/FdR_B followed by Adx_{4-108}/AdR (Table 3). However, CYP266A1 preferred Fdx2/FdR_B followed by Fdx8/FdR_B and has no activity with Adx_{4-108}/AdR (Table 3). Although the conversion percentage was different, there was no change in the regioselectivity of hydroxylation, thus highlighting the use of the autologous redox systems for P450s of *S. cellulosum* So ce56 in future whole-cell studies. It is, however, interesting to mention that the use of different redox partners for CYP267B1 revealed different regioselectivity of epothilone D oxidation, in which the combination of CYP267B1 with Fdx8/FdR_B and Adx_{4-108}/AdR preferred the 26-OH epothilone D/epothilone B product followed by 7-ketone epothilone D, whereas Fdx2/FdR_B showed a preference for 7-ketone epothilone D formation (Table 3). It can be assumed that the different ferredoxins mediate the electron flow to CYP267B1 with different efficiency and are, therefore, affecting the product distribution. An effect of different redox partner combinations on the regioselectivity of substrate hydroxylation has also been observed for P450 MycG[55].

The products of epothilone D conversion, 14-OH, 21-OH and 26-OH epothilone D, can currently only be obtained via biotransformation of epothilone D by *Amycolata autotrophica*[52], as natural products of So ce90/B2 and So ce90/D13[56] or via chemical synthesis[57]. Cytotoxic activity data (IC50, MCF7 breast cancer cell line) of 14-OH (29 nM), 21-OH (23 nM) and 26-OH epothilone D (95 nM) were published earlier, with values higher than for epothilone D (9 nM) or B (0.5 nM), respectively[52]. However, for the first time, we found P450s, which open the possibility of a P450-derived production of 14-OH, 21-OH and 26-OH epothilone D to perform further studies with those derivatives. Most interestingly, CYP267B1 was able to oxidize epothilone D at position C-7 to 7-ketone epothilone D (Table 3). The positions in the epothilone molecule surrounding position C-7 have been shown to be of importance for the pharmacological effect of this compound. Thus, the removal/insertion of the methyl group, the reduction of the C = O group or the extension/reduction of the size of the epothilone D ring result in a less cytotoxic effect[58]. In contrast, the function of substitutions at position C-7 have currently not been analyzed and need to be further investigated to be able to find a potential pharmacologically active derivative of epothilones.

In summary, our results demonstrate that the redox pair Fdx8/FdR_B from *S. cellulosum* So ce56 efficiently supports the epothilone D conversion catalyzed by EpoK thus indicating a potential similarity to natural redox partners from So ce90. This hypothesis is supported both by experimental results and bioinformatics study. Apart from Fdx8/FdR_B, several other efficient redox partners were also identified in this study, which enable for the first time the implementation of EpoK in semisynthetic[47], biotechnological[49] or putatively even light-dependent[44] epothilone B production. Following the hybrid system of *Anabaena* ferredoxin-NADP$^+$ reductase and *bovine* Adx described in 2003[59], the newly established *in vitro* hybrid system consisting of SynFdx from *Synechocystis* and FNR from *C. reinhardtii* reveals great potential for future EpoK *in vitro* and whole-cell studies and brings hybrid systems for P450 applications back into discussion.

With regard to the derivatization of epothilone D, eleven myxobacterial P450s have been investigated concerning their respective potential of converting epothilones and three of them were identified to convert epothilone D. Thereby, 14-OH, 21-OH and 26-OH epothilone D were found as novel P450-derived products. Additionally, a new epothilone derivative (7-ketone epothilone D) with a potential anti-tumor activity available by CYP267B1-dependent conversion was obtained (Fig. 5). Along with the autologous redox partners from *S. cellulosum* So ce56, further studies on protein engineering targeting higher yields and selectivity could lead to an important biotechnological application of myxobacterial P450s.

Methods

Chemicals. Phusion^{TM} High Fidelity DNA polymerase was purchased from Finnzymes (Espoo, Finland), Fast-Link^{TM} and DNA ligation kit from EPICENTRE Biotechnologies (Madison, WI, USA). Restriction enzymes were obtained from Promega (Madison, WI, USA). Oligonucleotides were purchased from BioTeZ Berlin-Buch GmbH (Berlin, Germany). Epothilone D was purchased via Biorbyt Ltd. (Cambridge, United Kingdom). Isopropyl ß-D-1-thiogalactopyranoside (IPTG) and 5-aminolevulinic acid were purchased from Carbolution chemicals (Saarbruecken, Germany). Bacterial media were purchased from Becton Dickinson (Heidelberg, Germany). All other chemicals were obtained from standard sources in the highest purity available.

Plasmids and strains. The gene encoding EpoK was amplified by polymerase chain reaction (PCR) using the primers EpoK_Bamfor (CAGTGGATCCATATGACACAGGAGCAAGCGAATCAG) and EpoKhis_hindrev (ATGAAGCTTAGTGATGGTGATGGTGATGT-CCAGCTTTGGAGGGCTTCAAG) as well as Phusion^{TM} High Fidelity DNA polymerase and genomic DNA of *S. cellulosum* So ce90 as template. The PCR primers introduced a sequence encoding a hexahistidine-tag in front of the stop codon as well as the restriction sites used for cloning into pCWori+. The FNR cDNA fragment coding for the full-length mature protein of *Chlamydomonas reinhardtii* was inserted into the pET-3d plasmid between the restriction sites NcoI and BamHI giving rise to the construct pET-FNR. The construct was designed in such a way that the N- and C-termini of the recombinant protein were MASLRKPS and NQWHVEVY, respectively. The *E. coli* strain BL21 (DE3) for the heterologous expression of the P450s was purchased from Agilent Technologies (Santa Clara, CA, USA).

Bioinformatics. Pairwise protein sequence alignments were performed using the Needlemann-Wunsch algorithm (EMBL-EBI: Needle (EMBOSS)). Protein sequences were taken from NCBI protein database (UniProtKB).

Heterologous expression and purification of P450s. *E. coli* BL21 (DE3) cells were transformed with the pCWori_EpoK plasmid encoding the C-terminal hexahistidine-tagged EpoK from *S. cellulosum* So ce90. An overnight culture was prepared from a single colony and was grown at 37 °C in lysogeny broth (LB) medium (10 g tryptone, 5 g yeast extract and 10 g NaCl per liter H_2O) containing 100 μg ml^{-1} ampicillin. For the heterologous expression of EpoK, a main culture of 500 ml terrific broth (TB) medium (24 g yeast extract, 12 g peptone, 4 ml glycerol, 2.31 g K_2HPO_4 and 12.54 g KH_2PO_4 per liter H_2O) containing 100 μg/ml ampicillin was inoculated with 5 ml of the overnight culture and grown at 37 °C. At an optical density (600 nm) of 0.9, 1 mM IPTG and 0.5 mM 5-aminolevulinic acid were added. After 24 h of expression at 25 °C, cells were harvested by centrifugation at 4000 × g for 20 min. Cell pellets were stored at −20 °C until purification. For protein purification, a cell pellet was thawed on ice and resuspended in lysis buffer (50 mM Tris-Cl (pH 7.5) buffer with 10% glycerol, 0.5 M sodium chloride, 5 mM ß-mercaptoethanol, 5 mM imidazole and 1 mM phenylmethylsulfonyl fluoride). Cells were disrupted by sonication and the separation of the cytosolic fraction was ensured by centrifugation at 30,000 rpm for 30 min. The supernatant was loaded on a 5 PRIME* PerfectPro* Ni-NTA Agarose column (Fisher scientific, Schwerte, Germany), washed with lysis buffer (twice the volume of packed column) and eluted with a linear gradient from 5 mM to 200 mM imidazole. Fractions of 2 ml were collected and analyzed via UV-Vis spectroscopy (UV- 2101PC, SHIMADZU, Japan). Fractions showing an absorption value ($A_{420\,nm}/A_{276\,nm}$) higher than 1.1 were pooled, washed with storage buffer (50 mM Tris-Cl (pH 7.5) buffer with 10% glycerol, 0.5 mM dithiothreitol and 1 mM EDTA) and concentrated using a Centricon ultrafiltration unit with 30-kDa cut-off (Millipore). The concentration of EpoK was determined by recording the oxidized spectra using ε (420 nm–490 nm) = 110 mM^{-1} cm^{-1} [60].

The P450s CYP109C1, CYP109C2, CYP109D1, CYP260A1, CYP260B1, CYP264A1, CYP264B1, CYP265A1, CYP266A1, CYP267A1, and CYP267B1 were expressed and purified as described previously[17,19,22,23,54].

Heterologous expression and purification of redox partners. The electron transfer partners $Adx_{4\text{-}108}$ and AdR from *Bos taurus* were expressed and purified as noted elsewhere[61,62]. The ferredoxin $Etp1^{fd}$ and the reductase Arh1 from *S. pombe* were expressed and purified as described[28,29]. The ferredoxins Fdx2 and Fdx8 as well as the reductase FdR_B from *S. cellulosum* So ce56 were expressed and purified analogous to previous studies in our laboratory[31].

E. coli BL21(DE3) was transformed with pET3d-FNR (ampicillin resistance) and pSBET (kanamycin resistance), the latter one encoding tRNAs for rare arginine codons[63] and colonies with double resistance were selected. SynFdx expression was performed from an ampicillin-resistant pCK5-Fdx plasmid in *E. coli* DH5α[64]. In both cases the antibiotic resistant strains were grown at 37 °C in 2.4 l LB medium supplemented with the required antibiotics (ampicillin at 100 μg ml^{-1} or kanamycin at 50 μg ml^{-1}) and in the case of SynFdx with additional 50 μM $FeSO_4$. Protein expression was induced at exponential phase by adding 100 μM IPTG for 4 h at 37 °C. The cultures were then centrifuged for 15 min at 4400 × g. The pellets were resuspended in 30 ml of 30 mM Tris–HCl (pH 8.0), 200 mM NaCl (Tris-NaCl buffer).

Cell lysis was performed by sonication (3 × 1 min with intervals of 1 min) and the soluble and insoluble fractions were separated by centrifugation for 30 min at 35,000 × g. The soluble part was then fractionated in two steps first up to 40% of the saturation in ammonium sulfate, then up to 80% for FNR or to 90% for SynFdx. After centrifugation (20 min, 20,000 × g), the recombinant proteins in the pellets from the 40 to 80/90% ammonium sulfate fractions were purified first by size exclusion chromatography after loading onto an ACA44 (5 × 75 cm) column equilibrated in Tris-NaCl buffer. The fractions containing the highest absorption values (SynFdx: $A_{420\,nm}/A_{275\,nm}$; FNR: $A_{455\,nm}/A_{275\,nm}$) were pooled, dialyzed by ultrafiltration to remove NaCl and loaded onto a DEAE (diethylaminoethyl) cellulose column (Sigma-Aldrich, Hannover, Germany) equilibrated in a 30 mM Tris–HCl (pH 8.0) buffer. The proteins were then eluted using a 0 to 0.4 M NaCl gradient. The fractions of interest were pooled, concentrated by ultrafiltration under nitrogen pressure (Amicon, YM10 membrane) and stored in the same buffer at −20 °C at concentrations higher than 5 mg/ml. Purified *Synechocystis* ferredoxin had ratios $A_{420\,nm}/A_{275\,nm}$ higher than 0.5. *Chlamydomonas reinhardtii* FNR preparations had ratios $A_{275\,nm}/A_{455\,nm}$ of about 7. Molecular extinction coefficients of the ferredoxins and ferredoxin reductases expressed and purified during this study are summarized in supplemental Table S0.

***In vitro* conversions.** To measure the *in vitro* conversion of epothilone D to B, a reconstituted *in vitro* system analogous to Julien *et al.* and Tang *et al.* was chosen[12,21]. EpoK (1.5 μM), the regeneration system consisting of glucose-6-phosphate (3.3 mM) and glucose-6-phosphate dehydrogenase (0.5 U), and epothilone D (100 μM) were used for each sample. The ratios of EpoK to the tested ferredoxins and reductases were selected corresponding to previous studies. *In vitro* conversions with *bovine* electron transfer partners were done using a ratio EpoK:$Adx_{4\text{-}108}$:AdR of 1:20:3[22] and the ratio of the redox partners from *S. cellulosum* So ce56 were chosen as 1:60:3 (both EpoK:Fdx2:FdR_B and EpoK:Fdx8:FdR_B) corresponding to published values[31]. The ratio for the electron transfer system from *S. pombe* was set as 1:8:0.8 (EpoK:$Etp1^{fd}$:Arh1) as described by Ewen *et al.*[29]. Ferredoxin from *Synechocystis* (SynFdx) was tested with different heterologous reductases (ratio EpoK:SynFdx:reductase 1:10:1 and 1:20:3). The total volume of the reaction was 200 μl. The reaction was started by the addition of NADPH (1 mM). After 1 h at 30 °C the reaction was quenched by adding ethyl acetate (400 μl). The aqueous phase was extracted twice with ethyl acetate (2 × 400 μl), unified and evaporated to dryness. All experiments were done twice and a negative control without P450 was implemented to verify the P450-dependent reaction.

In vitro conversions with P450s from *S. cellulosum* So ce56 were done as described before with potassium phosphate buffer (50 mM, pH 7.4, 1% glycerin) as reaction buffer.

Kinetic studies of epothilone D epoxidation by EpoK/SynFdx/FNR system were performed analogous to the reconstituted *in vitro* system described above. EpoK concentration was set as 0.25 μM with an EpoK:SynFdx:FNR ratio of 1:20:3. The reaction was stopped after 90 s at 30 °C by freezing the samples in liquid nitrogen.

Analysis of the *in vitro* conversions via HPLC. The HPLC analysis was performed on a Jasco (Gross-Umstadt, Germany) HPLC system 2000. The samples were dissolved in 100 μl acetonitrile and analyzed (samples of kinetics twice) on a reversed phase column (125/4 Nucleodur 100-5 C18ec, Macherey Nagel, Düren, Germany) at a flow rate of 1 ml min^{-1} and a temperature of 40 °C with the gradient: 80% solvent A (80:20 (v/v) water-acetonitrile) for 1 min, linear gradient for 8.5 min from 20% to 90% solvent B (100% acetonitrile) and holding 90% solvent B for 4 min. The injection volume was set as 20 μl (40 μl for kinetic studies) and the sample was monitored at 250 nm.

Analysis of the *in vitro* conversions via LC-MS/MS. Mass spectrometric analyses were performed using a Thermo-Fischer (Sunnyvale, CA, USA) Dionex UltiMate 3000 ultra-high performance liquid chromatography (UHPLC) system coupled to an AB Sciex (Concord, ON, Canada) QTRAP 5500 quadrupole linear ion trap (QqLIT) system. Samples were separated on a reversed-phase HPLC column (125/4 Nucleodur 100-5 C18ec, Macherey Nagel) at 40 °C using gradient elution at 0.5 mL min^{-1}. The mobile phase consisted of 80:20 (v/v) water-acetonitrile (A) and 100% acetonitrile (B). The gradient was as follows: B was increased from 20 to 90% within 17 min, held there for 5 min, and then returned to 20% within 0.1 min, followed by an equilibration period at 20% B for 7.9 min. For each analysis, 10 μl were injected. ESI-MS conditions were as follows: curtain gas: 55 psi, electrospray voltage: 5 kV, source heater temperature: 350 °C, ion source gas 1: 45 psi, ion source gas 2: 50 psi, collision gas: nitrogen, declustering potential: 48 V, entrance potential: 11 V. MS/MS experiments were performed using collision-induced dissociation (CID) between 15–35 V for the precursor ion *m/z* 508. The collision cell exit potential was 13 V; an isolation width of 1 u was used.

References

1. WHO. Decisions and list of resolutions of the 65th World Health Assembly: prevention and control of noncommunicable diseases—follow-up to the high-level meeting of the United Nations General Axssembly on the prevention and control of non-communicable diseases (A65/DIV/3). Report (2012).
2. Allemani, C. *et al.* Global surveillance of cancer survival 1995–2009: analysis of individual data for 25, 676, 887 patients from 279 population-based registries in 67 countries (concord-2). *Lancet*, **385(9972),** 977–1010 (2015).
3. Dall'Acqua, S. Natural products as antimiotic agents *Curr. Top. Med. Chem.* **14,** 2272–2285 (2014).
4. Mukhtar, E., Adhami, V. M. & Mukhtar, H. Targeting microtubules by natural agents for cancer therapy. *Mol. Cancer Ther.* **13(2),** 275–284 (2014).
5. Gerth, K., Bedorf, N., Höfle, G., Irschik, H. & Reichenbach, H. Epothilones A and B: antifungal and cytotoxic compounds from Sorangium cellulosum (Myxobacteria). Production, physico-chemical and biological properties. *J Antibiot (Tokyo)*, **49(6),** 560–3 (1996).
6. Höfle, G. *et al.* Epothilone A and B - Novel 16-membered macrolides with cytotoxic activity: Isolation, crystal structure, and conformation in solution. *Angew. Chem., Int. Ed. Engl.* **35(13-14),** 1567–1569 (1996).
7. Bollag, D. M. *et al.* Epothilones, a new class of microtubule-stabilizing agents with a taxol-like mechanism of action. *Cancer Res.* **55,** 2325–2333 (1995).
8. Brogdon, C. F., Lee, F. Y. & Canetta, R. M. Development of other microtubule-stabilizer families: the epothilones and their derivatives. *Anticancer Drugs.* **25(5),** 599–609 (2014).
9. Cartelli, D. *et al.* Microtubule alterations occur early in experimental parkinsonism and the microtubule stabilizer epothilone D is neuroprotective. *Sci. Rep.* **3,** 1837 (2013).
10. Zhang, B. *et al.* The microtubule-stabilizing agent, epothilone D, reduces axonal dysfunction, neurotoxicity, cognitive deficits, and Alzheimer-like pathology in an interventional study with aged tau transgenic mice. *J Neurosci.* **32(11),** 3601–11 (2012).
11. Molnár, I. *et al.* The biosynthetic gene cluster for the microtubule-stabilizing agents epothilones A and B from Sorangium cellulosum So ce90. *Chem. Biol.*, **7(2),** 97–109 (2000).
12. Tang, L. *et al.* Cloning and heterologous expression of the epothilone gene cluster. *Science.* **287(5453),** 640–2 (2000).
13. Bernhardt, R. Cytochromes P450 as versatile biocatalysts. *J. Biotechnol.*, **124(1),** 128–45 (2006).
14. Bernhardt, R. & Urlacher, V. B. Cytochromes P450 as promising catalysts for biotechnological application: chances and limitations. *Appl Microbiol Biotechnol.* **98(14),** 6185–203 (2014).
15. Hannemann, F., Bichet, A., Ewen, K. M. & Bernhardt, R. Cytochrome P450 systems-biological variations of electron transport chains. *Biochim Biophys Acta.* **1770(3),** 330–44 (2007).
16. Ogura, H. *et al.* EpoK, a Cytochrome P450 involved in biosynthesis of the anticancer agents epothilones A and B. Substrate-mediated rescue of a P450 Enzyme. *Biochemistry.* **43,** 14712–14721 (2004).
17. Khatri, Y. *et al.* A natural heme-signature variant of CYP267A1 from Sorangium cellulosum So ce56 executes diverse omega-hydroxylation. *FEBS J.* **282(1),** 74–88 (2015).
18. Litzenburger, M., Kern, F., Khatri, Y. & Bernhardt, R. Conversions of tricyclic antidepressants and antipsychotics with selected P450s from Sorangium cellulosum So ce56. *Drug Metab Dispos*, **43(3),** 392–9 (2015).
19. Ly, T. T., Khatri, Y., Zapp, J., Hutter, M. C. & Bernhardt, R. CYP264B1 from Sorangium cellulosum So ce56: a fascinating norisoprenoid and sesquiterpene hydroxylase. *Appl Microbiol Biotechnol.* **95(1),** 123–33 (2012).
20. Schifrin, A. *et al.* Characterization of the gene cluster CYP264B1-geoA from Sorangium cellulosum So ce56: Biosynthesis of (+)-eremophilene and its hydroxylation. *ChemBioChem.* **16(2),** 337–344 (2015).
21. Julien, B. *et al.* Isolation and characterization of the epothilone biosynthetic gene cluster from Sorangium cellulosum. *Gene.* **249(1-2),** 153–60 (2000).
22. Khatri, Y. *et al.* The CYPome of Sorangium cellulosum So ce56 and identification of CYP109D1 as a new fatty acid hydroxylase. *Chem Biol*, **17(12),** 1295–305 (2010).
23. Ringle, M., Khatri, Y., Zapp, J., Hannemann, F. & Bernhardt, R. Application of a new versatile electron transfer system for cytochrome P450-based Escherichia coli whole-cell bioconversions. *Appl Microbiol Biotechnol.* **97(17),** 7741–54 (2013).
24. Blum, W. *et al. In vivo* metabolism of epothilone B in tumor-bearing nude mice: identification of three new epothilone B metabolites by capillary high-pressure liquid chromatography/mass spectrometry/tandem mass spectrometry. *Rapid Commun. Mass Spectrom.*, **15(1),** 41–49 (2001).
25. Prota, A. E. *et al.* Molecular mechanism of action of microtubule-stabilizing anticancer agents. *Science.* **339(6119),** 587–90 (2013).
26. Gerber, A., Hannemann, F., Bleif, S., Kleser, M. & Bernhardt, R. Inventors; SANOFI, Inc., assignee. Whole-cell system for Cytochrome P450 monooxygenases biocatalysis. (2014). WIPO Patent Application WO/2014/202627.
27. Janocha, S. & Bernhardt, R. Design and characterization of an efficient CYP105A1-based whole-cell biocatalyst for the conversion of resin acid diterpenoids in permeabilized Escherichia coli. *Appl Microbiol Biotechnol.* **97(17),** 7639–49 (2013).
28. Bureik, M., Schiffler, B., Hiraoka, Y., Vogel, F. & Bernhardt, R. Functional expression of human mitochondrial CYP11B2 in fission yeast and identification of a new internal electron transfer protein, etp1. *Biochemistry.* **41(7),** 2311–2321 (2002).
29. Ewen, K. M., Schiffler, B., Uhlmann-Schiffler, H., Bernhardt, R. & Hannemann, F. The endogenous adrenodoxin reductase-like flavoprotein arh1 supports heterologous cytochrome P450-dependent substrate conversions in Schizosaccharomyces pombe. *FEMS Yeast Res.* **8(3),** 432–41 (2008).
30. Schneiker, S. *et al.* Complete genome sequence of the myxobacterium Sorangium cellulosum. *Nat. Biotechnol.* **25(11),** 1281–1289 (2007).
31. Ewen, K. M. *et al.* Genome mining in Sorangium cellulosum So ce56: identification and characterization of the homologous electron transfer proteins of a myxobacterial cytochrome P450. *J Biol Chem.* **284(42),** 28590–8 (2009).
32. Han, K. *et al.* Extraordinary expansion of a Sorangium cellulosum genome from an alkaline milieu. *Sci. Rep.* **3(2101),** (2013).
33. Zhao, L. *et al.* Glycosylation and production characteristics of epothilones in alkali-tolerant Sorangium cellulosum strain So0157-2. *J. Microbiol.* **48(4),** 438–444 (2010).
34. Kaneko, T. Structural analysis of four large plasmids harboring in a unicellular cyanobacterium, Synechocystis sp. PCC 6803. *DNA Res.* **10(5),** 221–228 (2003).
35. Bottin, H. & Lagoutte, B. Ferrodoxin and flavodoxin from the cyanobacterium Synechocystis sp PCC 6803. *Biochimi Biophys Acta*, **1101(1),** 48–56 (1992).

36. Cassier-Chauvat, C. & Chauvat, F. Function and regulation of ferredoxins in the cyanobacterium, Synechocystis PCC6803: Recent advances. *Life (Basel)*. **4(4),** 666–80 (2014).
37. Jacquot, J. P. *et al.* Residue Glu-91 of Chlamydomonas reinhardtii ferredoxin is essential for electron transfer to ferredoxin-thioredoxin reductase. *FEBS*. **400,** 293–296 (1997).
38. Decottignies, P., Le Maréchal, P., Jacquot, J. P., Schmitter, J. M. & Gadal, P. Primary structure and post-translational modification of ferredoxin-NADP+ reductase from Chlamydomonas reinhardtii. *Arch. Biochem. Biophys.* **316(1),** 249–259 (1995).
39. Ceccarelli, E. A., Arakaki, A. K., Cortez, N. & Carrillo, N. Functional plasticity and catalytic efficiency in plant and bacterial ferredoxin-NADP(H) reductases. *Biochim. Biophys. Acta*. **1698(2),** 155–65 (2004).
40. Chibani, K., Tarrago, L., Schürmann, P., Jacquot, J. P. & Rouhier, N. Biochemical properties of poplar thioredoxin z. *FEBS Lett.* **585(7),** 1077–1081 (2011).
41. Palma, P. N., Lagoutte, B., Krippahl, L., Moura, J. J. & Guerlesquin, F. Synechocystis ferredoxin/ferredoxin-NADP+ reductase/NADP+ complex: Structural model obtained by NMR-restrained docking. *FEBS Lett.* **579(21),** 4585–90 (2005).
42. Davydov, D. R. & Halpert, J. R. Allosteric P450 mechanisms: multiple binding sites, multiple conformers, or both? *Expert Opin. Drug Metab. Toxicol.* **4(12),** 1523–1535 (2008).
43. Cammack, R. *et al.* Midpoint redox potentials of plant and algal ferredoxins. *Biochem J.* **168(2),** 205–9 (1977).
44. Jensen, K., Johnston, J. B., Ortiz de Montellano, P. R. & Møller, B. L. Photosystem I from plants as a bacterial cytochrome P450 surrogate electron donor: terminal hydroxylation of branched hydrocarbon chains. *Biotechnol Lett.* **34(2),** 239–45 (2012).
45. Yang, H. *et al.* Preparative isolation and purification of epothilones from Sorangium cellulosum fermentation broth by high-speed counter-current chromatography. *J. Liq. Chromatogr. Relat. Technol.* **38(1),** 123–127 (2014).
46. Mulzer, J., Altmann, K. H., Höfle, G., Müller, R. & Prantz, K. Epothilones - A fascinating family of microtubule stabilizing antitumor agents. *C. R. Chim.* **11(11-12),** 1336–1368 (2008).
47. Boddy, C. N., Hotta, K., Tse, M. L., Watts, R. E. & Khosla, C. Precursor-directed biosynthesis of epothilone in Escherichia coli. *J Am Chem Soc*, **126(24),** 7436–7 (2004).
48. Julien, B. & Shah, S. Heterologous expression of epothilone biosynthetic genes in Myxococcus xanthus. *Antimicrob. Agents Chemother.* **46(9),** 2772–8 (2002).
49. Mutka, S. C., Carney, J. R., Liu, Y. & Kennedy, J. Heterologous production of epothilone C and D in Escherichia coli. *Biochemistry.* **45(4),** 1321–1330 (2006).
50. Zhang, H., Wang, K., Cheng, X., Lu, Y. & Zhang, Q. Synthesis and *in vitro* cytotoxicity of poly(ethylene glycol)-epothilone B conjugates. *J. Appl. Polym. Sci.* **131(23),** (2014).
51. Lu, C., Zhao, L. & Li, Y. Four natural epothilone derivatives isolated from Sorangium cellulosum strain So0157-2. *J Chin. Pharmaceutical Sci.* **22(1),** 28–31 (2013).
52. Tang, L., Qiu, R., Li, Y. & Katz, L. Generation of novel epothilone analogs with cytotoxic activity by biotransformation. *J. Antibiot.* **56(1),** 16–23 (2003).
53. Basch, J. & Chiang, S. J. Cloning and expression of a cytochrome P450 hydroxylase gene from Amycolatopsis orientalis: hydroxylation of epothilone B for the production of epothilone F. *J. Ind. Microbiol. Biotechnol.*, **34(2),** 171–176 (2007).
54. Khatri, Y. *et al.* Novel family members of CYP109 from Sorangium cellulosum So ce56 exhibit characteristic biochemical and biophysical properties. *Biotechnol Appl Biochem*, **60(1),** 18–29 (2013).
55. Zhang, W. *et al.* New reactions and products resulting from alternative interactions between the P450 enzyme and redox partners. *J. Am. Chem. Soc.* **136,** 3640–3646 (2014).
56. Hardt, I. H. *et al.* New natural epothilones from Sorangium cellulosum, strains So ce90/B2 and So ce90/D13: Isolation, structure elucidation, and SAR studies. *J. Nat. Prod.* **64(7),** 847–856 (2001).
57. Nicolaou, K. C., Finlay, M. R. V., Ninkovic, S. & Sarabia, F. Total synthesis of 26-hydroxy-epothilone B and related analogs via a macrolactonization based strategy. *Tetrahedron.* **54(25),** 7127–7166 (1998).
58. Altmann, K. H., Wartmann, W. & O'Reilly, T. Epothilones and related structures – a new class of microtubule inhibitors with potent *in vivo* antitumor activity. *Biochim. Biophys. Acta.*, **1470(3),** M79–91 (2000).
59. Faro, M. *et al.* Insights into the design of a hybrid system between Anabaena ferredoxin-NADP+ reductase and bovine adrenodoxin. *Eur. J. Biochem.* **270(4),** 726–735 (2003).
60. Omura, T. & Sato, R. The carbon monoxide-binding pigment of liver microsomes. *J Biol Chem.* **239(7),** 2379–2385 (1964).
61. Sagara, Y. *et al.* Direct expression of adrenodoxin reductase in Escherichia coli and the functional characterization. *Biol Pharm Bull.* **16(7),** 627–30 (1993).
62. Uhlmann, H., Kraft, R. & Bernhardt, R. C-terminal region of adrenodoxin affects its structural integrity and determines differences in its electron transfer function to cytochrome P450. *J Biol Chem.* **269(36),** 22557–22564 (1994).
63. Rogers, W. J. *et al.* Isolation of a cDNA fragment coding for Chlamydomonas reinhardtii ferredoxin and expression of the recombinant protein in Escherichia coli. *FEBS Lett.* **310(3),** 240–5 (1992).
64. Glauser, D. A., Bourquin, F., Manieri, W. & Schurmann, P. Characterization of ferredoxin:thioredoxin reductase modified by site-directed mutagenesis. *J Biol Chem*, **279(16),** 16662–9 (2004).
65. Dereeper, A. *et al.* Phylogeny.fr: robust phylogenetic analysis for the non-specialist. *Nucleic Acids Res.* **36,** W465–W469 (2008).
66. Grinberg, A. V. *et al.* Adrenodoxin: Structure, stability, and electron transfer properties. *Proteins: Struct., Funct., Genet.* **40(4),** 590–612 (2000).
67. Schiffler, B. *et al.* The adrenodoxin-like ferredoxin of Schizosaccharomyces pombe mitochondria. *J Inorg Biochem.* **98(7),** 1229–37 (2004).
68. Tagawa, K. & Arnon, D. I. Oxidation-reduction potentials and stoichiometry of electron transfer in ferredoxins. *Biochim Biophys Acta*. **153(3),** 602–613 (1968).
69. Hiwatashi, A., Ichikawa, Y., Maruya, N., Yamano, T. & Aki, K. Properties of crystalline reduced nicotinamide adenine dinucleotide phosphate-adrenodoxin reductase from bovine adrenocortical mitochondria. I. Physicochemical properties of holo- and apo-NADPH-adrenodoxin reductase and interaction between non-heme iron proteins and the reductase. *Biochemistry.* **15(14),** 3082–3090 (1976).
70. Decottignies, P., Flesch, V., Gérard-Hirne, C. & Le Maréchal, P. Role of positively charged residues in Chlamydomonas reinhardtii ferredoxin-NADP+ reductase. *Plant Physiol. Biochem.* **41(6-7),** 637–642 (2003).
71. Kitayama, M., Kitayama, K. & Togasaki, R. K. A cDNA clone encoding a ferredoxin-NADP+ reductase from Chlamydomonas reinhardtii. *Plant Physiol.* **106,** 1715–1716 (1994).
72. Süss, K. H., Prokhorenko, I. & Adler, K. *In situ* association of calvin cycle enzymes, ribulose-l,5-bisphosphate carboxylase/oxygenase activase, ferredoxin-NADP+ reductase, and nitrite reductase with thylakoid and pyrenoid membranes of Chlamydomonas reinhardtii chloroplasts as revealed by immunoelectron microscopy. *Plant Physiol.* **107,** 1387–1397 (1995).

Acknowledgements

We would like to thank Michael R. Waterman, Vanderbilt University School of Medicine, Nashville, USA, for the gift of the *E. coli* expression vector pCWori+. Special thanks to Rolf Müller, Saarland University, Germany, for the gift of the genomic DNA from *S. cellulosum* So ce90 and to Nicolas Rouhier, Nancy University, France, for SynFdx purification. We would also like to thank Birgit Heider-Lips, Alexander Schifrin, Tanja Sagadin and Michael Ringle for protein purifications. This work was partially funded by the DFG (Be1343/23) and a grant from Laboratory of Excellence ARBRE (ANR-LABXARBRE-01).

Author Contributions

F.K. and R.B. conceived the experiments, F.K., T.D., Y.K., K.M.E. and J.P.J. conducted the experiments, F.K., T.D. and D.V. analyzed the results. All authors reviewed the manuscript.

Additional Information

Supplementary information accompanies this paper at http://www.nature.com/srep

Competing financial interests: The authors declare no competing financial interests.

How to cite this article: Kern, F. *et al.* Highly Efficient CYP167A1 (EpoK) dependent Epothilone B Formation and Production of 7-Ketone Epothilone D as a New Epothilone Derivative. *Sci. Rep.* **5**, 14881; doi: 10.1038/srep14881 (2015).

SUPPORTING INFORMATION

Highly efficient CYP167A1 (EpoK) dependent epothilone B formation and production of 7-ketone epothilone D as a new epothilone derivative

Fredy Kern[1], Tobias K. F. Dier[2], Yogan Khatri[1], Kerstin M. Ewen[1], Jean-Pierre Jacquot[3], Dietrich A. Volmer[2] and Rita Bernhardt[1]

[1]From the Department of Biochemistry, Saarland University, 66123 Saarbrücken, Germany

[2]Institute of Bioanalytical Chemistry, Saarland University, 66123 Saarbrücken, Germany

[3]Unité Mixte de Recherches, 1136 Interaction arbres microorganismes INRA, Nancy University, 54506 Vandoeuvre-lès-Nancy cedex, France

To whom correspondence should be addressed: Rita Bernhardt, Department of Biochemistry, Saarland University, 66123 Saarbrücken, Germany, Tel.: +49 (0)681 302 4241; Fax: +49 (0)681 302 4739; E-mail: ritabern@mx.uni-saarland.de

Molecular extinction coefficients of ferredoxins and ferredoxin reductases - The summarized extinction coefficients of ferredoxins and ferredoxin reductases expressed and purified in this study are listed in Table S0.

Table S0. Overview: molecular extinction coefficients of ferredoxins and ferredoxin reductases. (Values were taken from literature as referred in Table 1 and Table 2; results section)

Ferredoxin	Organism	Extinction coefficient [mM^{-1} cm^{-1}]	Reductase	Organism	Extinction coefficient [mM^{-1} cm^{-1}]
$Adx_{4\text{-}108}$	*Bos taurus*	ε_{414nm}: 9.8	AdR	*Bos taurus*	ε_{450nm}: 11.3
$Etp1^{fd}$	*S. pombe*	ε_{414nm}: 9.8	Arh1	*S. pombe*	ε_{450nm}: 11.3
Fdx2	*S. cellulosum So ce56*	ε_{390nm}: 6.181	FdR_B	*S. cellulosum* So ce56	ε_{457nm}: 8.73
Fdx8		ε_{400nm}: 9.7			
SynFdx	*Synechocystis*	ε_{422nm}: 9.7	FNR	*C. reinhardtii*	ε_{450nm}: 11.3

Structure of products - During this study, 4 new P450-derived epothilone D derivatives were found and characterized via LC-MS/MS. An overview of the chemical structures is presented in Figure S1.

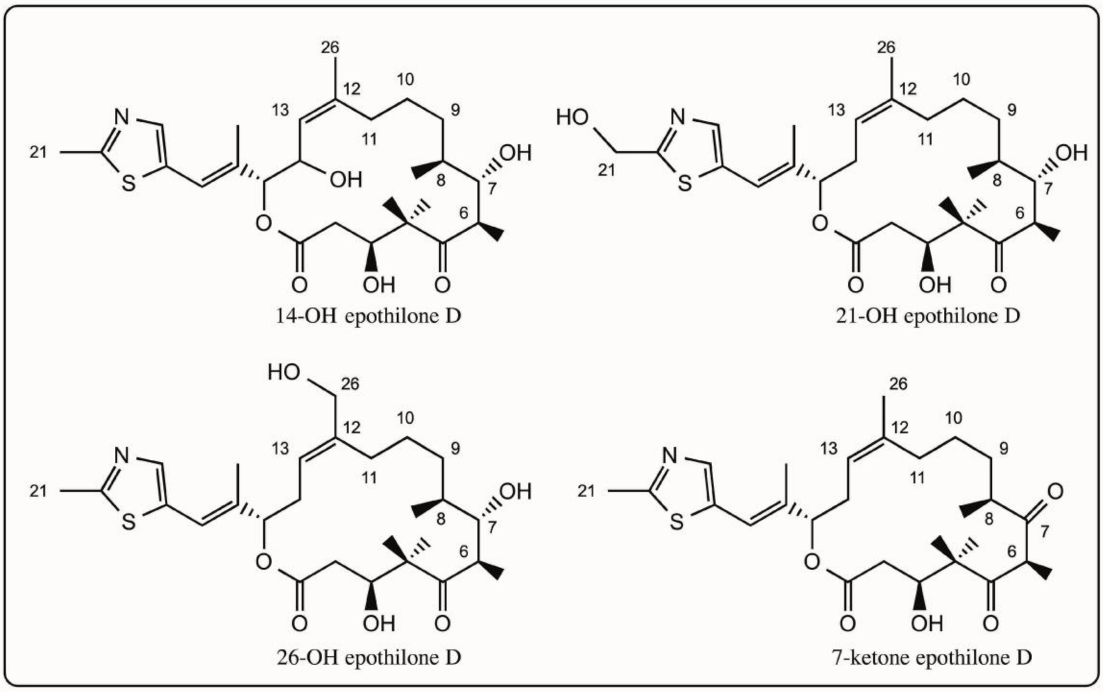

Figure S1. Overview of major epothilone D products formed by myxobacterial P450s from *S. cellulosum* So ce56 (CYP265A1 and CYP266A1: 14-OH epothilone D; CYP267B1: 14-OH, 21-OH, 26-OH and 7-ketone epothilone D).

2/5

LC-MS/MS data - The chromatograms of LC-MS/MS experiments are presented in Figure S2. Products A and B are already labeled as 21-OH epothilone D as well as product C (14-OH epothilone D), product D (26-OH epothilone D) and product E (7-ketone epothilone D).

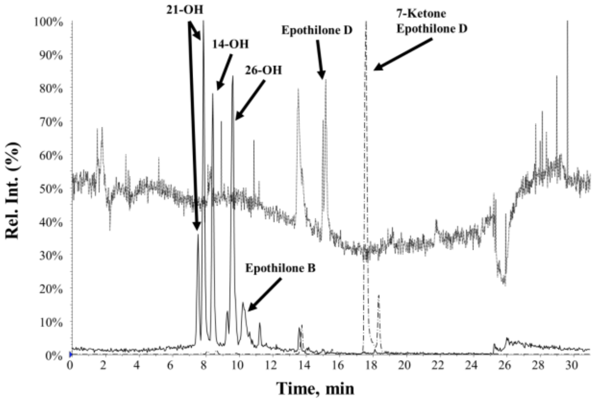

Figure S2. LC-MS/MS chromatograms of epothilone D conversion.

The MS/MS spectrum of the new epothilone derivative 7-ketone epothilone D is presented in Figure S3.

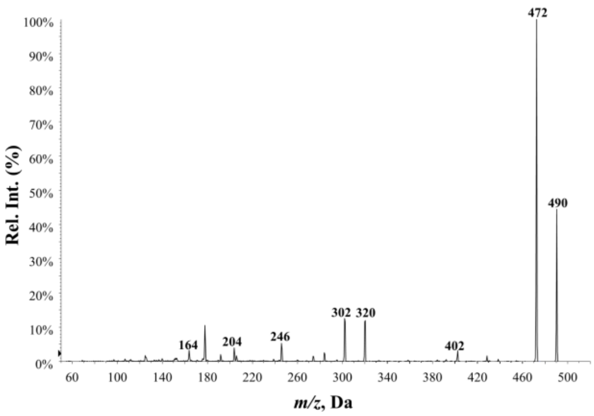

Figure S3. MS/MS spectrum of 7-ketone epothilone D.

An overview of the chemical structures assigned to the fragments observed in the LC-MS/MS spectra of the identified products is listed in Table S1. For further information on 7-ketone epothilone D, see Figure 5 in the discussion section.

Table S1. Overview of conversion products tentatively identified by LC-MS/MS (a: taken from [37]; *: fragments observed in 14-OH, 21-OH, 26-OH and 7-ketone epothilone D MS/MS spectra; b: see Figure 5 in the manuscript for fragment structures).

Name (m/z of $[M+H]^+$)	Chemical structure	MS^2/CID product ions (m/z)
Epothilone B (508)	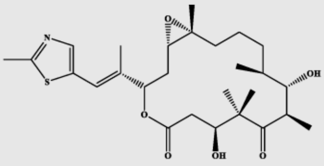	508-H_2O (490)[a*]; 490-H_2O (472)[*]; 508-$C_3H_4O_3$ (420)[a*]; 420-H_2O (402)[*]; 508-$C_7H_{12}O_5$ (332)[a*]; 508-$C_8H_{14}O_4$ (320)[a*]; 320-H_2O (302)[a*]; 166[a*]
14-OH epothilone D (508)	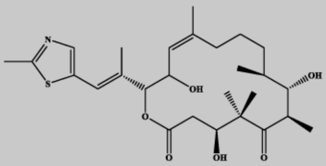	206 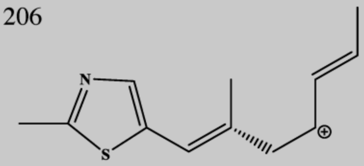
21-OH epothilone D (508)	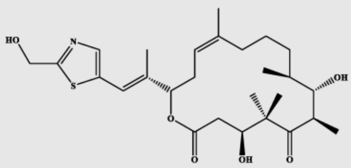	168 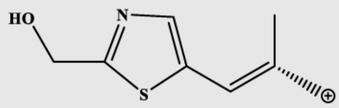
26-OH epothilone D (508)	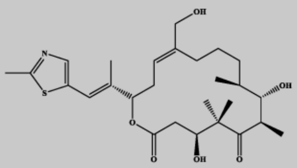	220 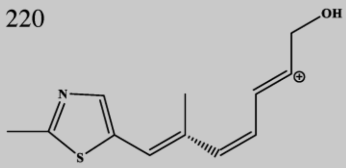
7-Ketone epothilone D (490)	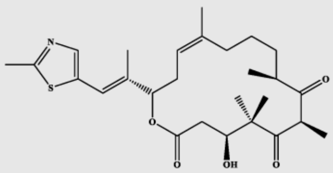	490-H_2O (472)[b]; 490-CO_2,C_2H_4O; (402)[b]; 320[b]; 246[b]; 204[b]; 164[b]

Bioinformatic analysis of the putative Fdx2, Fdx8 and FdR_B-like ferredoxins and ferredoxin reductase of S. cellulosum So0157-2 - Among UniProtKB Bacteria database, the Proteome of *Sorangium cellulosum* So0157-2 (GenBank: CP003969.1, length = 14782125) was found producing significant alignments with protein sequences of Fdx2, Fdx8 and FdR_B from *S. cellulosum* So ce56 (NCBI BLAST+). Pairwise protein sequence alignments were performed using the Needlemann-Wunsch algorithm (EMBL-EBI: Needle (EMBOSS).

Table S2. Summarized alignment results of Fdx2, Fdx8 and FdR_B from *S. cellulosum* So ce56 with *S. cellulosum* So0157-2.

Protein (So ce56)	**Gene name in So0157-2**	**Identity**	**Similarity**	**Gaps**
Fdx2	SCE1572_46000 [4Fe-4S] ferredoxin	94/101 (93.1%)	98/101 (97.0%)	0/101 (0.0%)
Fdx8	SCE1572_33470 Hypothetical protein	86/110 (78.2%)	89/110 (80.9%)	11/110 (10.0%)
FdR_B	SCE1572_31190 Hypothetical protein	227/245 (92.7%)	235/245 (95.9%)	1/245 (0.4%)

3.2 Kern et al. 2016

CYP267A1 and CYP267B1 from *Sorangium cellulosum* So ce56 are Highly Versatile Drug Metabolizers.

Fredy Kern, Yogan Khatri, Martin Litzenburger and Rita Bernhardt

Drug Metabolism and Disposition, 2016, 44(4): 495-504.

1521-009X/44/4/495–504$25.00
Drug Metabolism and Disposition

http://dx.doi.org/10.1124/dmd.115.068486
Drug Metab Dispos 44:495–504, April 2016

DRUG METABOLISM & DISPOSITION

CYP267A1 and CYP267B1 from *Sorangium cellulosum* So ce56 are Highly Versatile Drug Metabolizers [S]

Fredy Kern, Yogan Khatri, Martin Litzenburger, and Rita Bernhardt

Department of Biochemistry, Saarland University, Saarbruecken, Germany

Received November 19, 2015; accepted February 2, 2016

ABSTRACT

The guidelines of the Food and Drug Administration and International Conference on Harmonization have highlighted the importance of drug metabolites in clinical trials. As a result, an authentic source for their production is of great interest, both for their potential application as analytical standards and for required toxicological testing. Since we have previously shown promising biotechnological potential of cytochromes P450 from the soil bacterium *Sorangium cellulosum* So ce56, herein we investigated the CYP267 family and its application for the conversion of commercially available drugs including nonsteroidal anti-inflammatory, antitumor, and antihypotensive drugs. The CYP267 family, especially CYP267B1, revealed the interesting ability to convert a broad range of substrates. We established substrate-dependent extraction protocols and also optimized the reaction conditions for the in vitro experiments and *Escherichia coli*–based whole-cell bioconversions. We were able to detect activity of CYP267A1 toward seven out of 22 drugs and the ability of CYP267B1 to convert 14 out of 22 drugs. Moderate to high conversions (up to 85% yield) were observed in our established whole-cell system using CYP267B1 and expressing the autologous redox partners, ferredoxin 8 and ferredoxin-NADP$^+$ reductase B. With our existing setup, we present a system capable of producing reasonable quantities of the human drug metabolites 4′-hydroxydiclofenac, 2-hydroxyibuprofen, and omeprazole sulfone. Due to the great potential of converting a broad range of substrates, wild-type CYP267B1 offers a wide scope for the screening of further substrates, which will draw further attention to future biotechnological usage of CYP267B1 from *S. cellulosum* So ce56.

Introduction

The emergence of new diseases, rising concerns about drug resistance, and the decreasing efficacy of the existing drugs are of great pharmaceutical concern. As a result, drug research during the past century, driven by chemistry, pharmacology, and clinical science, has shown an increasing contribution to the development of new therapeutic agents (Drews, 2000). Despite the success in combating the majority of genetic, infectious, and bacterial diseases, novel drugs and drug derivatives are consistently demanded. However, the efficacy of such drugs and their related metabolites need to be tested and approved. The guidelines published by the Food and Drug Administration and the International Conference on Harmonization highlight the importance of qualifying metabolite exposure in clinical trials, in which a metabolite formed greater than 10% needs to be specifically tested for toxicity (Food and Drug Administration, 2008; International Conference on Harmonization, 2009, 2012). Due to the frequent introduction of novel drugs and drug candidates with new or modified chemical structure, implementation of costly multistep chemical syntheses may not be sufficient enough to overcome the demand of the respective metabolites (Rushmore et al., 2000).

This work was supported by Deutsche Forschungsgemeinschaft [Grant Be1343/23].
This manuscript describes original work and is not under consideration by any other journal. All authors approved the manuscript and this submission. The authors declare no competing financial interests.
dx.doi.org/10.1124/dmd.115.068486.
[S] This article has supplemental material available at dmd.aspetjournals.org.

Although the purification of major metabolites from urine is relatively easy and cheap (Gao et al., 2012), a constant and subject-independent large-scale production of drug metabolites, for instance, by using human liver, is hindered by very limited availability. To circumvent such limitations, alternative approaches of using microorganisms have been practiced, in which several microorganisms such as the fungus *Cunninghamella* sp. or bacterial variants of *Streptomyces* strains were shown to transform drugs and xenobiotics to mammalian metabolites (Zhang et al., 1996; Asha and Vidyavathi, 2009; Bright et al., 2011; Murphy and Sandford, 2012; Diao et al., 2013). However, because of the release of side products and the difficulty on handling the microbes during such biotransformation process, there is now a great interest in cytochrome P450 (P450) enzymes for the production of drug metabolites. In general, P450 enzymes are versatile, heme-containing enzymes, which catalyze a variety of reactions highlighting them as essential candidates for biotechnological and pharmaceutical research (Bernhardt and Urlacher, 2014). It has been shown that the utilization of human P450 enzymes enables the sufficient production of human drug metabolites employing baculovirus-infected insect cells expressing CYP3A4 or CYP2D9 (Rushmore et al., 2000), fission yeast expressing CYP2D6 (Peters et al., 2007) or CYP2C9 (Drăgan et al., 2011; Neunzig et al., 2012), and *Escherichia coli* cells expressing CYP3A4, CYP2C9, and CYP1A2 (Vail et al., 2005). Since it is not mandatory to employ associated human P450 enzymes to synthesize human drug metabolites (Schroer et al., 2010; Geier et al., 2015), microbial, especially bacterial, P450 enzymes serve as a good alternative because they are convenient to handle and usually hold higher expression levels and activities, recommending the possibility to employ them as useful

ABBREVIATIONS: AdR, adrenodoxin NADP$^+$ reductase; Adx_{4-108}, truncated adrenodoxin; BM3, cytochrome P450 102A1; CO, carbon monoxide; FdR_B, ferredoxin-NADP$^+$ reductase B; Fdx8, ferredoxin 8; Fpr, ferredoxin NADP$^+$ reductase; HPLC, high-performance liquid chromatography; MS/MS, tandem mass spectrometry; P450, cytochrome P450.

biocatalysts (Bernhardt, 2006). The genetic manipulation of bacterial P450 enzymes toward a drug metabolizing activity has been successfully demonstrated for several P450 enzymes including the most studied P450 102A1 (BM3), CYP102A1 (Whitehouse et al., 2012; Ren et al., 2015). However, the engineering of enzymes against their native, narrow substrate range, or in general the screening for enzymes to produce certain drug metabolites, is time consuming and complex, which can be overcome by employing versatile wild-type P450 enzymes showing an untypically broad substrate range (Yin et al., 2014).

During our recent investigations on P450 enzymes from the myxobacterium *Sorangium cellulosum* So ce56, several interesting enzymes displaying new properties and substrate specificities have been discovered, which lead us to investigate the potential of these P450 enzymes for an application as drug metabolizing biocatalysts (Khatri et al., 2010, 2013; Schifrin et al., 2015; Litzenburger and Bernhardt, 2016). Therefore, we used bioinformatics analysis to identify myxobacterial P450 enzymes that are closely related to drug metabolizing P450 enzymes. Among others, the two members of the CYP267 family, CYP267A1 and CYP267B1, were found to be potential candidates. Although purified CYP267A1 and CYP267B1 have been previously shown to convert certain drugs (Kern et al., 2015; Litzenburger et al., 2015) and CYP267A1 was found to catalyze the hydroxylation of fatty acids (Khatri et al., 2015), a broader analysis of their substrate spectrum has never been tested. Therefore, in this study, we have tested the in vitro and whole-cell conversion of 22 widely used drugs (Fig. 1) by CYP267A1 and CYP267B1 for the first time. Compounds showing significant in vitro conversion were further chosen for a whole-cell biotransformation to upscale the metabolite production for the structural elucidation of the product(s) via NMR spectroscopy. We demonstrate that seven out of 22 drugs can be converted by CYP267A1 and that CYP267B1 shows activity toward 14 out of 22 drugs.

Materials and Methods

Chemicals. Amitriptyline, amodiaquine, haloperidol, losartan, olanzapine, quinine, repaglinide, ritonavir, tamoxifen, and thioridazine were kindly provided by Dr. Stephan Lütz (Novartis, Basel, Switzerland). Isopropyl-β-D-1-thiogalactopyranoside and δ-aminolevulinic acid were purchased from Carbolution Chemicals (Saarbruecken, Germany). Bacterial media were purchased from Becton Dickinson (Heidelberg, Germany). All other chemicals were obtained from standard sources at the highest purity available.

Strains. The *E. coli* strains Top 10 and NovaBlue Singles Competent Cells for cloning purpose were obtained from Invitrogen (San Diego, CA) and Merck (Duesseldorf, Germany). The *E. coli* strains BL21-Gold(DE3) for the heterologous expression of CYP267A1 and C43(DE3) for the heterologous expression of CYP267B1 were purchased from Agilent Technologies (Santa Clara, CA), whereby C43(DE3) was also used for whole-cell conversions.

Plasmids. The genes of CYP267A1 and CYP267B1 were cloned into a pET22b plasmid (Novagen, Darmstadt, Germany) as described elsewhere (Litzenburger et al., 2015). The pKKHC plasmids for the heterologous expression of the autologous redox partners ferredoxin 8 (Fdx8) and ferredoxin-NADP$^+$ reductase B (FdR_B) originate from previous work done in our laboratory (Ewen et al., 2009).

For the expression of the redox partners in the whole-cell system, the pCDF_dFA plasmid from Litzenburger et al. (2015) was used and changed as follows. The gene encoding ferredoxin NADP$^+$ reductase (Fpr) was excised using the restriction enzymes NdeI and KpnI and substituted with the FdR_B gene obtained from pKKHC_FdR_B using the same restriction enzymes. The ligation reactions were performed with the Fast-Link DNA Ligase Kit (Biozym Scientific GmbH, Hessisch Oldendorf, Germany). From the resulting plasmid pCDF_AFB containing the truncated adrenodoxin (Adx_{4-108}) from *Bos taurus* and ferredoxin-NADP$^+$ reductase FdR_B from *S. cellulosum* So ce56, the gene of Adx_{4-108} was excised with NcoI and HindIII. The resulting open plasmid was ligated with the gene of Fdx8 previously obtained from pKKHC_Fdx8 using the mentioned restriction enzymes. The resulting plasmid pCDF_F8B contains the genes for expressing the autologous Fdx8 and FdR_B from *S. cellulosum* So ce56 (see also Supplemental Fig. 1).

Expression and Purification. CYP267A1 and CYP267B1 have been expressed and purified as previously described (Khatri et al., 2015) using the T7 promoter–based expression construct of CYP267A1 and CYP267B1 (pET22b_CYP267A1 and pET22b_CYP267B1). The electron transfer partners Fdx8 and FdR_B were expressed and purified as noted elsewhere (Ewen et al., 2009).

Media and Buffers. For the heterologous expression of CYP267A1 and CYP267B1, terrific broth medium (24 g yeast extract, 12 g peptone, 4 ml glycerol, 2.31 g K_2HPO_4, and 12.54 g KH_2PO_4 per liter H_2O) was used. The whole-cell conversions were performed in M9CA medium (6 g Na_2HPO_4, 3 g KH_2PO_4, 0.5 g NaCl, 1 g NH_4Cl, 4 g Bacto Casamino Acids (BD Diagnostics, Sparks, NV), 4 g glucose, 50 μl 1M $CaCl_2$, 2 ml 1 M $MgSO_4$, 2 ml of trace elements solution per liter H_2O; trace elements solution contained 2.5 g EDTA, 250 mg $FeSO_4$, 25 mg $ZnCl_2$, and 5 mg $CuSO_4$ per 50 ml H_2O).

Spectral Characterization of the CYP267 Family. UV-visible spectra for the purified P450 enzymes were recorded at room temperature on a double-beam spectrophotometer (UV-2101PC, Shimadzu, Kyoto, Japan). The enzyme solution (2 μM) in 10 mM potassium phosphate buffer, pH 7.4, was dosed with a few grains of sodium dithionite to reduce the heme-iron and the sample was split into two cuvettes. The baseline was recorded between 400 and 700 nm. The sample cuvette was bubbled gently with carbon monoxide (CO) for 1 minute and a spectrum was recorded. The concentration of the P450 enzymes was estimated by CO-difference spectroscopy assuming molar extinction coefficient ε (450–490 nm) = 91 $mM^{-1}cm^{-1}$ according to the method of Omura and Sato (1964).

In Vitro Conversions. A reconstituted in vitro system containing the corresponding P450 (0.5 μM), FdR_B (1.5 μM), and Fdx8 (10 μM), and a cofactor regenerating system with glucose-6-phosphate (5 mM) and glucose-6-phosphate dehydrogenase (2 U/ml) in potassium phosphate buffer (20 mM, pH 7.4, 1% glycerin) was used. The potential substrates, except olanzapine and omeprazole (both dissolved in dimethylsulfoxide), were dissolved in ethanol (10 mM) and added to an end concentration of 200 μM. The total volume of the reaction was 250 μl. The reaction was started by the addition of NADPH (800 μM) and carried out for 3 hours at 30°C. For substrates 1, 9, 11–15, and 18–21, 1 M glycine buffer (pH 11) or acetate buffer (pH 4) was added after reaction to enable improved recovery of the analytes. Therefore, the reaction was stopped by adding buffer (300 μl) or organic solvent (500 μl). The extraction was performed twice with 500 μl of the appropriate solvent (see (Supplemental Table 0). A negative control without P450 was implemented for each substrate to verify the P450-dependent reaction.

Whole-Cell Conversions. The experiments were performed with C43(DE3) cells, which were transformed with two plasmids, one encoding CYP267A1 (pET22b_CYP267A1) or CYP267B1 (pET22b_CYP267B1) and the second one encoding the redox partners Fdx8 and FdR_B (pCDF_F8B). For the main culture, 50 ml M9CA medium containing ampicillin (100 μg/ml) and streptomycin (50 μg/ml), inoculated with the corresponding overnight culture in lysogeny broth medium (dilution 1:100), was used. At an optical density of 0.9–1, the induction was initiated by adding 1 mM isopropyl β-D-1-thiogalactopyranoside and 0.5 mM 5-aminolevulinic acid and the temperature was set to 28°C. After 21 hours of expression, the temperature was set to 30°C and the substrate was added to a final concentration of 200 μM. To enable higher substrate conversion, EDTA (20 mM) or polymyxin B (32 μg/l) was added to increase permeability and substrate uptake of the *E. coli* cells (Janocha and Bernhardt, 2013). After 48 hours at 30°C, a 500 μl sample was removed, quenched by adding buffer or organic solvent, and extracted two times with 500 μl of organic solvent (see Supplemental Table 0). The organic phases were collected and evaporated to dryness. The extracts were stored at −20°C until analysis. All experiments were done twice, including a negative control (cells only transformed with pCDF_F8B).

Analysis of the In Vitro and Whole-Cell Conversions via High-Performance Liquid Chromatography (HPLC). The HPLC analysis was performed on a Jasco (Gross-Umstadt, Germany) HPLC 2000 system consisting of a PU-2080 Plus Pump, a AS-2050 Plus Sampler and a UV-2075 Plus UV/Vis-Detector. For the HPLC analysis, samples of substrates 3, 10, 13, and 22 were dissolved in 75 μl acetonitrile and 75 μl Milli-Q water. The remaining substrates were dissolved in the same volumes of solvents containing 0.1% trifluoroacetic acid. Analyses were performed on a reversed-phase column (125/4 Nucleodur

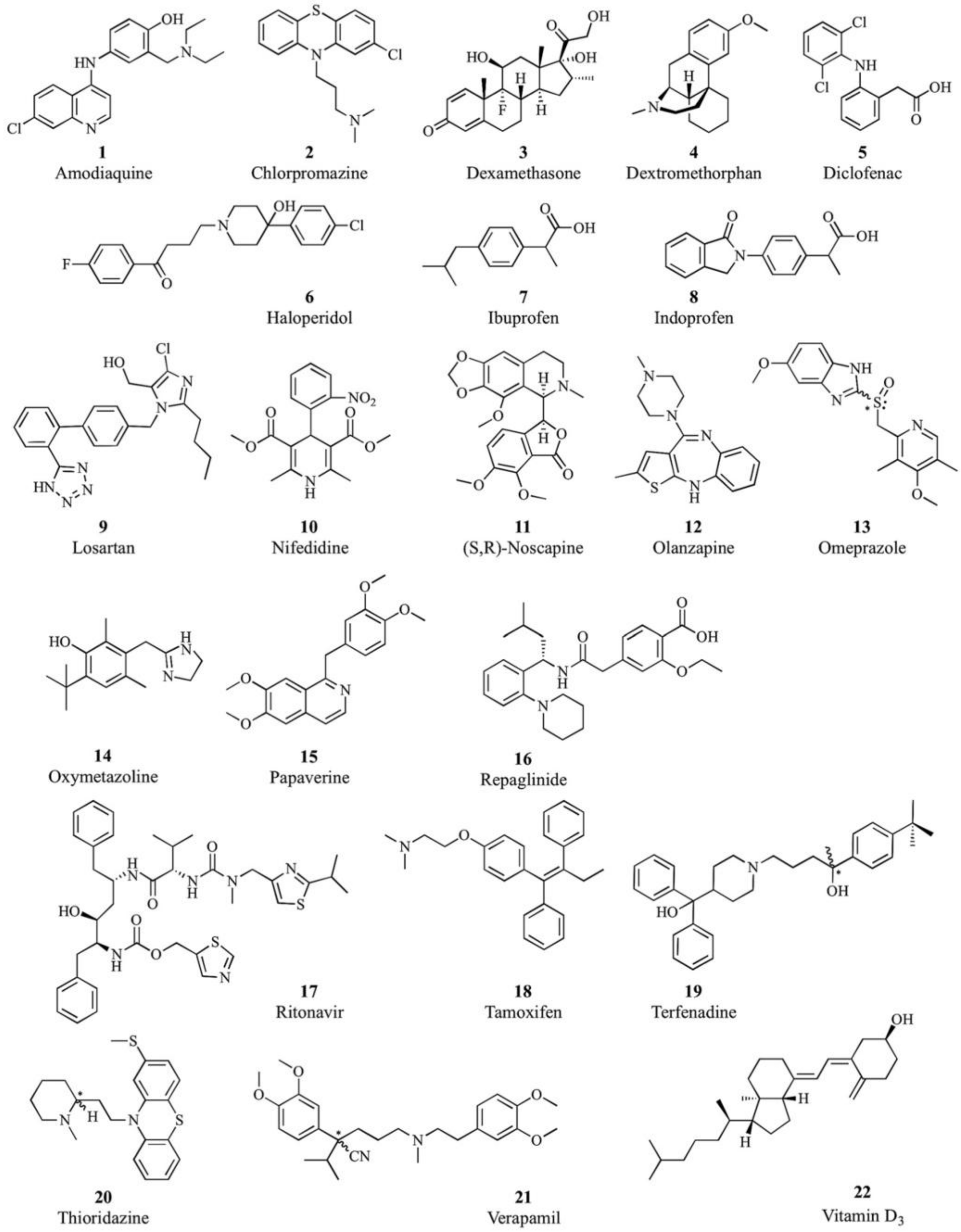

Fig. 1. Structural illustration of the tested drugs. In the case of drugs 13, 19, 20, and 21, racemic mixtures were used in all experiments.

100-5 C18ec; Macherey Nagel, Düren, Germany) at a flow rate of 1 ml/min and a temperature of 40°C. The injection volume was set to 30 μl. Due to the amount of different substrates the HPLC methods (including detection wavelengths) were substrate dependent and are presented in the Supplemental Material (Supplemental Table 1).

Upscaling of the Whole-Cell Biotransformation System and Purification of the Products. To obtain sufficient amounts of products for structure elucidation via NMR analysis, the previously described whole-cell conversions were up-scaled to a total volume of 2.5 l. After 48 hours, the reaction was stopped with the same volume of the appropriate solvent (see Supplemental Table 0). Before extraction of the product of substrate 13, the culture was set to a pH of 11 using 2 M KOH and subsequently purified as described previously (Litzenburger et al., 2015). The purification of product 13a was done in the absence of trifluoroacetic acid.

NMR Analysis. The structures of the products were analyzed by NMR spectroscopy (Institute for Pharmaceutical Biology, Saarland University). The ^{1}H- and ^{13}C-NMR were recorded on a Bruker (Rheinstetten, Germany) 500 MHz NMR spectrometer. Two-dimensional NMR spectra were recorded as gs-H, H-COSY, gs-HSQC, and gs-HMBC. All chemical shifts are relative to $CDCl_3$ (δ = 77.00 for ^{13}C-NMR; δ = 7.24 for ^{1}H-NMR) or CD_3OD (δ = 49.00 for ^{13}C-NMR; δ = 3.31 for ^{1}H-NMR) using the standard δ notion in parts per million.

Tandem Mass Spectrometry (MS/MS) Analysis. Product 13a was additionally characterized by MS/MS analysis (Institute of Bioanalytical Chemistry, Saarland University) with a API 2000 Qtrap (ABSciex, Darmstadt, Germany). Detailed settings of the MS/MS experiments can be found in section 8 (MS/MS settings) of the Supplemental Material.

Results

Bioinformatics Studies and Comparison of CYP267A1 with CYP267B1

To identify homologs of potentially drug metabolizing P450 enzymes from *S. cellulosum* So ce56, all of the 21 P450 enzymes (Khatri et al., 2010) from this bacterium were aligned with the known bacterial drug metabolizing P450 enzymes (Supplemental Table 2). We observed that the CYP265A1, CYP266A1, and the CYP267 family of this bacterium clustered within the same clan of the drug metabolizing P450 enzymes such as CYP107E4 from *Actinoplanes* sp. ATCC 53771 and CYP105 and CYP256 from *Rhodococcus jostii* RHA1, showing amino acid sequence identities of 38.9%, 34.2%, and 33.4%, respectively (Fig. 2; Supplemental Table 2). These bacterial P450 enzymes are considered to be active drug metabolizers for several drugs including amitriptyline, chlorpromazine (2), and diclofenac (5) (Prior et al., 2010; Kulig et al., 2015). In addition, we have previously shown that CYP264A1 was able to convert tricyclic drug molecules (Litzenburger et al., 2015), and CYP265A1 and CYP266A1 were able to hydroxylate the antitumor drug epothilone D (Kern et al., 2015). As a result, our homology study with the drug metabolizing bacterial P450 enzymes suggested that the two members of the CYP267 family (in addition to CYP265A1 and CYP266A1) are potential candidates for metabolizing certain drugs. The amino acid sequence alignment of CYP267A1 and CYP267B1 showed an identity of 38%. CYP267B1 possesses a conserved heme-binding domain ($_{347}$**F**GG**G**IHF**CLG**$_{356}$), the conserved threonine in the I-helix ($_{243}$AGHE**TT**$_{248}$), and glutamic acid and arginine in the K-helix ($_{281}$**E**EAL**R**$_{285}$), whereas in CYP267A1 the conserved phenylalanine in the heme-domain is replaced by leucine (L366) (Khatri et al., 2015). Amino acid sequence alignment of the CYP267 family with human P450 enzymes demonstrated that CYP267B1 showed the highest identities of 20.7%, 20.2%, 19.6%, 19.3%, and 19.0% with CYP2W1, CYP2C8, CYP2A6, CYP2D6, and CYP3A4, respectively (Supplemental Table 2), which are considered to be efficient drug metabolizers (Wrighton and Stevens, 1992; Guengerich, 1999).

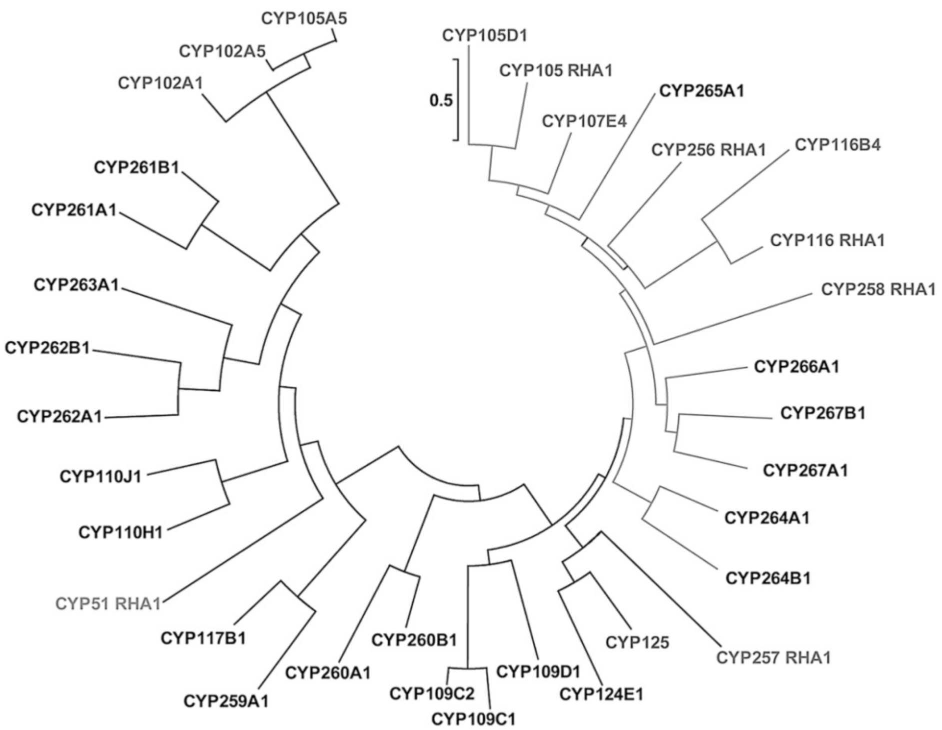

Fig. 2. The radial view of an unrooted phylogenetic tree obtained by MEGA4 (version 4.0, (Tamura 2007)) analysis for the determination of relatedness of the 21 P450 enzymes from *S. cellulosum* So ce56 (in black) with respect to drug metabolizing bacterial P450 enzymes CYP105D1 (P26911.1) from *Streptomyces griseus*; CYP51_RHA1 (Q0S7M9), CYP105_RHA1 (Q0SDH7), CYP116_RHA1 (Q0RUR9), CYP125_RHA1 (Q0S7N3), CYP256_RHA1 (Q0RXF8), and CYP257_RHA1 (Q0RVH0) from *Rhodococcus jostii* RHA1; CYP107E4 (ACN71221.1) from *Actinoplanes* sp. ATCC 53771; and CYP116B4 (EAV41564.1) from *Labrenzia aggregate* (in gray). The cluster of drug metabolizing P450 enzymes is shown in the gray clan. The bar in the tree indicates 0.5 amino acid substitutions per amino acid for the branch length.

Expression, Purification, and Characterization of the CYP267 Family Members

First expression studies for CYP267B1 were realized using the vector pCWori+. However, the yield of CYP267B1 using the pCWori+-based expression construct was very low (<20 nmol/l *E. coli* culture after purification). Therefore, the protein has been expressed and purified using a T7-based expression construct (pET22b_CYP267B1) (Litzenburger et al., 2015), in which the protein yield was increased 5-fold (100 nmol/l).

As shown in Fig. 3, the UV-visible absorption spectrum of the oxidized CYP267B1 showed the presence of the Soret band (γ) at 416 nm, and the *Q*-bands at 567 nm (β) and 533 nm (α). The reduction of CYP267B1 with sodium dithionite showed a slightly diminished absorption peak for the Soret band at 410 nm and a single peak in the *Q*-region (538 nm). The reduced CO-complex of CYP267B1 showed a typical peak maximum at 449 nm. The purified CYP267A1 showed the same spectroscopic features as previously described (Khatri et al., 2015), with the characteristic peak maximum at 448 nm in the CO-difference spectroscopy experiment and a peak maximum at 418 nm in the oxidized form of CYP267A1.

Optimization of the In Vitro Conversion

Since P450 enzymes are monooxygenases, they require electrons from NADPH, which are transferred by autologous or heterologous redox partners (Hannemann et al., 2007). The substrate turnover also depends on the coupling and the efficiency of the redox partner proteins. In the case of the CYP267 family we observed limited in vitro conversions (Kern et al., 2015; Litzenburger et al., 2015) when using the bovine redox partners Adx_{4-108}/adrenodoxin NADP+ reductase (AdR). Therefore, we substituted the heterologous Adx_{4-108} and AdR with the autologous redox partners Fdx8 and FdR_B from *S. cellulosum* So ce56, which were previously shown to increase the CYP267B1-dependent epothilone D conversion (Kern et al., 2015). In our previous studies on the conversion of tricyclic antipsychotics and antidepressants (Litzenburger et al., 2015), thioridazine (20) could be identified as a substrate for CYP267A1 and amitriptyline as well as chlorpromazine (2) for CYP267B1, respectively; however, with low in vitro and whole-cell conversion. The substitution of Adx_{4-108}/AdR with the autologous redox partners Fdx8/FdR_B showed increased thioridazine-5-sulfoxide (20a) formation (from 43% to 50%) during the in vitro conversion of substrate 20. Likewise, the in vitro conversion of amitriptyline by CYP267B1 showed a significant enhancement of 10-hydroxyamitriptyline formation (from 15% to 60%), whereas the in vitro conversion of chlorpromazine (2) showed no difference.

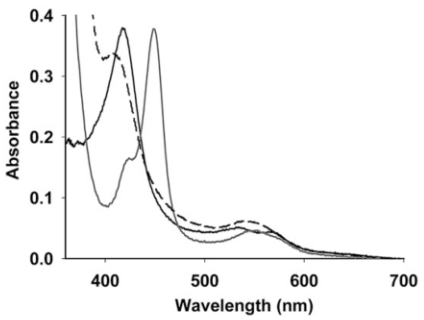

Fig. 3. Spectroscopic characterization of CYP267B1. The UV-visible spectra of oxidized (black line), dithionite reduced (dashed line), and CO-bound (gray line) CYP267B1 were recorded in 10 mM potassium phosphate buffer, pH 7.5.

Optimization of the *E. coli*–Based Whole-Cell Bioconversion System

Since we observed a significant increase in the product formation when using the autologous redox partners, we investigated the coexpression of the autologous redox partners Fdx8 and FdR_B for our whole-cell bioconversion experiments. For comparison, a whole-cell system coexpressing Adx_{4-108} and Fpr was used, since it has been shown previously that the whole-cell conversion of 4-methyl-3-phenyl-coumarin by CYP264A1 from *S. cellulosum* So ce56 increased when Fpr instead of AdR was used (Ringle et al., 2013). However, when substituting Adx_{4-108}/Fpr with the autologous redox partners Fdx8/FdR_B, the yield of the product was even further increased. In the case of CYP267A1, a nine times higher conversion of substrate 20 was observed (from 5% to 45% thioridazine-5-sulfoxide 20a) (Table 1). Likewise, the formation of chlorpromazine sulfoxide (2a) was nearly doubled by the CYP267B1-Fdx8-FdR_B whole-cell bioconversion system compared with CYP267B1-Adx_{4-108}-Fpr (from 18% to 30% 2a) (Table 1). In addition, we also observed a higher yield (from 7.5% to 26%) of the product 10-hydroxyamitriptyline from amitriptyline (Table 1). On the basis of these results, all further drug conversions were performed using Fdx8/FdR_B as redox partners in all in vitro and *E. coli*–based whole-cell bioconversion experiments.

When establishing a whole-cell system for P450 enzymes, indole-dependent inhibition should also be considered. The metabolism of tryptophan by the tryptophanase TnaA of *E. coli* results in the formation of indole (Li and Young, 2013). Since tryptophan is present in terrific broth medium, a concentration of over 600 μM indole was detected after 72 hours (Ringle et al., 2013). It was observed that indole acts as an inhibitor of CYP264A1 from *S. cellulosum* So ce56 (Ringle et al., 2013) and CYP109B1 from *Bacillus subtilis* (Girhard et al., 2010). In addition, some P450 enzymes are known to convert indole, and in this way competing with the normal substrate (Gillam et al., 2000). In case of the two members of the CYP267 family, the presence of 600 μM indole decreases the product formation in vitro by up to 40% for CYP267B1 and by up to 85% in the case of CYP267A1 (Supplemental Fig. 3). Therefore, we performed the whole-cell bioconversions in a defined M9CA minimal medium, which was previously shown to exhibit a very low amount of indole when using *E. coli* as a host (<5 μM) (Ringle et al., 2013).

Furthermore, the effect of the additives EDTA and polymyxin B was also investigated during the whole-cell conversions, since it has been shown previously that the presence of EDTA or polymyxin B enhances substrate uptake of *E. coli* cells for resin acid diterpenoid conversion by a CYP105A1-based whole-cell biocatalyst (Janocha and Bernhardt, 2013). We observed that the highest product formation was obtained when 20 mM EDTA for substrates 1, 2, 5, 7, 9, 15, and 16, and 32 $\mu g\ ml^{-1}$ polymyxin B for substrates 11, 13, 18, 19, and 20 were applied in the whole-cell system. Higher concentrations of both additives did not alter the product pattern for the tested drugs.

Optimization of Product Extraction and HPLC Conditions for the Investigation of Drug Conversions

Due to the diverse chemical structures and functional groups of the tested drug molecules, we established a substrate-dependent extraction protocol to improve our experimental conditions for efficient analyses and product purification (Supplemental Table 0). We also optimized the HPLC conditions as listed in the Supplemental Table 1.

CYP267-Dependent Substrate Conversion

In Vitro and Whole-Cell Conversions by CYP267A1. The in vitro conversions revealed that seven out of 22 drugs were converted by CYP267A1. In comparison with CYP267B1, the product pattern of

TABLE 1

Comparison of the whole-cell conversions with CYP267A1 and CYP267B1 using different redox partners

Model Substrate	CYP267	Conversion with heterologous Adx_{4-108}/Fpr[a]	Conversion with autologous Fdx8/FdR_B	Product
		%	%	
Amitriptyline	B1	7.5	26	10-Hydroxyamitriptyline[a]
Chlorpromazine (2)	B1	18	30	Chlorpromazine sulfoxide[a] (2a)
Thioridazine (20)	A1	5	45	Thioridazine-5-sulfoxide[a] (20a)

[a]Taken from Litzenburger et al. (2015).

CYP267A1 differs only for chlorpromazine (2; 2.4%) for which one single product was observed. For ibuprofen (7), tamoxifen (18), and terfenadine (19) the yields of the product formation were significantly lower compared with the respective CYP267B1-dependent conversions (7: 1.5%, 18: 3.7%, and 19: 2.1%). Despite having lower conversions with CYP267A1, five new substrates for CYP267A1 were identified (4, 6, 7, 18, and 19) (Fig. 4A). However, during in vitro conversion of substrates 18 and 20, one side product has been observed for substrate 18 (1.9% ± 1.1%) and in the case of substrate 20 two minor side products (3.7% ± 0.3% and 2.6% ± 0.1%) were found.

Only dextromethorphan (4), haloperidol (6), and thioridazine (20) were further employed for the investigation in the whole-cell system with CYP267A1-Fdx8-FdR_B, in which compounds 4 and 6 showed no conversion. Due to the higher in vitro conversion of substrates 2, 18, and 19 with CYP267B1, these substrates were only tested in the CYP267B1-Fdx8-FdR_B whole-cell system. However, using CYP267A1, substrate 20 was successfully converted to product 20a yielding a 44.7% product formation in our *E. coli*–based whole-cell bioconversion (Fig. 4A).

In Vitro and Whole-Cell Conversions by CYP267B1. It is very interesting to note that the in vitro conversions of the 22 tested drugs showed that CYP267B1 was able to convert 14 out of 22 compounds (Fig. 4B), seven more than CYP267A1. The highest in vitro yield was observed for oxymetazoline (14; 77.7%) and moderate in vitro conversions were detected for chlorpromazine (2; 37%), diclofenac (5; 37.5%), ibuprofen (7; 31.1%), and repaglinide (16; 41.4%). In addition, amodiaquine (1, 10.2%), losartan (9; 8.9%), noscapine (11; 12.1%), olanzapine (12; 16.5%), omeprazole (13; 13.7%), papaverine (15; 12.6%), and tamoxifen (18; 15%) were converted by CYP267B1. Very low conversion was observed for ritonavir (17; 1.4%) and terfenadine (19; 4.1%). However, during the in vitro experiments, also one minor side product was observed for substrates 7 (2.2% ± 0.1%), 9 (1.9% ± 0.4%), 11 (1.85% ± 0.45%), 12 (2% ± 0.1%), 13 (7% ± 0.4%), 15 (2.2% ± 0.1%), 16 (7.8% ± 1.4%), and 18 (2.55% ± 0.45%). In the case of substrate 14, two minor side products were found (5.1% ± 1.0% and 3% ± 0.5%).

The 14 drugs identified as substrates for CYP267B1 during the in vitro experiments were further investigated in the corresponding whole-cell experiments, where the highest yield was observed for omeprazole (13; 78.1%). The compounds 2 (30.3%), 5 (38%), and 7 (44.1%) showed similar yields compared with the corresponding in vitro experiments. We also observed a high conversion of losartan (9) to one product; however, without expressing CYP267B1 in the whole-cell experiment. This observation leads to the assumption that substrate 9 might have been oxidized by *E. coli* C43(DE3) to losartan carboxy acid. Due to the limited availability of a reference standard, we were not able to further investigate this assumption. The CYP267B1-Fdx8-FdR_B whole-cell system was also able to convert substrates 1, 11, 15, 16, 18, and 19, but in lower yields (≤10%). In the CYP267B1-dependent whole-cell experiments, minor side products were only formed in the case of substrates 11 (1.25% ± 0.15%), 13 (5.3% ± 0.2%), 15 (5.4% ± 0.5%), and 16 (5.2% ± 0.4%), showing identical retention time to those

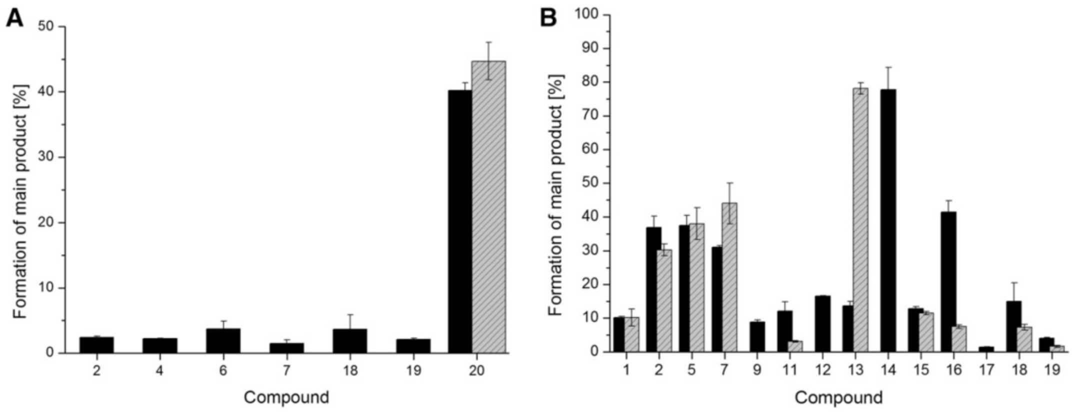

Fig. 4. The main metabolite formation in vitro (black bar) and in the whole-cell (gray bar) system by CYP267A1-Fdx8-FdR_B (A) and CYP267B1-Fdx8-FdR_B (B). (A) The compounds 1, 3, 5, 8–17, 21, and 22 were not converted by CYP267A1 and are therefore not shown. Only the substrates 4, 6, and 20 were further tested in the whole-cell system, whereby compounds 4 and 6 showed no conversion. The highest whole-cell conversion for substrate 20 was achieved with the supplement of polymyxin B (32 μg/ml). (B) The highest yields for the whole-cell conversions of compounds 1, 2, 5, 7, 9, 15, and 16 by CYP267B1 were achieved in the presence of 20 mM EDTA. In the case of compounds 11, 13, 18, and 19, the highest conversions were observed with the addition of polymyxin B (32 μg/ml). Despite the in vitro conversions of compounds 12 and 14 by CYP267B1, no conversion was observed in the corresponding whole-cell experiments. Due to the absence of conversion in the in vitro experiments, compounds 3, 4, 6, 8, 10, and 20–22 are not presented in this diagram.

observed in the corresponding in vitro experiments. For compounds 12 and 14, all attempts to utilize them in the whole-cell conversion system were unsuccessful, despite having high in vitro conversions (16.5% for compound 12 and 83% for compound 14). For the substrates that were not converted (3, 4, 6, 8, 10, 20, 21, and 22) or showed poor conversion (17) during the in vitro assay, attempts of investigating these drugs within the whole-cell system were discarded. Due to the high conversion in the whole-cell experiments, compounds 2, 5, 7, and 13 were further chosen for upscale and product characterization.

Production of Drug Metabolites Using an *E. coli*–Based Whole-Cell Bioconversion System and Purification of Products via Preparative HPLC

The whole-cell system of CYP267B1-Fdx8-FdR_B was up-scaled to 2.5 l of M9CA medium for substrates 2, 5, and 7. For compound 13, an upscaling to 500 ml was sufficient enough to produce 5 mg of product 13a. In the case of whole-cell system CYP267A1-Fdx8-FdR_B and substrate 20, the conversion was also up-scaled to 2.5 l M9CA medium. For the compounds converted in a larger scale, comparable yields as previously described (Fig. 4, A and B) were observed, revealing the great potential of the established bioconversion system for future biotechnological upscaling. The products were purified via preparative HPLC and the purity of the isolated products was further verified by an additional HPLC measurement. The chromatograms of the purified products (5a, 7a, and 13a) and the pure substrates (5, 7, and 13) are shown in the Supplemental Material (Supplemental Fig. 2), confirming the high purity of the corresponding products. For products 2a and 20a, the chromatograms coincide with previous data and can be found in the Supplemental Material (Litzenburger et al., 2015).

Drug Metabolites Formed by the CYP267 Family

As previously presented, CYP267A1 is able to convert seven out of 22 drugs and CYP267B1 catalyzes the conversion of 14 out of 22 drugs in vitro. However, only drug 20 for CYP267A1 and 10 drugs (1, 2, 5, 7, 11, 12, 15, 16, 18, and 19) for CYP267B1 were successfully converted in our whole-cell system. For drugs 2, 5, 7, 13, and 20 showing high yields after whole-cell biotransformation, the respective metabolites were additionally elucidated with an up-scaled production and via NMR measurements. A comprehensive overview of the analyzed drugs, and the human metabolites produced by the two members of the CYP267 family, is presented in (Supplemental Fig. 6). CYP267B1 is able to catalyze an aromatic hydroxylation of drug 5 to the human metabolite 4′-hydroxydiclofenac (5a) and an aliphatic hydroxylation of drug 7 to 2-hydroxyibuprofen (2a). Furthermore, the sulfoxidation of drugs 2 and 13 is catalyzed by CYP267B1 and the sulfoxidation of drug 20 is catalyzed by CYP267A1. All products were obtained with high purity and sufficient amounts (5–10 mg) for the structure elucidation via NMR spectroscopy. The NMR (^{1}H and ^{13}C) data for products 5a, 7a, and 13a are shown in the (Supplemental Material). In the case of product 13a, an additional MS/MS measurement provided an unambiguous assignment to omeprazole sulfone (Supplemental Fig. 5). The NMR data of products 2a and 20a were identical to those previously described (Litzenburger et al., 2015) and match the corresponding reference standards (Zhang et al., 1996; Morrow et al., 2005). However, we achieved significantly increased yields in this study by our new whole-cell constructs (see Supplemental Fig. 1), which also gave better access to high product amounts for characterization of the respective products.

Discussion

In recent years, the number of publications about the potential applications of P450 enzymes for the production of drug or drug-related compounds of pharmaceutical interest has continuously grown (Julsing et al., 2008). This progress can directly be of use for efficient and time-saving production of human drug metabolites. High yields and conversion rates can already be achieved by using corresponding human (Rushmore et al., 2000; Vail et al., 2005; Schroer et al., 2010; Geier et al., 2012; Schiffer et al., 2015) or suitable nonhuman (Taylor et al., 1999; Otey et al., 2006; Sawayama et al., 2009; Reinen et al., 2011; Di Nardo and Gilardi, 2012; Kiss et al., 2015; Ren et al., 2015) P450 enzymes in a whole-cell system to produce respective metabolites. The majority of published bacterial P450 enzymes used for the conversion of drugs are mutants of CYP102A1 (BM3) from *Bacillus megaterium*. We investigated the native myxobacterial P450 enzymes from *S. cellulosum* So ce56 for their application as drug metabolizers since soil bacteria should be able to convert and metabolize different xenobiotics present in their environment. Therefore, special attention was given to the CYP267 family.

It is interesting to note that CYP267B1 revealed the remarkable ability to accept substrates with completely different chemical structures and functions. In addition to the capability of converting tricyclic compounds (Litzenburger et al., 2015), the large 16-membered macrolide epothilone D (Kern et al., 2015), and small structures such as apocarotenoids (Litzenburger and Bernhardt, 2016), CYP267B1 also showed activity toward the conversion of 14 out of 22 different drugs. In contrast, CYP267A1 was only able to convert seven out of 22 drugs. The drugs converted by CYP267A1 and CYP267B1 feature a variety of chemical structures such as heterocyclic aromatics, morphinan class compounds, and alkaloids, thus increasing both the known substrate spectrum for this P450 family and the conceivable fields of their application. The metabolism of a drug molecule by a human P450 usually results in the formation of several side products (Table 2) since the main aspect of drug metabolism is excretion out of the body. Hence, the application of myxobacterial P450 enzymes is favorable in enabling the production of a single human drug metabolite, highlighting their ability for biotechnological processes to produce a metabolite in large quantity.

However, an important bottleneck in the application of P450 enzymes in biotechnological processes is often the efficiency of the redox system (Bernhardt and Urlacher, 2014). Therefore, we first identified efficient autologous redox partners to transfer electrons to the CYP267 family. Although the autologous redox system Fdx8/FdR_B from *S. cellulosum* So ce56 has already been shown to transfer electrons to myxobacterial CYP109D1, CYP260A1, and CYP264A1 (Khatri et al., 2010; Ringle et al., 2013), the heterologous bovine Adx_{4-108} with AdR or the *E. coli* Fpr has been shown to be more efficient (Khatri et al., 2013; Ringle et al., 2013). However, in this study, the substitution of Adx_{4-108}/Fpr by Fdx8/FdR_B showed a significant increase of product yields for drug molecules (Table 1) when using the members of the CYP267 family. As a result, an *E. coli*–based whole-cell bioconversion system has been established containing the autologous redox partners of the CYP267 family.

Another bottleneck in whole-cell conversions that we faced during our studies was substrate uptake and indole inhibition. As a result, we established a substrate-dependent protocol, where EDTA and polymyxin B, which are shown to enhance substrate uptake into *E. coli* cells (Janocha and Bernhardt, 2013), significantly increased the limited whole-cell conversions (Fig. 4, A and B). To overcome inhibition of CYP267A1 and CYP267B1 by indole (Supplemental Fig. 3), we performed the whole-cell experiments in defined M9CA medium. However, for substrates 2, 11, 14, 16, 18, and 19 the CYP267B1-dependent whole-cell conversion showed lower yields compared with the in vitro assay, which might be a limitation caused by the low permeability of the *E. coli* cells for these substrates during the whole-cell

TABLE 2

Comprehensive overview of human drug metabolites formed by the members of the CYP267 family from *S. cellulosum* So ce56 and the corresponding human P450 enzymes

Metabolites marked with # and * are selectively formed by CYP267A1 and CYP267B1, respectively. The order of the listed metabolites is not representative for the product distribution.

Drug	Human P450	Desired Metabolite	Expected Side Products of Human P450 Enzymes	Reference
Chlorpromazine (2)	CYP2D6 CYP3A4	Chlorpromazine sulfoxide (2a) *	7-Hydroxychlorpromazine Chlorpromazine-*N*-oxide	Cashman et al. (1993)
Diclofenac (5)	CYP1A2	4′-Hydroxydiclofenac (5a) *	—	Bort et al. (1999)
	CYP2C8 CYP2C18 CYP2C19		5-Hydroxydiclofenac 4,5-Dihydroxydiclofenac	
	CYP2C9		3-Hydroxydiclofenac 5-Hydroxydiclofenac	
Ibuprofen (7)	CYP2C8 CYP2C9	2-Hydroxyibuprofen (7a) *	3-Hydroxyibuprofen Carboxyibuprofen	Hamman et al. (1997); Neunzig et al. (2012)
Omeprazole (13)	CYP3A4	Omeprazole sulfone (13a) *	5-Hydroxyomeprazole	Yamazaki et al. (1997); Abelö et al. (2000)
Thioridazine (20)	CYP2D6	Thioridazine-5-sulfoxide (20a) #	*N*-desmethylthioridazine 7-Hydroxythioridazine Mesoridazine	Daniel et al. (2000)

conversion. In contrast, substrates 7 and 13 showed higher yields in the whole-cell system compared with the in vitro conversion, suggesting that the conditions established for these substrates support an efficient metabolite production with our whole-cell system.

It has been shown recently that several members of a P450 fusion library, constructed by P450 enzymes and their autologous redox system RhfRED from *R. jostii* RHA1, are able to convert five out of 48 selected drugs (Kulig et al., 2015). Compared with our system consisting of the wild-type CYP267B1 and its autologous redox partners Fdx8 and FdR_B, we observed a larger substrate range (14 out of 22 drugs) and significantly higher activity toward the conversion of drugs. This leads to the suggestion that CYP267B1 features a great potential for the biotechnological production of various drug metabolites when using bacterial P450 enzymes. Our thus far not optimized whole-cell system was able to convert 38% of 160 mg of diclofenac (5) within 48 hours, which is a good starting point for the production of 4′-hydroxydiclofenac (5a). In this regard, the production of product 5a has previously been shown using an optimized fermentation process. The recombinant expression of CYP2C9 in fission yeast strain CAD68 resulted in an efficient formation of product 5a (468 mg/l) after the optimization of the pH value, the glucose concentration, and the establishment of a favorable host organism for the hydroxylation of substrate 5 (Drăgan et al., 2011). The engineering of BM3 toward the metabolism of drugs resulted in the BM3 mutant Asp251Gly/Gln307His, capable of the metabolism of drug 5 to product 5a in vitro (Tsotsou et al., 2012). This BM3 mutant was also shown to produce 2-hydroxyibuprofen (7a) from ibuprofen (7) (Tsotsou et al., 2012); however, experiments were only done in vitro or in a microtiter plate. Likewise, the production of product 7a in a preparative in vitro scale was described yielding 74.3 mg of product 7a (96% conversion) (Rentmeister et al., 2011). However, in this study, we were able to produce product 7a in a more relevant, biotechnological way using an *E. coli*–based whole-cell bioconversion system for CYP267B1 consisting of autologous redox partners and necessary cofactors within the cells. In this regard, the conversion of 115 mg of drug 7 to product 7a giving 44% product yield by the wild-type CYP267B1 demonstrated a promising scope for further optimization since we have not yet focused on the optimization or the engineering of the respective P450 toward higher space-time yields. In addition, our CYP267B1-Fdx8-FdR_B whole-cell system also presents the first method to produce omeprazole sulfone (13a) using a biotechnological approach with a high conversion yield (nearly 80%, 68 mg/l of drug 13) and high selectivity (<5% formation of unknown side product). Although CYP3A4 is responsible for the formation of omeprazole sulfone (13a) in the human body (Yamazaki et al., 1997), to the best of our knowledge, the biotechnological production of product 13a with CYP3A4 (Table 2) or another P450 has thus far not been described.

The established CYP267-Fdx8-FdR_B whole-cell systems are an excellent starting point for further optimizations in view of biotechnological upscaling and optimization (Bernhardt and Urlacher, 2014). Optimizations such as changing expression and reaction conditions or engineering P450 enzymes could be potential topics of interest. Several approaches for increasing the performance of the whole-cell system have been published, describing that an increased number of ferredoxin gene copies (Schiffer et al., 2015) or coexpressing a NADPH regenerating system (Zehentgruber et al., 2010) could enhance product formation. In a recent review, numerous approaches and examples were presented to enhance the catalytic activity of P450 enzymes toward potential practical purposes (Gillam, 2008). It is remarkable that the wild-type CYP267B1 is already able to catalyze three different reaction types (hydroxylation, sulfoxidation, and epoxidation) without any directed or evolutionary modification. In fact, the catalyzed hydroxylation reactions can be diversified to aliphatic (in the case of drug 7), allylic (as described for sesquiterpenes) (Litzenburger and Bernhardt, 2016), and aromatic (as shown for drug 5) hydroxylations, whereby the aromatic hydroxylation has not yet been described for a myxobacterial P450 enzyme.

Although in previous studies the bioconversion of drugs and xenobiotics was performed using different strains of *Streptomyces* or *Cunninghamella* sp. (Zhang et al., 1996; Asha and Vidyavathi, 2009; Bright et al., 2011; Murphy and Sandford, 2012; Diao et al., 2013), the systems were not selective and side products were usually observed. In addition, the nonoptimized media conditions used in these approaches could also interfere with the product identification. In contrast, in this study, we established a whole-cell biocatalyst for the conversion of widely used therapeutically important drugs and xenobiotics using two bacterial P450 enzymes (CYP267A1 and CYP267B1) and we also optimized this whole-cell system to allow convenient and effective product isolation for identification by NMR and MS/MS. In this way, the substrate spectrum of the CYP267 family—and especially for CYP267B1—was extended to commercially used drugs and their associated diverse chemical structures, demonstrating the potential of myxobacterial P450 enzymes as drug metabolizers. Due to the great potential to convert a broad range of substrates, it can be concluded that CYP267B1 is an efficient and promising candidate for further substrate screening and protein engineering attempts, particularly with regard to its biotechnological applicability.

Acknowledgments

The authors thank Dr. Stephan Lütz, Novartis (Basel, Switzerland), for providing some of the substrates and Dr. Josef Zapp, Institute of Pharmaceutical Biology (Saarland University), for measuring the NMR samples. The authors also thank Tobias K. F. Dier, Institute of Bioanalytical Chemistry (Saarland University) for the MS/MS measurement of omeprazole and omeprazole sulfone.

Authorship Contributions

Participated in research design: Kern, Bernhardt.

Conducted experiments: Kern, Litzenburger, Khatri.

Performed data analysis: Kern, Litzenburger, Khatri.

Wrote or contributed to the writing of the manuscript: Kern, Khatri, Litzenburger, Bernhardt.

References

Abelö A, Andersson TB, Antonsson M, Naudot AK, Skånberg I, and Weidolf L (2000) Stereoselective metabolism of omeprazole by human cytochrome P450 enzymes. *Drug Metab Dispos* **28**:966–972.

Asha S and Vidyavathi M (2009) *Cunninghamella*—a microbial model for drug metabolism studies—a review. *Biotechnol Adv* **27**:16–29.

Bernhardt R (2006) Cytochromes P450 as versatile biocatalysts. *J Biotechnol* **124**:128–145.

Bernhardt R and Urlacher VB (2014) Cytochromes P450 as promising catalysts for biotechnological application: chances and limitations. *Appl Microbiol Biotechnol* **98**:6185–6203.

Bort R, Macé K, Boobis A, Gómez-Lechón MJ, Pfeifer A, and Castell J (1999) Hepatic metabolism of diclofenac: role of human CYP in the minor oxidative pathways. *Biochem Pharmacol* **58**:787–796.

Bright TV, Clark BR, O'Brien E, and Murphy CD (2011) Bacterial production of hydroxylated and amidated metabolites of flurbiprofen. *J Mol Catal, B Enzym* **72**:116–121.

Cashman JR, Yang Z, Yang L, and Wrighton SA (1993) Stereo- and regioselective N- and S-oxidation of tertiary amines and sulfides in the presence of adult human liver microsomes. *Drug Metab Dispos* **21**:492–501.

Daniel WA, Syrek M, Haduch A, and Wójcikowski J (2000) Pharmacokinetics and metabolism of thioridazine during co-administration of tricyclic antidepressants. *Br J Pharmacol* **131**:287–295.

Diao X, Deng P, Xie C, Li X, Zhong D, Zhang Y, and Chen X (2013) Metabolism and pharmacokinetics of 3-*n*-butylphthalide (NBP) in humans: the role of cytochrome P450s and alcohol dehydrogenase in biotransformation. *Drug Metab Dispos* **41**:430–444.

Di Nardo G and Gilardi G (2012) Optimization of the bacterial cytochrome P450 BM3 system for the production of human drug metabolites. *Int J Mol Sci* **13**:15901–15924.

Drăgan CA, Peters FT, Bour P, Schwaninger AE, Schaan SM, Neunzig I, Widjaja M, Zapp J, Kraemer T, and Maurer HH, et al. (2011) Convenient gram-scale metabolite synthesis by engineered fission yeast strains expressing functional human P450 systems. *Appl Biochem Biotechnol* **163**:965–980.

Drews J (2000) Drug discovery: a historical perspective. *Science* **287**:1960–1964.

Ewen KM, Hannemann F, Khatri Y, Perlova O, Kappl R, Krug D, Hüttermann J, Müller R, and Bernhardt R (2009) Genome mining in *Sorangium cellulosum* So ce56: identification and characterization of the homologous electron transfer proteins of a myxobacterial cytochrome P450. *J Biol Chem* **284**:28590–28598.

Food and Drug Administration (2008) *Guidance for Industry Safety Testing of Drug Metabolites*, U.S. Department of Health and Human Services, Food and Drug Administration, Rockville, MD.

Gao R, Li L, Xie C, Diao X, Zhong D, and Chen X (2012) Metabolism and pharmacokinetics of morinidazole in humans: identification of diastereoisomeric morpholine N^{+}-glucuronides catalyzed by UDP glucuronosyltransferase 1A9. *Drug Metab Dispos* **40**:556–567.

Geier M, Bachler T, Hanlon SP, Eggimann FK, Kittelmann M, Weber H, Lütz S, Wirz B, and Winkler M (2015) Human FMO2-based microbial whole-cell catalysts for drug metabolite synthesis. *Microb Cell Fact* **14**:82.

Geier M, Braun A, Emmerstorfer A, Pichler H, and Glieder A (2012) Production of human cytochrome P450 2D6 drug metabolites with recombinant microbes—a comparative study. *Biotechnol J* **7**:1346–1358.

Gillam EMJ (2008) Engineering cytochrome P450 enzymes. *Chem Res Toxicol* **21**:220–231.

Gillam EMJ, Notley LM, Cai H, De Voss JJ, and Guengerich FP (2000) Oxidation of indole by cytochrome P450 enzymes. *Biochemistry* **39**:13817–13824.

Girhard M, Klaus T, Khatri Y, Bernhardt R, and Urlacher VB (2010) Characterization of the versatile monooxygenase CYP109B1 from *Bacillus subtilis*. *Appl Microbiol Biotechnol* **87**:595–607.

Guengerich FP (1999) Cytochrome P-450 3A4: regulation and role in drug metabolism. *Annu Rev Pharmacol Toxicol* **39**:1–17.

Hamman MA, Thompson GA, and Hall SD (1997) Regioselective and stereoselective metabolism of ibuprofen by human cytochrome P450 2C. *Biochem Pharmacol* **54**:33–41.

Hannemann F, Bichet A, Ewen KM, and Bernhardt R (2007) Cytochrome P450 systems—biological variations of electron transport chains. *Biochim Biophys Acta* **1770**:330–344.

International Conference on Harmonization (2009) *Guidance of Nonclinical Safety Studies for the Conduct of Human Clinical Trials and Marketing Authorization for Pharmaceuticals M3 (R2)*, European Medicines Agency, London.

International Conference on Harmonization (2012) *ICH Guideline M3 (R2)—Questions and Answers*, European Medicines Agency, London.

Janocha S and Bernhardt R (2013) Design and characterization of an efficient CYP105A1-based whole-cell biocatalyst for the conversion of resin acid diterpenoids in permeabilized *Escherichia coli*. *Appl Microbiol Biotechnol* **97**:7639–7649.

Julsing MK, Cornelissen S, Bühler B, and Schmid A (2008) Heme-iron oxygenases: powerful industrial biocatalysts? *Curr Opin Chem Biol* **12**:177–186.

Kern F, Dier TKF, Khatri Y, Ewen KM, Jacquot JP, Volmer DA, and Bernhardt R (2015) Highly efficient CYP167A1 (EpoK) dependent epothilone B formation and production of 7-ketone epothilone D as a new epothilone derivative. *Sci Rep* **5**:14881.

Khatri Y, Hannemann F, Ewen KM, Pistorius D, Perlova O, Kagawa N, Brachmann AO, Müller R, and Bernhardt R (2010) The CYPome of *Sorangium cellulosum* So ce56 and identification of CYP109D1 as a new fatty acid hydroxylase. *Chem Biol* **17**:1295–1305.

Khatri Y, Hannemann F, Girhard M, Kappl R, Hutter M, Urlacher VB, and Bernhardt R (2015) A natural heme-signature variant of CYP267A1 from *Sorangium cellulosum* So ce56 executes diverse ω-hydroxylation. *FEBS J* **282**:74–88.

Khatri Y, Hannemann F, Girhard M, Kappl R, Même A, Ringle M, Janocha S, Leize-Wagner E, Urlacher VB, and Bernhardt R (2013) Novel family members of CYP109 from *Sorangium cellulosum* So ce56 exhibit characteristic biochemical and biophysical properties. *Biotechnol Appl Biochem* **60**:18–29.

Kiss FM, Lundemo MT, Zapp J, Woodley JM, and Bernhardt R (2015) Process development for the production of 15β-hydroxycyproterone acetate using *Bacillus megaterium* expressing CYP106A2 as whole-cell biocatalyst. *Microb Cell Fact* **14**:1–13.

Kulig JK, Spandolf C, Hyde R, Ruzzini AC, Eltis LD, Grönberg G, Hayes MA, and Grogan G (2015) A P450 fusion library of heme domains from *Rhodococcus jostii* RHA1 and its evaluation for the biotransformation of drug molecules. *Bioorg Med Chem* **23**:5603–5609.

Li G and Young KD (2013) Indole production by the tryptophanase TnaA in *Escherichia coli* is determined by the amount of exogenous tryptophan. *Microbiology* **159**:402–410.

Litzenburger M and Bernhardt R (2016) Selective oxidation of carotenoid-derived aroma compounds by CYP260B1 and CYP267B1 from *Sorangium cellulosum* So ce56. *Appl Microbiol Biotechnol* DOI:10.1007/s00253-015-7269-7 [published ahead of print].

Litzenburger M, Kern F, Khatri Y, and Bernhardt R (2015) Conversions of tricyclic antidepressants and antipsychotics with selected P450s from *Sorangium cellulosum* So ce56. *Drug Metab Dispos* **43**:392–399.

Morrow RJ, Millership JS, and Collier PS (2005) Facile syntheses of the three major metabolites of thioridazine. *Helv Chim Acta* **88**:962–967.

Murphy CD and Sandford G (2012) Fluorinated drug metabolism in microorganisms. *Chim Oggi Chem Today* **30**:16–19.

Neunzig I, Göhring A, Drăgan CA, Zapp J, Peters FT, Maurer HH, and Bureik M (2012) Production and NMR analysis of the human ibuprofen metabolite 3-hydroxyibuprofen. *J Biotechnol* **157**:417–420.

Omura T and Sato R (1964) The carbon monoxide-binding pigment of liver microsomes. I. Evidence. *J Biol Chem* **239**:2370–2378.

Otey CR, Bandara G, Lalonde J, Takahashi K, and Arnold FH (2006) Preparation of human metabolites of propranolol using laboratory-evolved bacterial cytochromes P450. *Biotechnol Bioeng* **93**:494–499.

Peters FT, Dragan CA, Wilde DR, Meyer MR, Zapp J, Bureik M, and Maurer HH (2007) Biotechnological synthesis of drug metabolites using human cytochrome P450 2D6 heterologously expressed in fission yeast exemplified for the designer drug metabolite 4′-hydroxymethyl-α-pyrrolidinobutyrophenone. *Biochem Pharmacol* **74**:511–520.

Prior JE, Shokati T, Christians U, and Gill RT (2010) Identification and characterization of a bacterial cytochrome P450 for the metabolism of diclofenac. *Appl Microbiol Biotechnol* **85**:625–633.

Reinen J, van Leeuwen JS, Li Y, Sun L, Grootenhuis PDJ, Decker CJ, Saunders J, Vermeulen NPE, and Commandeur JNM (2011) Efficient screening of cytochrome P450 BM3 mutants for their metabolic activity and diversity toward a wide set of drug-like molecules in chemical space. *Drug Metab Dispos* **39**:1568–1576.

Ren X, Yorke JA, Taylor E, Zhang T, Zhou W, and Wong LL (2015) Drug oxidation by cytochrome P450BM3: metabolite synthesis and discovering new P450 reaction types. *Chem A Eur J* **21**:15039–15047.

Rentmeister A, Brown TR, Snow CD, Carbone MN, and Arnold FH (2011) Engineered bacterial mimics of human drug metabolizing enzyme CYP2C9. *ChemCatChem* **3**:1065–1071.

Ringle M, Khatri Y, Zapp J, Hannemann F, and Bernhardt R (2013) Application of a new versatile electron transfer system for cytochrome P450-based *Escherichia coli* whole-cell bioconversions. *Appl Microbiol Biotechnol* **97**:7741–7754.

Rushmore TH, Reider PJ, Slaughter D, Assang C, and Shou M (2000) Bioreactor systems in drug metabolism: synthesis of cytochrome P450-generated metabolites. *Metab Eng* **2**:115–125.

Sawayama AM, Chen MMY, Kulanthaivel P, Kuo MS, Hemmerle H, and Arnold FH (2009) A panel of cytochrome P450 BM3 variants to produce drug metabolites and diversify lead compounds. *Chemistry* **15**:11723–11729.

Schiffer L, Anderko S, Hobler A, Hannemann F, Kagawa N, and Bernhardt R (2015) A recombinant CYP11B1 dependent *Escherichia coli* biocatalyst for selective cortisol production and optimization towards a preparative scale. *Microb Cell Fact* **14**:25.

Schifrin A, Ly TTB, Günnewich N, Zapp J, Thiel V, Schulz S, Hannemann F, Khatri Y, and Bernhardt R (2015) Characterization of the gene cluster CYP264B1-geoA from *Sorangium cellulosum* So ce56: biosynthesis of (+)-eremophilene and its hydroxylation. *ChemBioChem* **16**:337–344.

Schroer K, Kittelmann M, and Lütz S (2010) Recombinant human cytochrome P450 monooxygenases for drug metabolite synthesis. *Biotechnol Bioeng* **106**:699–706.

Taylor M, Lamb DC, Cannell R, Dawson M, and Kelly SL (1999) Cytochrome P450105D1 (CYP105D1) from *Streptomyces griseus*: heterologous expression, activity, and activation effects of multiple xenobiotics. *Biochem Biophys Res Commun* **263**:838–842.

Tsotsou GE, Sideri A, Goyal A, Di Nardo G, and Gilardi G (2012) Identification of mutant Asp251Gly/Gln307His of cytochrome P450 BM3 for the generation of metabolites of diclofenac, ibuprofen and tolbutamide. *Chemistry* **18**:3582–3588.

Vail RB, Homann MJ, Hanna I, and Zaks A (2005) Preparative synthesis of drug metabolites using human cytochrome P450s 3A4, 2C9 and 1A2 with NADPH-P450 reductase expressed in *Escherichia coli*. *J Ind Microbiol Biotechnol* **32**:67–74.

Whitehouse CJC, Bell SG, and Wong LL (2012) P450(BM3) (CYP102A1): connecting the dots. *Chem Soc Rev* **41**:1218–1260.

Wrighton SA and Stevens JC (1992) The human hepatic cytochromes P450 involved in drug metabolism. *Crit Rev Toxicol* **22**:1–21.

Yamazaki H, Inoue K, Shaw PM, Checovich WJ, Guengerich FP, and Shimada T (1997) Different contributions of cytochrome P450 2C19 and 3A4 in the oxidation of omeprazole by human liver microsomes: effects of contents of these two forms in individual human samples. *J Pharmacol Exp Ther* **283**:434–442.

Yin YC, Yu HL, Luan ZJ, Li RJ, Ouyang PF, Liu J, and Xu JH (2014) Unusually broad substrate profile of self-sufficient cytochrome P450 monooxygenase CYP116B4 from *Labrenzia aggregata*. *ChemBioChem* **15**:2443–2449.

Zehentgruber D, Hannemann F, Bleif S, Bernhardt R, and Lütz S (2010) Towards preparative scale steroid hydroxylation with cytochrome P450 monooxygenase CYP106A2. *ChemBioChem* **11**:713–721.

Zhang D, Freeman JP, Sutherland JB, Walker AE, Yang Y, and Cerniglia CE (1996) Biotransformation of chlorpromazine and methdilazine by *Cunninghamella elegans*. *Appl Environ Microbiol* **62**:798–803.

Address correspondence to: Dr. Rita Bernhardt, Institut für Biochemie, Universität des Saarlandes, Campus Geb. B2.2, 66123 Saarbrücken, Germany. E-mail: ritabern@mx.uni-saarland.de

DMD # 68486

SUPPORTING INFORMATION

Drug Metabolism and Disposition

CYP267A1 and CYP267B1 from *Sorangium cellulosum* So ce56 are highly versatile drug metabolizers

Fredy Kern, Yogan Khatri, Martin Litzenburger and Rita Bernhardt

Department of Biochemistry, Saarland University, 66123 Saarbruecken, Germany

To whom correspondence should be addressed: Rita Bernhardt, Department of Biochemistry, Saarland University, 66123 Saarbrücken, Germany, Tel.: +49 (0)681 302 4241; Fax: +49 (0)681 302 4739; Email: ritabern@mx.uni-saarland.de

Optimized extraction procedure - Due to the different substrates, and thus, the diversity of chemical structures and functional groups, we established a substrate-dependent extraction protocol as shown in Table S 0 accompanied by substrate-dependent HPLC methods listed in Table S 1.

Table S 0. The optimized extraction procedure for the tested drugs and respective metabolites. To improve the extraction efficiency, the addition of acidic (pH 4) or basic (pH 11) buffer before extraction is needed.

#	Substrate	Added before extraction	Solvent used for extraction
1	Amodiaquine	Glycine buffer	Chloroform
2	Chlorpromazine	-	Chloroform
3	Dexamethasone	-	Chloroform
4	Dextromethorphan	-	Chloroform
5	Diclofenac	-	Ethyl acetate
6	Haloperidol	-	Ethyl acetate
7	Ibuprofen	-	Ethyl acetate
8	Indoprofen	-	Ethyl acetate
9	Losartan	Acetic acid/Acetate buffer	Hexane 95%/ 5% Isopropyl alcohol
10	Nifedepine	-	Ethyl acetate
11	Noscapine	Glycine buffer	Ethyl acetate
12	Olanzapine	Glycine buffer	Chloroform
13	Omeprazole	Glycine buffer	Ethyl acetate
14	Oxymetazoline	Glycine buffer	Ethyl acetate
15	Papaverine	Glycine buffer	Chloroform
16	Repaglinide	-	Chloroform
17	Ritonavir	-	Chloroform
18	Tamoxifen	Glycine buffer	Hexane 95%/ 5% Isopropyl alcohol
19	Terfenadine	Glycine buffer	Chloroform
20	Thioridazine	Glycine buffer	Ethyl acetate
21	Verapamil	Glycine buffer	Chloroform
22	Vitamin D3	-	Chloroform

HPLC methods – The HPLC analysis of the substrates **3**, **10**, **13**, and **22** were performed using 20% acetonitrile/80% Milli-Q water (*v/v*) as solvent A and 100% acetonitrile as solvent B. All other substrates (**1**, **2**, **4**-**9**, **11**, **12** and **14**-**21**) were analyzed by using 100% Milli-Q water containing 0.1% TFA as solvent A and 100% acetonitrile containing 0.1% TFA as solvent B. Unless otherwise specified, the flow rate for all methods was set as 1 ml min^{-1} and the oven temperature as 40°C.

Table S 1. HPLC Methods for the tested compounds.

#	Substrate	Molecular weight [g mol^{-1}]	Wavelength [nm]	Method [minutes / % of solvent A]
1	Amodiaquine	464.81	344	0/90
				5/90
				10/60
				13/60
				13.1/20
				14/20
				14.1/90
				16/90
2	Chlorpromazine	318.86	256	0/80
				1/80
				9/20
				12/20
				12.1/80
				14/80
3	Dexamethasone	392.47	240	0/90
				7/90
				13/50
				13.1/90
				15/90
4	Dextromethorphan	271.40	280	Same method as **3**
5	Diclofenac	318.10	276	0/70
				1/70
				12/20
				14/20
				14.5/70
				15/70
6	Haloperidol	375.86	244	0/80
				2/80
				8/50
				12/50
				12.1/80
				14/80
				1.2 ml min^{-1}
7	Ibuprofen	229.28	224	0/80
				4/80

				13/20
				15/20
				15.1/80
				17/80
8	Indoprofen	281.31	284	Same method as **7**
9	Losartan	461.91	244	0/90
				2/90
				10/40
				12/40
				12.1/20
				14/20
				14.1/90
				16/90
10	Nifedepine	346.34	236	Same method as **7**
11	Noscapine	413.42	232	Same method as **7**
12	Olanzapine	312.43	260	0/90
				12/70
				12.1/50
				13.5/50
				13.6/90
				16/90
13	Omeprazole	345.42	300	Same method as **3**
14	Oxymetazoline	296.84	228	Same method as **7**
15	Papaverine	375.75	252	0/90
				2/90
				7/60
				10/60
				10.1/20
				11/20
				11.1/90
				13/90
16	Repaglinide	452.59	244	0/90
				1/90
				10/10
				12/10
				12.5/90
				15/90
17	Ritonavir	720.94	240	0/70
				1/70
				9/10
				10/10
				10.1/70
				13/70
				0.8 ml min^{-1}

18	Tamoxifen	371.51	240	0/60 3/60 10/20 13/20 13.1/60 15/60
19	Terfenadine	471.67	228	Same method as **7**
20	Thioridazine	407.04	264	Same method as **7**
21	Verapamil	491.06	232	Same method as **11**
22	Vitamin D_3	384.64	265	0/40 15/0 26/0 30/40

Phylogenetic analysis of CYP267B1 with drug metabolizing P450s of human and bacterial origin – In addition to the phylogenetic analysis of CYP267B1 with respect to drug metabolizing human and bacterial P450s as depicted in Figure 2, we performed pairwise alignments with EMBOSS Needle and present the identities and similarities in Table S 2.

Table S 2. Overview of identities and similarities of drug metabolizing human and bacterial P450s with respect to CYP267B1 from *Sorangium cellulosum* So ce56.

CYP267B1 to	P450	UniProtKB	Identity	Similarity
human	CYP1A1	P04798.1	96/612 (15.7%)	152/612 (24.8%)
	CYP1A2	P05177.3	107/572 (18.7%)	166/572 (29.0%)
	CYP1B1	Q16678.2	96/600 (16.0%)	167/600 (27.8%)
	CYP2A6	P11509.3	105/537 (19.6%)	181/537 (33.7%)
	CYP2A7	P20853.2	99/592 (16.7%)	160/592 (27.0%)
	CYP2A13	Q16696.3	103/540 (19.1%)	175/540 (32.4%)
	CYP2B6	P20813.1	100/570 (17.5%)	164/570 (28.8%)
	CYP2C8	P10632.2	106/524 (20.2%)	173/524 (33.0%)
	CYP2C9	P11712.3	97/554 (17.5%)	168/554 (30.3%)
	CYP2C18	P33260.3	89/583 (15.3%)	159/583 (27.3%)
	CYP2C19	P33261.3	101/559 (18.1%)	172/559 (30.8%)
	CYP2D6	P10635.2	110/569 (19.3%)	164/569 (28.8%)
	CYP2E1	P05181.1	101/567 (17.8%)	160/567 (28.2%)
	CYP2F1	P24903.2	90/605 (14.9%)	138/605 (22.8%)
	CYP2J2	P51589.2	106/552 (19.2%)	160/552 (29.0%)
	CYP2R1	Q6VVX0.1	91/599 (15.2%)	150/599 (25.0%)
	CYP2S1	Q96SQ9.2	91/568 (16.0%)	154/568 (27.1%)
	CYP2U1	Q7Z449.1	93/615 (15.1%)	155/615 (25.2%)
	CYP2W1	Q8TAV3.2	112/540 (20.7%)	169/540 (31.3%)
	CYP3A4	P08684.4	95/565 (16.8%)	164/565 (29.0%)
	CYP3A5	P20815.1	102/536 (19.0%)	184/536 (34.3%)
	CYP3A7	P24462.2	92/565 (16.3%)	164/565 (29.0%)
	CYP3A43	Q9HB55.1	97/536 (18.1%)	168/536 (31.3%)
Streptomyces griseus	P450-SOY	P26911.1	147/433 (33.9%)	200/433 (46.2%)
Actinoplanes sp. ATCC 53771	CYP107E4	ACN71221.1	163/419 (38.9%)	216/419 (51.6%)
Labrenzia aggregate	CYP116B4	EAV41564.1	129/819 (15.8%)	189/819 (23.1%)
Bacillus cereus	CYP102A5	Q81BF4	100/1141 (8.8%)	169/1141 (14.8%)
Rhodococcus jostii RHA1	CYP51_RHA1	Q0S7M9	104/481 (21.6%)	176/481 (36.6%)
	CYP105_RHA1	Q0SDH7	144/434 (33.2%)	209/434 (48.2%)
	CYP116_RHA1	Q0RUR9	135/460 (29.3%)	202/460 (43.9%)
	CYP125_RHA1	Q0S7N3	139/429 (32.4%)	207/429 (48.3%)
	CYP256_RHA1	Q0RXF8	131/446 (29.4%)	205/446 (46.0%)
	CYP257_RHA1	Q0RVH0	122/445 (27.4%)	195/445 (43.8%)
	CYP258_RHA1	Q0RUW2	130/451 (28.8%)	194/451 (43.0%)
Sorangium cellulosum So ce56	CYP264A1	CAN96490.1	147/430 (34.2%)	207/430 (48.1%)
	CYP267A1	CAN90832.1	173/453 (38.2%)	235/453 (51.9%)

Whole-cell biotransformation construct **–** The established pCDF_dFA plasmid[1] (Figure S 1 A) containing the genes for an expression of bovine adrenodoxin ($Adx_{4\text{-}108}$) and Fpr reductase from *E. coli* was optimized with the substitution of the mentioned genes with Fdx8 and FdR_B from *Sorangium cellulosum* So ce56 as described in the materials and methods section. The resulting plasmid was named as pCDF_F8B and is presented in Figure S 1 B.

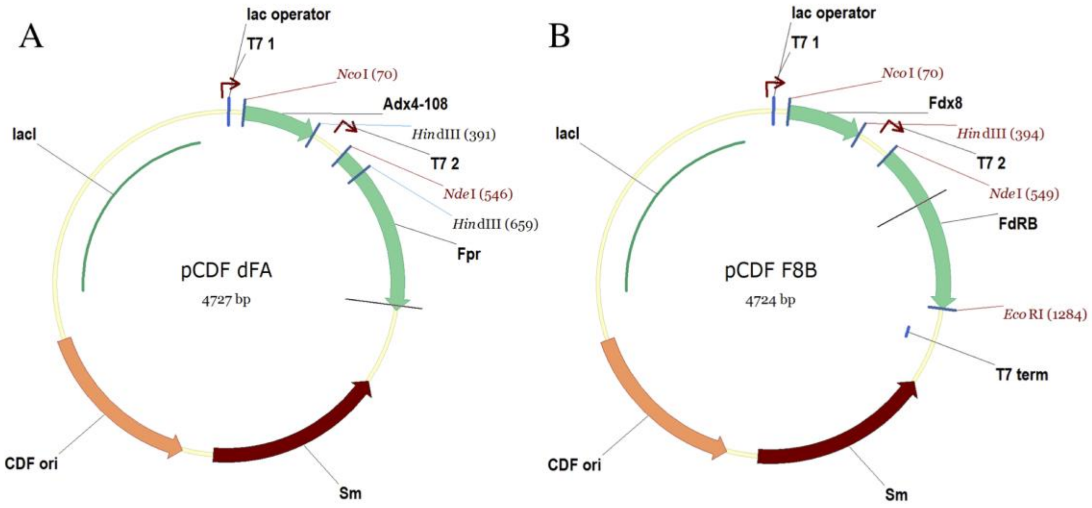

Figure S 1. Vector map of pCDF_dFA plasmid (A) and the optimized pCDF_F8B plasmid (B).

[1] Litzenburger M, Kern F, Khatri Y, and Bernhardt R (2015) Conversions of Tricyclic Antidepressants and Antipsychotics with Selected P450s from Sorangium cellulosum So ce56. *Drug Metab Dispos* **43**:392–399.

HPLC chromatograms of the purified products – To validate the purity of the metabolites produced by the whole-cell system CYP267B1-Fdx8-FdR_B, all purified products were analyzed via preparative HPLC and compared with the respective substrate as presented in Figure S 2.

For **13**, we detected an additional peak at 7 min in the chromatogram of the pure substrate (red line, 11.8 min, Figure S 2 C). As described by Brändström et al. in 1989, omeprazole is able to form a more hydrophilic positively charged intermediate in a reversible chemical equilibrium[2], which explains the second peak (red line, 7 min, Figure S 2 C) in the pure substrate chromatogram.

However, for the purified product **13a**, only a minor amount of the substrate peak at 11.8 min was observed indicating a high purity of the product (blue line, 4 min, Figure S 2 C).

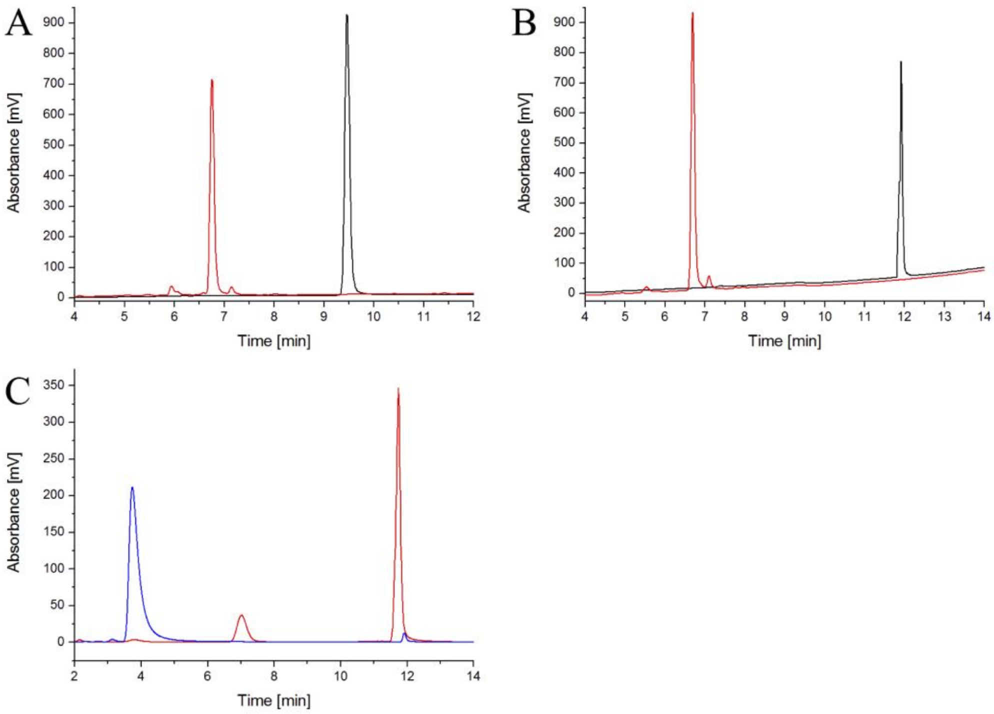

Figure S 2. HPLC chromatograms of the substrates and products. A: diclofenac (**5**, black line), 4-hydroxydiclofenac (**5a**, red line); B: ibuprofen (**7**, black line), 2-hydroxyibuprofen (**7a**, red line); C: omeprazole (**13**, red line) and omeprazole sulfone (**13a**, blue line).

[2] A. Brändström et al. (1989) Chemical Reactions of Omeprazole and Omeprazole Analogues. VI. The Reactions of Omeprazole in the Absence of 2-Mercaptoethanol. *Acta Chem. Scand.* **43**, 595-611

Determination of inhibition of CYP267 family by indole – To validate the necessity to use a defined minimal medium (M9CA) in our whole-cell system, we performed *in vitro* conversions of 200 μM β-ionone with increasing concentrations of indole (Figure S 3). The conditions of this assay were chosen analogous to our previous work[3] with a shorter reaction time of 20 min.

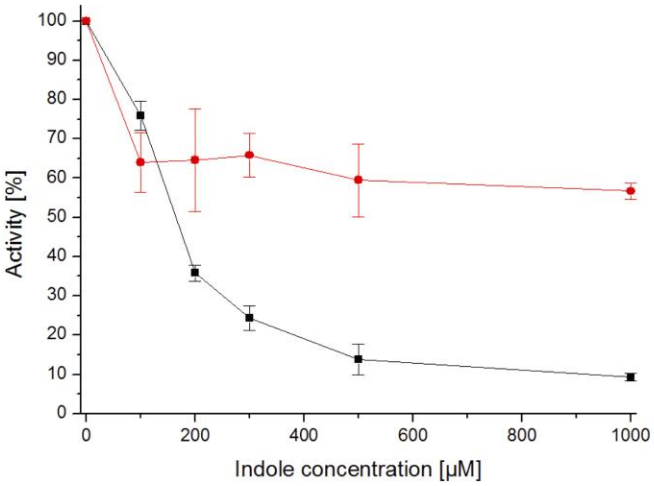

Figure S 3. Inhibition of product formation by increased indole concentration. The data were produced with the conversion of β-ionone. The results of the product inhibition catalyzed by CYP267A1 (black line) and CYP267B1 (red line) in the presence of increasing concentrations of indole is shown.

[3] Litzenburger M, and Bernhardt R (2015) Selective oxidation of carotenoid-derived aroma compounds by CYP260B1 and CYP267B1 from *Sorangium cellulosum* So ce56. *Appl. Microbiol. Biotechnol.* **in press**

DMD # 68486

***NMR data of the purified products 5a, 7a and 13a* –** The chemical structures of the products (inclusive numbering) are presented in Figure S 4.

4-Hydroxydiclofenac (**5a**):
^{1}H-NMR (CDCl$_3$, 500 MHz): δ 3.63 (s, 2H, CH$_2$), 6.11 (d, 1H, ArH-3), 6.73 (t, 1H, ArH-5), 6.94 (s, 2H, ArH-3' and ArH-5'), 6.99 (t, 1H, ArH-4), 7.12 (d, 1H, ArH-6).
^{13}C-NMR (CDCl$_3$, 125 MHz): δ 40.43 (C-a), 113.64 (C-3), 115.80 (C-3' and C-5'), 118.92 (C-5), 127.46 (C-4), 128.06 (C-1), 129.10 (C-2), 130.72 (C-6), 132.94 (C-1'), 144.12 (C-2' and C-6'), 155.34 (C-4'), 173.10 (COOH).

2-Hydroxyibuprofen (**7a**):
^{1}H-NMR (CDCl$_3$, 500 MHz): δ 1.19 (s, 6H, H-3), 1.45 (d, 3H, H-b), 2.78 (s, 2H, H-a), 3.65 (q, 1H, H-1), 7.28 (m, 4H, ArH-1 to ArH-4).
^{13}C-NMR (CDCl$_3$, 125 MHz): δ 17.6 (C-3), 27.7 (C-b), 45.0 (C-1), 48.2 (C-a), 71.8 (C-2), 127.2 (C-2', C-6'), 131.3 (C-3', C-5'), 137.3 (C-4'), 138.9 (C-1').

Omeprazole sulfone (**13a**):
^{1}H-NMR (CD$_3$OD, 500 MHz): δ 1.86 (s, 3H, ArCH$_3$), 1.89 (s, 3H, ArCH$_3$), 3.19 (s, 3H, OCH$_3$), 3.70 (s, 3H, OCH$_3$) 4.30 (s, 2H, CH$_2$), 6.74 (dd, 1H, ArH-6), 6.87 (s, 1H, ArH-4), 7.27 (s, 1H, ArH-7), 7.47 (s, 1H, ArH-13).

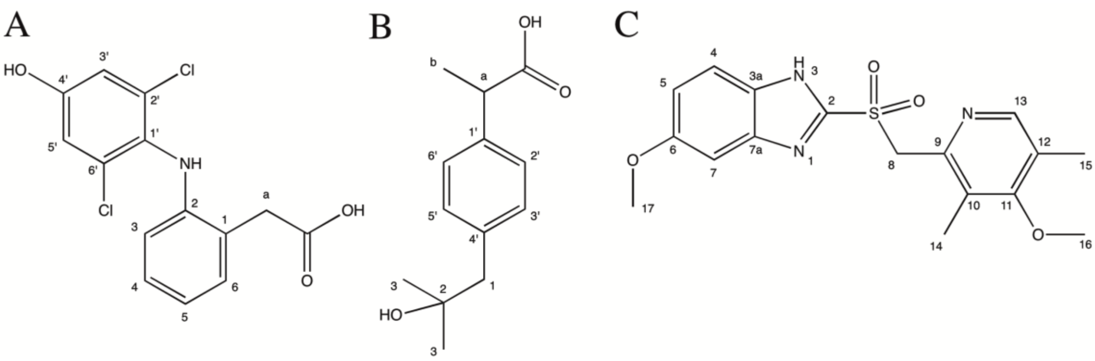

Figure S 4. Chemical formula of 4-hydroxydiclofenac (A), 2-hydroxyibuprofen (B) and omeprazole sulfone (C).

Settings of the MS/MS measurements of omeprazole (13) and omeprazole sulfone (13a) – The MS/MS experiments were performed on an API 2000 Qtrap (ABSciex, Darmstadt, Germany) in positive mode (*m/z* 100-400) with a flow rate of 4.0 μL min^{-1} using a syringe pump with ID 4.6 mm. Additional settings are presented in Table S 3.

Table S 3. Detailed settings for the MS/MS measurements of **13** and **13a**.

Name	Value	Name	Value
Curtain Gas (CUR)	20.0 psi	Collision Potential	25 V
Ion Spray Voltage (IS)	5500.0 V	Declustering Potential (DP)	80.0 V
Ion Source Gas 1 (GS1)	25.0 psi	Entrance Potential (EP)	10.0 V
Ion Source Gas 2 (GS2)	0.0 psi	Temperature (TEM)	230.0 C

MS data of omeprazole sulfone (13a) – Clear elucidation of product **13a** exclusively by NMR was unsatisfactory since no ^{33}S NMR was measured. We therefore performed MS/MS analysis (Figure S 5) and compared the results with the MS/MS spectrum from 5'-hydroxyomeprazole published by Woolf et al.[4] to exclude a hydroxylation of **13** by CYP267B1 in 5' position. The fragmentation of the precursor ion **13a** (*m/z* 362) results in four characteristic fragments, which is related to the fragment pattern published for 5'-hydroxyomeprazole [4]. The characteristic fragment for **13** (*m/z* 198) can be found as *m/z* 214 fragment in the product spectrum of **13a** indicating the insertion of an oxygen (*m/z* +16) to the pyridine part of the compound resulting in $[SO_2\text{-}CH_2\text{-}C_8H_{10}ON]^+$. However, taken the results of the mass spectrometric analysis (precursor *m/z* 362, fragment *m/z* 214) and the NMR data into account, we were able to conclusively assign the product **13a** as omeprazole sulfone.

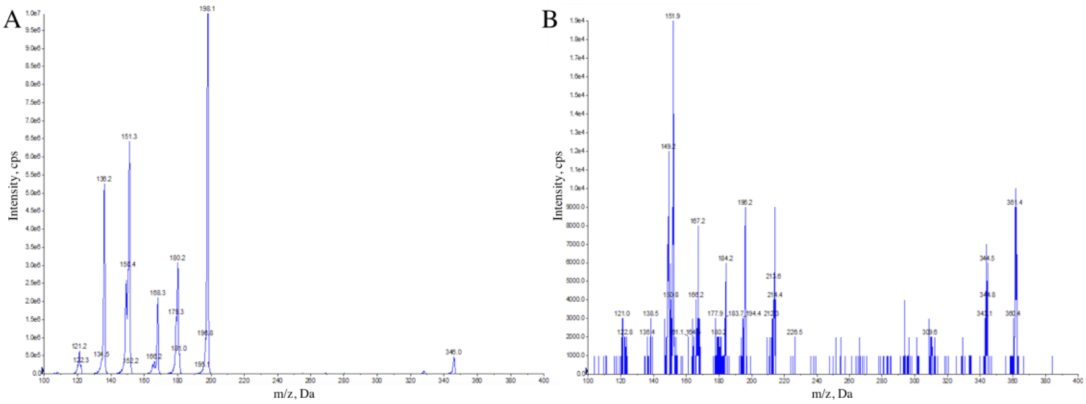

Figure S 5. Positive product ion mass spectra of the protonated substrate omeprazole (**13**, A) and omeprazole sulfone (**13a**, B).

[4] E. J. Woolf, B. K. Matuszewski. (1998) Simultaneous determination of omeprazole and 5'-hydroxyomeprazole in human plamsa by liquid chromatography - tandem mass spectrometry. *J. Chromatogr. A.* **828**, 229-238.

DMD # 68486

Overview of drugs metabolized by the CYP267 family - A comprehensive overview of the analyzed drugs, and the human metabolites produced by the two members of the CYP267 family, is presented in supplemental Figure S 6.

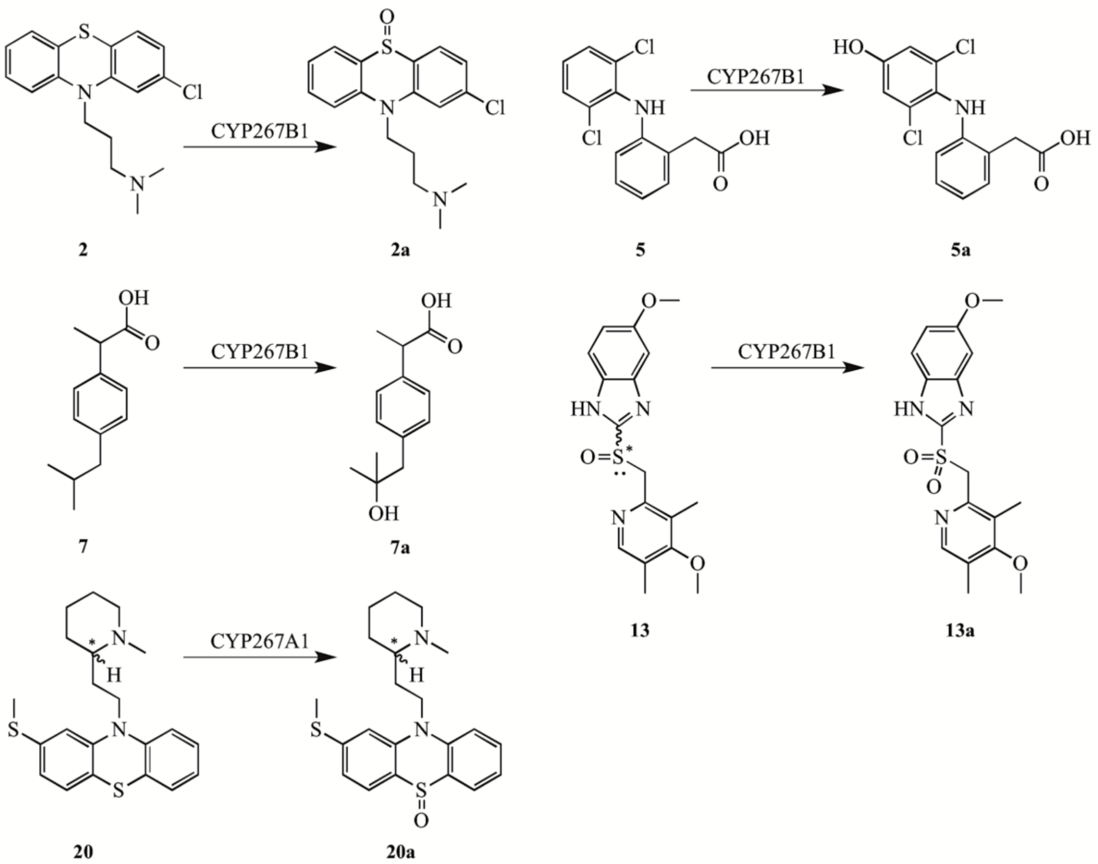

Figure S 6. Overview of drugs converted by the CYP267 family: Conversion of **20** to thioridazine-5-sulfoxide (**20a**) by CYP267A1 and conversion of **2** to chlorpromazine sulfoxide (**2a**), **5** to 4-hydroxydiclofenac (**5a**), **7** to 2-hydroxyibuprofen (**7a**) and **13** to omeprazole sulfone (**13a**) by CYP267B1.

3.3 Litzenburger et al. 2015

Conversions of tricyclic antidepressants and antipsychotics with selected P450s from *Sorangium cellulosum* So ce56.

Martin Litzenburger, **Fredy Kern**, Yogan Khatri and Rita Bernhardt

Drug Metabolism and Disposition, 2015, 43(3): 392-9.

Supplemental material to this article can be found at:
http://dmd.aspetjournals.org/content/suppl/2014/12/30/dmd.114.061937.DC1.html

1521-009X/43/3/392–399$25.00
DRUG METABOLISM AND DISPOSITION
http://dx.doi.org/10.1124/dmd.114.061937
Drug Metab Dispos 43:392–399, March 2015

Conversions of Tricyclic Antidepressants and Antipsychotics with Selected P450s from *Sorangium cellulosum* So ce56 [S]

Martin Litzenburger, Fredy Kern, Yogan Khatri, and Rita Bernhardt

Institut für Biochemie, Universität des Saarlandes, Saarbruecken, Germany (M.L., F.K., Y.K., R.B.)

Received November 13, 2014; accepted December 30, 2014

ABSTRACT

Human cytochromes P450 (P450s) play a major role in the biotransformation of drugs. The generated metabolites are important for pharmaceutical, medical, and biotechnological applications and can be used for derivatization or toxicological studies. The availability of human drug metabolites is restricted and alternative ways of production are requested. For this, microbial P450s turned out to be a useful tool for the conversion of drugs and related derivatives. Here, we used 10 P450s from the myxobacterium *Sorangium cellulosum* So ce56, which have been cloned, expressed, and purified. The P450s were investigated concerning the conversion of the antidepressant drugs amitriptyline, clomipramine, imipramine, and promethazine; the antipsychotic drugs carbamazepine, chlorpromazine, and thioridazine, as well as their precursors, iminodibenzyl and phenothiazine. Amitriptyline, chlorpromazine, clomipramine, imipramine, and thioridazine are efficiently converted during the in vitro reaction and were chosen to upscale the production by an *Escherichia coli*–based whole-cell bioconversion system. Two different approaches, a whole-cell system using M9CA medium and a system using resting cells in buffer, were used for the production of sufficient amounts of metabolites for NMR analysis. Amitriptyline, clomipramine, and imipramine are converted to the corresponding 10-hydroxylated products, whereas the conversion of chlorpromazine and thioridazine leads to a sulfoxidation in position 5. It is shown for the first time that myxobacterial P450s are efficient to produce known human drug metabolites in a milligram scale, revealing their ability to synthesize pharmaceutically important compounds.

Introduction

Cytochromes P450 (P450s) are heme-thiolate monooxygenases. They are present in nearly all organisms and belong to one of the largest superfamilies of enzyme proteins (Nelson, 2011). P450s are involved in the degradation and detoxification of drugs and xenobiotics, as well as in the metabolism of steroid hormones, lipids, and antibiotics (Bernhardt, 2006; Bernhardt and Urlacher, 2014). In general, P450s catalyze the insertion of a molecular oxygen atom into organic molecules while the other oxygen atom is reduced to water. Beside the hydroxylation, they catalyze a broad range of reactions such as sulfoxidation, epoxidation, deamination, dehalogenation, and N-, O-, and S-dealkylation (Sono et al., 1996; Bernhardt and Urlacher, 2014). To catalyze such reactions, these enzymes are dependent on redox partners, either homologous or heterologous, which provide electrons from NAD(P)H via an electron transfer chain (Hannemann et al., 2007).

Human P450s play a major role in the metabolism of drugs. The human liver P450s CYP3A4/5, CYP2D6, CYP2C9, CYP1A2, and CYP2C19 are responsible for the conversion of about 80% of all drugs (Zanger and Schwab, 2013). One important group of pharmaceuticals is psychotherapeutic drugs. Antipsychotic drugs and tricyclic antidepressants are used for the treatment of psychiatric disorders. In 1952, these psychotherapeutic drugs started with the discovery of chlorpromazine and since that time many drugs, mainly based on phenothiazine or iminodibenzyl, have been discovered and are used for psychiatric medication (Shen, 1999; Owens, 2014). The involvement of human liver P450s in the phase I biotransformation of these psychotherapeutics is well studied (Tanaka and Hisawa, 1999). Most of the drug metabolites are produced by P450s (see Table 1), with the exception of N-oxide products that are formed by the flavin-containing monooxygenases (Ziegler, 1993). Since some of the drug metabolites might have adverse effects, the U.S. Food and Drug Administration (FDA) published the guidance for safety testing of drug metabolites. Any human metabolite representing >10% of the parent drug exposure at steady state has to be tested in safety studies (FDA, 2008). However, this FDA guidance is superseded by the guidelines of the International Conference on Harmonization (Frederick and Obach, 2010; Haglund et al., 2014). Concerning these guidelines, further safety testing is recommended for human metabolites that are observed at exposures >10% of total drug-related exposure and at significantly greater levels in humans than the maximum exposure seen in toxicity studies (European Medicines Agency, 2009). As a result, ways for the production of these drug metabolites are demanded by the pharmaceutical industry. Production of such metabolites for toxicological studies and further derivatization can be achieved either by chemical synthesis or biocatalysis. The enzymatic production has many benefits such as high selectivity or the absence of employing toxic chemicals (Koeller and Wong, 2001). Microbial enzymes play an increasing role in the production of known human drugs and secondary metabolites, which are used for drug development (Demain, 1999; Patel, 2002). In this respect, microbial P450s are often involved in the production of these metabolites (Urlacher and Girhard, 2012) due to their ability to hydroxylate inactive carbon-hydrogen bonds in complex molecules.

The work is supported by Deutsche Forschungsgemeinschaft (DFG 1343/23-1).
dx.doi.org/10.1124/dmd.114.061937.
[S]This article has supplemental material available at dmd.aspetjournals.org.

ABBREVIATIONS: Adx_{4-108}, adrenodoxin (truncated form); FDA, Food and Drug Administration; Fpr, ferredoxin-NADP$^+$ reductase; GC, gas chromatography; HPLC, high-performance liquid chromatography; MS, mass spectrometry; P450, cytochrome P450; RT, retention time.

TABLE 1

Overview of psychotherapeutic drugs, their metabolites, and the human P450s capable for the metabolism

Drug	Human P450	Main metabolite	Reference
Amitriptyline	CYP1A2, CYP3A4, CYP2B6, CYP2C8, CYP2C9, CYP2C19, CYP2D6	2-Hydroxyamitriptyline 3-Hydroxyamitriptyline 2,11-Dihydronortriptyline 10-Hydoxyamitriptyline 10-,11-Dihydroxyamitriptyline 10-Oxy-amitriptyline Amitriptyline-*N*-oxide Amitriptyline dihydrodiol Desmethylamitriptyline	Prox and Breyer-Pfaff, 1987; Venkatakrishnan et al., 2001
Carbamazepine	CYP1A2, CYP2A6, CYP3A4, CYP2B6, CYP2C8, CYP2E1	10-,11-Epoxycarbamazepine 2-Hydroxycarbamazepine 3-Hydroxycarbamazepine	Kerr et al., 1994; Pearce et al., 2002
Chlorpromazine	CYP1A2, CYP3A4, CYP2B6, CYP2C19, CYP2D6	7-Hydroxychlorpromazine Chlorpromazine-*N*-oxide Chlorpromazine sulfoxide Desmethylchlorpromazine Didesmethylchlorpromazine	Murray, 2006; Wójcikowski et al., 2010
Clomipramine	CYP1A2, CYP3A4, CYP2C19, CYP2D6	2-Hydroxyclomipramine 8-Hydroxyclomipramine 10-Hydroxyclomipramine Clomipramine-*N*-oxide Desmethylclomipramine	Nielsen et al., 1996; Yokono et al., 2001
Imipramine	CYP1A2, CYP3A4, CYP2C9, CYP2D6	2-Hydroxyimipramine 10-Hydroxyimipramine Desmethylimipramine Didesmethylimipramine Imipramine-*N*-oxide	Singh, 2012
Promethazine	CYP2B6, CYP2D6	3-Hydroxypromethazine 4-Hydroxypromethazine Desmethylpromethazine Promethazine sulfoxide	Nakamura et al., 1996
Thioridazine	CYP2D6	*N*-desmethylthioridazine 7-Hydroxythioridazine Mesoridazine Thioridazine-5-sulfoxide	Daniel et al., 2000

Myxobacteria are known for the production of pharmaceutically and chemically important compounds, which attracted the attention of the pharmaceutical industry (Weissman and Müller, 2010). In 2007, the myxobacterium *Sorangium cellulosum* So ce56 was sequenced and 21 P450 genes were identified (Schneiker et al., 2007; Khatri et al., 2010b). Although, the physiologic roles of those P450s are still not known, some of them are able to convert exogenous substrates such as terpenes and terpenoids or fatty acids (Khatri et al., 2010b; Ly et al., 2012). However, the potential for the conversion of pharmaceutically interesting compounds has not yet been tested.

In this study, 10 P450s (CYP109C1, CYP109C2, CYP109D1, CYP260A1, CYP260B1, CYP264A1, CYP264B1, CYP266A1, CYP267A1, and CYP267B1) from *S. cellulosum* So ce56 were selected and employed for the in vitro conversion of seven psychotherapeutic drugs and their precursors. Compounds showing significant in vitro conversion were further chosen for the conversion with an *Escherichia coli*–based whole-cell biotransformation system to upscale the production and facilitate structure elucidation via NMR spectroscopy. The purified compounds were compared with known human metabolites to check for specific derivatives and to elucidate possible new metabolites, which could be useful for further drug development.

Materials and Methods

Chemicals. Amitriptyline and thioridazine were provided by Dr. Stephan Lütz (Novartis, Basel, Switzerland). Isopropyl β-D-1-thiogalactopyranoside and 5-aminolevulinic acid were purchased from Carbolution Chemicals (Saarbruecken, Germany). Bacterial media were purchased from Becton Dickinson (Heidelberg, Germany). All other chemicals were obtained from standard sources in the highest purity available.

Strains. The *E. coli* strain Top 10 for cloning purpose was obtained from Invitrogen (San Diego, CA). The *E. coli* strain BL21(DE3) for the heterologous expression of the P450s and BL21-Gold(DE3) for the whole-cell conversions were purchased from Agilent Technologies (Santa Clara, CA).

Molecular Cloning and Preparation of Expression Vectors. The 10 P450s from *S. cellulosum* So ce56 (CYP109C1, CYP109C2, CYP109D1, CYP260A1, CYP260B1, CYP264A1, CYP264B1, CYP266A1, CYP267A1, and CYP267B1) were selected for this study. The genes of those P450s were cloned in pCWori$^+$ plasmids as described elsewhere (Khatri et al., 2010b). To improve the expression yield, the genes of the P450s (CYP109C1, CYP109C2, CYP109D1, CYP260A1, CYP260B1, CYP264A1, and CYP264B1) were excised from their corresponding pCWori$^+$ plasmids and cloned into a pET17b plasmid (Novagen, Darmstadt, Germany) (Ringle et al., 2013). Likewise, the genes of CYP266A1, CYP267A1, and CYP267B1 were excised and cloned into a pET22b plasmid (Novagen).

For the expression of the redox partners ferredoxin-NADP$^+$ reductase (Fpr) and adrenodoxin (truncated form) (Adx_{4-108}) in the *E. coli*–based whole-cell system, the pCDFDuet-1 (Merck, Darmstadt, Germany) vector with a streptomycin resistance marker gene was used. The DNA fragment encoding Adx_{4-108} was amplified by Polymerase chain reaction (forward primer, 5′- AAT GAC ATG CTT GAT CTG GCC TAT GGA CTA ACA GAT AGA T -3′, and reverse primer, 5′- ATC TAT CTG TTA GTC CAT AGG CCA GAT CAA GCA TGT CAT T-3′) using pKKHC_Adx_{4-108} as a template (Uhlmann et al., 1994). Then, the DNA fragment was inserted between NcoI and *Hind*III of the multiple cloning site MS-I of pCDFDuet-1 (Merck). The forward primer was used to delete the NdeI restriction site. The fragment encoding Fpr was amplified by Polymerase chain reaction (forward primer, 5′- CAT ATG GCT GAT TGG GTA ACA GGC AAA GTC ACT AAA GTG CAG AAC TGG -3′, and reverse primer, 5′- CGG GGT ACC TTA CCA GTA ATG CTC CGC TGT CAT GTG GCC CGG TCG GC-3′) using the pET16_Fpr plasmid as a template (Girhard et al., 2010). The fragment was subcloned in the pCR4 blunt vector and finally inserted between NdeI and KpnI, resulting in the pCDF_dFA expression vector.

Media and Buffers. For the heterologous expression of the related P450s, terrific broth medium (24 g yeast extract, 12 g peptone, 4 ml glycerol, 2.31 g K_2HPO_4, and 12.54 g KH_2PO_4 per liter H_2O) was used. The whole-cell conversion was performed in M9CA medium (6 g Na_2HPO_4, 3 g KH_2PO_4, 0.5 g NaCl, 1 g NH_4Cl, 4 g casamino acids, 4 g glucose, 50 μl 1M $CaCl_2$, 2 ml 1 M $MgSO_4$, 2 ml of trace elements solution per liter H_2O; Trace elements solution contained 2.5 g EDTA, 250 mg $FeSO_4$, 25 mg $ZnCl_2$ and 5 mg $CuSO_4$ per 50 ml H_2O). The conversion with resting cells was done in 50 mM potassium phosphate buffer (pH 7.4) containing 2% glycerol as the carbon source.

Expression and Purification of the Enzymes. The corresponding P450s were expressed and purified as described previously (Khatri et al., 2010b). The electron transfer partners Adx_{4-108} and adrenodoxin reductase from *Bos taurus* were expressed and purified as described elsewhere (Sagara et al., 1993; Uhlmann et al., 1994).

In Vitro Conversions. A reconstituted in vitro system containing the corresponding P450 (0.5 μM), adrenodoxin reductase (1.5 μM), Adx_{4-108} (10 μM), $MgCl_2$ (1 mM), and a cofactor regenerating system with glucose-6-phosphate (5 mM) and glucose-6-phosphate dehydrogenase (2 U ml^{-1}) in the end volume of 250 μl of potassium phosphate buffer (20 mM, pH 7.4) was used. The compounds (10 mM), except carbamazepine (MeOH), phenothiazine (EtOH), and iminodibenzyl (EtOH), were dissolved in water and added to an end-concentration of 200 μM. The reaction was started by the addition of NADPH (500 μM). After 3 hours at 30°C the reaction was quenched by adding chloroform (500 μl). The aqueous phase was extracted twice with chloroform (2 × 500 μl). A negative control in the absence of P450 in the reaction sample was employed for each substrate to verify the P450-dependent reaction.

Whole-Cell System Using M9CA. The experiments were performed with *E. coli* BL21(DE3) gold cells. The cells were transformed with two plasmids, one for the corresponding P450 (pET17b or pET22b) and the other one for the redox partners Fpr and Adx_{4-108} (pCDF_dFA). The overnight culture was prepared in nutrient broth containing ampicillin (100 μg/ml) and streptomycin (50 μg/ml). The main culture with M9CA medium was inoculated with the overnight culture (dilution 1:100) and incubated at 37°C. The induction of the corresponding genes was initiated by adding 1 mM isopropyl β-D-1-thiogalactopyranoside and 0.5 mM 5-aminolevulinic acid when the optical density reached 0.9–1 and the culture was grown further at 28°C. After 21 hours of expression, the temperature was set to 30°C and the substrates [stock solution 50 mM in water except for carbamazepine (MeOH), phenothiazine (EtOH) and iminodibenzyl (EtOH)] were added to a final concentration of 200 μM. To permeabilize the cells, EDTA was also added to a final concentration of 20 mM. The reaction was carried out for 48 hours under the same conditions. Samples were harvested, quenched with the same volume of chloroform and extracted twice. The organic phase was collected, pooled, and evaporated to dryness. The extracts were stored at −20°C until purification.

Whole-Cell System Using Resting Cells. The overnight culture was prepared as described before. Terrific broth medium was inoculated with the overnight culture (dilution 1:100). The expression was induced by adding 1 mM isopropyl β-D-1-thiogalactopyranoside and 0.5 mM 5-aminolevulinic acid at an optical density of 0.7–0.8. After 24 hours of expression at 28°C, the cells were harvested by centrifugation for 20 minutes at 4500*g*. The cell pellet was resuspended and washed in the buffer [20 mM potassium phosphate buffer (pH 7.4) containing 2% glycerol] following the centrifugation step. The 2.4 g cell mass was suspended in 100 ml buffer containing 2% glycerol. The substrates (200 μM) and EDTA (20 mM) were added and the cells were incubated for 24 hours at 30°C. The reaction was stopped by adding the same volume of chloroform. The extraction was done as described previously. Until purification, the extracts were stored at −20°C.

Analysis of the In Vitro and Whole-Cell Conversions via High-Performance Liquid Chromatography (HPLC)-Diode Array Detector. HPLC analysis was performed on a system consisting of a PU-2080 HPLC pump, an AS-2059-SF autosampler, and a MD-2010 multi wavelength detector (Jasco, Gross-Umstadt, Germany). A Nucleodur 100-5 C18 column (125 × 4 mm; Macherey-Nagel, Düren, Germany) was used at 40°C. The mobile phase consisted of water containing 0.1% trifluoroacetic acid (A) and acetonitrile containing 0.1% trifluoroacetic acid (B). A gradient from 20% to 80% of B with a flow rate of 1 ml/min was used for the separation of the compounds. The detection wavelengths were substrate dependent: amitriptyline (215 nm), carbamazepine (288 nm), chlorpromazine (256 nm), clomipramine (252 nm), iminodibenzyl (288 nm), imipramine (252 nm), phenothiazine (252 nm), promethazine (252 nm), and thioridazine (264 nm).

Purification of the Products. The extracts produced by the whole-cell system were purified via HPLC with a Nucleodur 100-5 C18 column (250 × 5 mm; Macherey-Nagel). For the preparative column, a gradient from 20% to 80% of B was also used but the flow rate was increased to 1.5 ml/min. The fractions containing product were collected, pooled, and treated with the same volume of 1 M glycine buffer (pH 11.4). After four times of extraction with chloroform, the combined organic fractions were evaporated to dryness and prepared for the NMR analysis.

Analysis of the Products via Gas Chromatography-Mass Spectrometry (GC-MS). GC-MS analysis was performed on a system consisting of an AI/AS 3000 autosampler, a DSQII quadrupole, a Focus GC column oven (Thermo Fisher Scientific, Waltham, MA), and a DB-5 column with a length of 30 m, 0.25 mm i.d., and 0.25 μm film thickness (Agilent Technologies). The compounds were analyzed in an *m/z* range of 30–450. The starting oven temperature was 100°C for 1 minute, and then the temperature was ramped to 320°C for 20°C/min and held for 10 minutes with a flow rate of 1 ml/min. The EI-mass spectra were compared with the NIST Mass Spectral Library (version 2.0; Gaithersburg, MD).

NMR Analysis. The structures of the products were analyzed by NMR spectroscopy (Institut für Pharmazeutische Biologie, Universität des Saarlandes). The ^1H and ^{13}C NMR were recorded on a Bruker (Rheinstetten, Germany) 500 NMR spectrometer. Two-dimensional NMR spectra were recorded as gs-HH-COSY, gs-HSQC, and gs-HMBC. All chemical shifts are relative to $CDCl_3$ (δ = 77.00 for ^{13}C-NMR; δ = 7.24 for ^1H-NMR) using the standard δ notion in parts per million.

Results

In Vitro Conversions. Initially, 10 P450s were used for the in vitro conversion of seven drugs (amitriptyline, carbamazepine, chlorpromazine, clomipramine, imipramine, promethazine, and thioridazine) and two precursors (iminodibenzyl and phenothiazine) to evaluate their ability for the conversion of those compounds. As shown in Table 2, CYP260A1, CYP264A1, CYP267A1, and CYP267B1 were able to convert some of the compounds; however, the remaining six enzymes did not show any conversion. CYP264A1 converts four substrates (amitriptyline, chlorpromazine, clomipramine, and imipramine) with appropriate yields. The main products of amitriptyline, chlorpromazine, and imipramine formed by CYP264A1 and CYP267B1 are identical. However, none of the P450s were able to convert carbamazepine. In general, CYP260A1 and the CYP267 family show lower conversions for the substrates compared with CYP264A1.

The obtained product patterns were different for each substrate. Besides the expected hydrophilic products, several hydrophobic products were also found. CYP260A1, CYP267A1, and CYP267B1 showed different product patterns for the conversion of promethazine. Four products were observed with CYP260A1 and CYP267A1, whereas CYP267B1 gave five products, in which two products [retention time (RT) = 11.2 and 11.6 minutes] were much more hydrophobic than the substrate (RT = 7.6 minutes). We observed that the most hydrophobic product (RT = 11.6 minutes) showed the same RT as that of phenothiazine (see Fig. 1). The conversion of chlorpromazine by CYP260A1 also forms a hydrophobic product (RT = 11.2 minutes). Likewise, low amounts of a hydrophobic product (RT = 12.4 minutes) were also found using CYP267A1 for thioridazine conversion (RT = 9.0 minutes). All other products were more hydrophilic compared with the substrates.

In accordance with these in vitro results, amitriptyline, chlorpromazine, clomipramine, and imipramine were chosen for the *E. coli*–based whole-cell biotransformation by CYP264A1. Amitriptyline and chlorpromazine were chosen for the conversion by CYP267B1. Thioridazine was chosen for the conversion by CYP267A1 to upscale the production for structure elucidation of the products.

TABLE 2

In vitro conversions of the drugs with the corresponding myxobacterial P450s (the observed products are arranged according to their RTs) Dashes mark that there is no conversion.

Substrate	Conversion by			
	CYP260A1	CYP264A1	CYP267A1	CYP267B1
RT [min]	RT [min]	RT [min]	RT [min]	RT [min]
Amitriptyline 8.2	—	P1: 70%/6.2	—	P1: 15%/6.2
		P2: 3%/6.8		
		P3: 18%/7.0		
Carbamazepine 7.7	—	—	—	—
Chlorpromazine 8.5	P1: 9%/11.2	P1: 62%/6.2	—	P1: 39%/6.2
Clomipramine 8.7	—	P1: 69%/7.0	—	Traces of product
		P2: 23%/7.4		
		P3: 2%/8.5		
Imipramine 8.0	—	P1: 52%/6.1	—	P1: 9%/6.1
		P2: 10%/6.5		
		P3: 4%/7.6		
Iminodibenzyl 12.1	—	P1: 3%/8.4	—	P1: 31%/9.3
Phenothiazine 11.6	—	P1: 4%/6.5	—	P1: 8%/6.5
Promethazine 7.6	—	—	—	P1: 4%/6.5
	P2: 15%/7.4		P2: 2%/7.4	P2: 23%/7.4
	P3: 5%/7.9		P3: 3%/7.9	—
	—		—	P4: 3%/10.8
	P5: 17%/11.2		P5: 4%/11.2	P5: 3%/11.2
	P6: 20%/11.6		P6: 5%/11.6	P6: 3%/11.6
Thioridazine 9.0	—	—	P1: 34%/6.9	—
			P2: 5%/7.9	
			P3: 4%/12.4	

Whole-Cell Conversions Using M9CA Medium and Resting Cells. Two different systems for the whole-cell conversions, either using M9CA medium or applying resting cells in buffer, were used to obtain larger amounts of products for NMR characterization. Interestingly, these two systems showed a clear difference concerning substrate conversion. A close correlation between the tested P450s and the conversion of the compounds was not observed (see Fig. 2). CYP264A1 showed higher product yields from amitriptyline, chlorpromazine, and clomipramine with resting cells, whereas a higher yield of the imipramine product was obtained in M9CA medium. In contrast, the yields of the whole-cell conversions with members of the CYP267 family were always higher in M9CA medium. Nevertheless, the ability of CYP267 to convert tricyclic compounds showed their potential pharmaceutical importance to generate derivatives from such compounds.

Product Purification via Preparative HPLC. The products of the corresponding whole-cell conversions were purified via preparative HPLC. The purity of the isolated products was further verified by an additional HPLC measurement before employing it for the NMR measurement. The chromatograms of the purified products and the pure substrates are shown in Supplemental Fig. 1, confirming the successful purifications of the corresponding products. All products were obtained with high purity and sufficient amounts (5–25 mg) for the structure elucidation via NMR spectroscopy.

Structure Elucidation via NMR Spectroscopy and GC-MS. The main products of the CYP264A1-dependent conversion of amitriptyline, chlorpromazine, clomipramine, and imipramine as well as the CYP267A1-dependent conversion of thioridazine were purified and analyzed by NMR spectroscopy. To substantiate the NMR results, the products were additionally analyzed by GC-MS. The ^{1}H NMR,

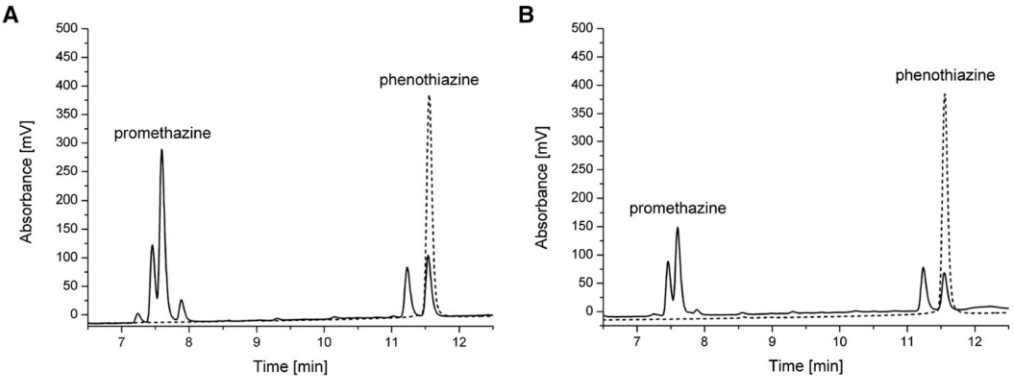

Fig. 1. HPLC chromatograms of the conversions of promethazine (solid lines) with CYP260A1 (A) and CYP267A1 (B) as well as pure phenothiazine (dashed lines). The hydrophobic product at 11.6 minutes shows the same RT as phenothiazine.

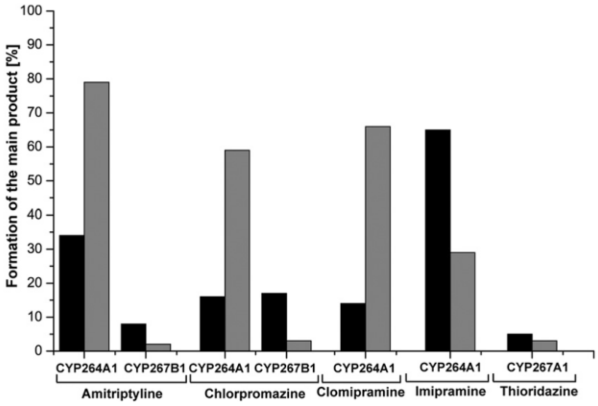

Fig. 2. Conversions of the tricyclic substrates to the corresponding main products. The conversions using M9CA medium (black bar) and resting cells (gray bar) are shown for each substrate.

^{13}C NMR, and GC-MS data are shown in the Supplemental Material (section 2: ^{1}H-NMR, ^{13}CNMR, and GC-MS data).

We observed that the EI-spectra showed a peak with *m/z* of 58, which is correlated to the tertiary ammonium moiety of the dimethylamino propyl group (Frigerio et al., 1972). This peak indicated that the dimethylamino group was intact and a demethylation can be excluded for amitriptyline, chlorpromazine, clomipramine, and imipramine. For clomipramine and imipramine conversion the database comparison of the fragmentation pattern showed the highest identity to the corresponding 10-hydroxy products, whereas chlorpromazine conversion showed the highest identity to chlorpromazine 5-sulfoxide. For the product of thioridazine, an ion with *m/z* of 386 was detected, indicating the insertion of a single oxygen atom. The corresponding 5-sulfoxidated thioridazine product was not available in the NIST database, and therefore it was only elucidated by NMR spectroscopy.

In summary, we showed that the myxobacterial P450s were able to oxidize the heterocyclic ring of the tricyclic compounds (see Fig. 3), in which CYP264A1 and CYP267B1 convert amitriptyline and imipramine to the corresponding 10-hydroxy products, whereas CYP264A1 additionally converts clomipramine to the 10-hydroxy product. In addition, chlorpromazine is sulfoxidated at position 5 by CYP264A1 and CYP267B1. Furthermore, CYP267A1 converts thioridazine to thioridazine 5-sulfoxide. The structures of the products are illustrated in Fig. 3.

Discussion

For the past few years, we have been engaged in the study of novel P450s from myxobacteria, and some P450s from *S. cellulosum* So ce56 have shown a potential for industrial and biotechnological applications (Khatri et al., 2010a,b, 2013, 2014; Ly et al., 2012; Ringle et al., 2013). We were also able to develop an efficient *E. coli*–based whole-cell bioconversion system for some myxobacterial P450s (Ringle et al., 2013). However, the potential applications of those P450s for the production of novel or known drug-related compounds have not yet been studied. Therefore, 10 myxobacterial P450s were investigated concerning their ability to produce human-like or novel drug metabolites from tricyclic psychotherapeutic drugs.

The production of human drug metabolites is an important challenge in the pharmaceutical industry. Drug metabolites formed at greater than 10% of the parent drug systemic exposure at steady state (FDA, 2008) or total drug-related exposure (European Medicines Agency, 2009) need to be tested in toxicological studies, whereby the International Conference on Harmonization guidelines take precedence over the FDA guidelines (Frederick and Obach, 2010; Haglund et al., 2014). For such studies, small (μg) to large quantities (in a gram scale) of these drug metabolites are necessary to provide standards for analytical and toxicological studies, respectively. Utilization of human liver or human liver microsomes is restricted due to limited availability of this human organ. Therefore, alternative ways of producing such metabolites have been investigated. Several approaches, including cell cultures and different microbial systems expressing human P450s as whole-cell biocatalysts to convert drugs, have been described (Crespi et al., 1993; Döhmer, 2001; Drăgan et al., 2011; Geier et al., 2012). However, the low activity and stability of the mammalian P450s compared with the bacterial and fungal P450s are limiting their application at an industrial scale (Julsing et al., 2008; Sakaki, 2012). In addition, the membrane association of the mammalian P450s hinders a simple handling of these enzymes for biotechnological applications, in contrast to the soluble bacterial P450s (Urlacher et al., 2004; Bernhardt and Urlacher, 2014). As a result, bacterial P450s become an alternative method to produce the identical metabolites as those provided by mammalian P450s (Yun et al., 2007; Caswell et al., 2013). Using wild-type microorganisms such as *Cunninghamella* ssp. or *Streptomyces* ssp. for the conversion of drugs is another possibility to obtain sufficient amounts of metabolites (Asha and Vidyavathi, 2009; Murphy, 2015). However, employing such microbial organisms for the production of drug metabolites can be a time-consuming process because of the lack of information regarding the involving enzyme in the biotransformation of the corresponding drug. Therefore, improvements of such a system to obtain higher amounts of a specific product are limited. This can be overcome by the utilization of specific bacterial P450s efficiently expressed in a bacterial whole-cell system as a biocatalyst. In this regard, one of the best characterized bacterial P450s is CYP102A1 (P450BM3) from *Bacillus megaterium*, which has been the target of most engineering efforts to improve activity, selectivity, and the range of substrates (Jung et al., 2011; Whitehouse et al., 2012). However, screening a variety of bacterial P450s for their ability to convert various drugs will certainly lead to a broad range of substrates with high structural diversity to be converted by these P450s. Therefore, we investigated 10 P450s from *S. cellulosum*—a bacterium typically found in soil (Shimkets et al., 2006), where it is exposed to a variety of xenobiotics—for their ability to convert tricyclic drugs.

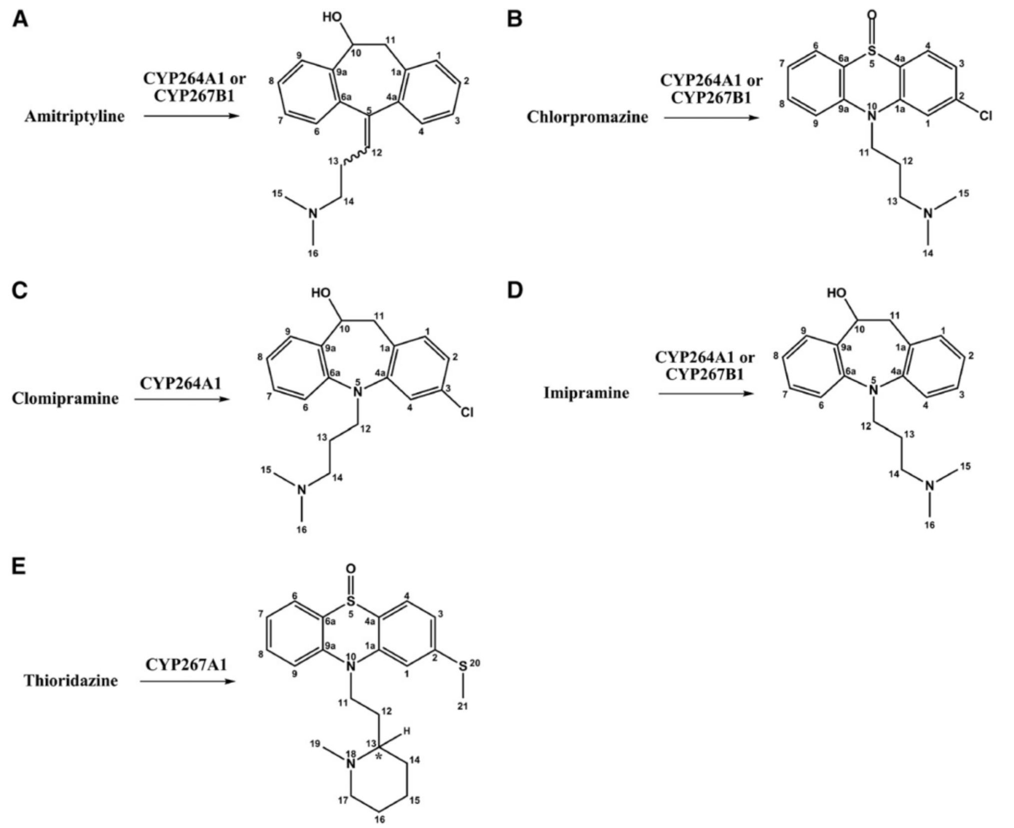

Fig. 3. Conversions of the substrates amitriptyline (A), chlorpromazine (B), clomipramine (C), imipramine (D), and thioridazine (E) by the myxobacterial P450s.

Terpenes and terpenoids as well as fatty acids have already been identified as substrates for these wild-type P450s in previous studies (Khatri et al., 2010a,b, 2014; Ly et al., 2012; Schifrin et al., 2014). Moreover, 4-methyl-3-phenyl-coumarin, a tricyclic molecule, was identified as a substrate for CYP264A1 (Ringle et al., 2013). Here, we can demonstrate that all tricyclic compounds except carbamazepine are converted in vitro by the myxobacterial P450s CYP260A1, CYP264A1, CYP267A1, and CYP267B1. To obtain sufficient amounts of products for structural elucidation, we used an *E. coli*–based whole-cell biotransformation system. The obtained products of amitriptyline, chlorpromazine, clomipramine, imipramine, and thioridazine were purified and characterized by NMR spectroscopy. It is remarkable that these products were indeed the same compounds as those obtained by human liver P450s. The 10-hydroxy products of amitriptyline and imipramine are predominantly formed by CYP2D6, whereas CYP1A2 and CYP3A4 are mainly capable of sulfoxidations of chlorpromazine and thioridazine. Moreover, the myxobacterial P450s show high selectivity for the production of a single major product, whereas the human P450s produce several other side products (see Table 1). Therefore, the ability to produce pure metabolites in a large quantity by the myxobacterial P450s is more suitable compared with the application of human P450s producing several metabolites.

Although 4-methyl-3-phenyl-coumarin has been previously identified as the only substrate for CYP264A1 (Ringle et al., 2013), its product has neither pharmaceutical nor chemical interest. However, the tricyclic moiety of this substrate indicated that CYP264A1 probably needs this structure for substrate recognition. This suggestion was supported by our observation that amitriptyline, chlorpromazine, clomipramine, and imipramine—all containing a tricyclic moiety—were converted by this P450. In addition, CYP264A1 is sensitive to the side chain moiety of the selected tricyclic compounds, since promethazine shows no conversion, whereas chlorpromazine is converted. In this regard, the dimethylamino propyl side chain seems to be necessary for the conversion. In agreement with this assumption, the two precursors, iminodibenzyl and phenothiazine, lacking the side chain, were also nearly not converted. Likewise, thioridazine containing a sterically demanding side chain is also not converted. However, amitriptyline, which possesses a side chain with reduced flexibility caused by the double bond, is converted. Comparing imipramine and clomipramine, there is no significant difference between their conversions, suggesting that the halogen group at the aromatic ring does not seem to play a notable role in the reaction. Unexpectedly, the homolog of this enzyme from the same strain, CYP264B1, which shows no activity toward the tested tricyclic compounds (see Table 2), acts as a norisoprenoid and sesquiterpene hydroxylase (Ly et al., 2012).

Interestingly, we also observed the formation of products being more hydrophobic than the substrate from the conversion of promethazine by CYP260A1 as well as CYP267A1 and CYP267B1. One single hydrophobic product showing an identical RT as phenothiazine has been identified, suggesting that the side chain of promethazine might have been cleaved. Although the oxidative thermal degradation of promethazine has been previously described (Underberg, 1978), the dealkylation of promethazine by P450s has not yet been described. In addition, CYP260A1 also forms a more hydrophobic product from chlorpromazine. However, the formation of N-oxide products could also lead to more hydrophobic products, although these products are mainly formed by flavin-containing monooxygenases (Ziegler, 1993). In addition, ring-opening products are also unlikely due to the fact that these products are obviously more hydrophilic compared with the substrate. However, because of the very low yield we were not able to characterize these products. Interestingly, although tricyclic substrates for CYP267A1 and CYP267B1 were not known before, we identified the psychotherapeutic drugs as substrates for these P450s for the first time. Despite being homologous to each other, CYP267A1 and CYP267B1 showed quite different affinity for the tested substrates. Promethazine is the only common substrate converted by both P450s. However, the ability of CYP267B1 to convert most of the selected drugs makes this enzyme a promising candidate for the conversion of other drugs or drug-related derivatives. Furthermore, improvements of these P450s by protein engineering could lead to higher yields or an increased substrate range (Gillam, 2008).

We also observed that the conversion of tricyclic compounds by the myxobacterial CYP264A1 showed identical main products as those observed by human CYP2D6. There are no crystal structures for human CYP2D6 with the tested substrates or for the myxobacterial P450s available. Therefore, we performed an alignment of CYP2641 and CYP267A1 with human CYP2D6 to determine the substrate binding residues that have been shown in the crystal structure of CYP2D6 (Rowland et al., 2006) and the recent docking study of imipramine with CYP2D6.1 (Handa et al., 2014). Interestingly, the conserved Phe120 and Val374 of CYP2D6, which control the orientation of the substrate, are conserved as Phe61 and Val279, respectively, in CYP264A1, but not in CYP267A1 (see Supplemental Fig. 2). It is assumed that this observation might be the reason for the similar conversion patterns of both CYP264A1 and CYP2D6.

In our study carbamazepine is the only compound that has not been converted by any of the tested myxobacterial P450s. The presence of a double bond in the middle ring forms a higher electron density, which might subsequently hinder the oxidation at this specific position. In addition, the presence of the urea moiety may influence the hydrogen bonds of the substrate-enzyme interactions, which can lead to an incorrect substrate orientation in the active site of the P450. Taken together, our results showed the potential of the myxobacterial P450s as an efficient source for the production of drug metabolites or their derivatives. The products could be used as analytical standards or for toxicological investigations showing their significance for pharmaceutical studies.

Acknowledgments

The authors thank Birgit Heider-Lips for protein purification, Dr. Michael Ringle for providing the pCDF_dFA vector, and Dr. Josef Zapp for measuring the NMR samples. Special thanks are given to Dr. Stephan Lütz for providing two of the substrates.

Authorship Contributions

Participated in research design: Litzenburger, Kern, Bernhardt.
Conducted experiments: Litzenburger, Kern.
Performed data analysis: Litzenburger, Kern.
Wrote or contributed to the writing of the manuscript: Litzenburger, Kern, Khatri, Bernhardt.

References

Asha S and Vidyavathi M (2009) *Cunninghamella*—a microbial model for drug metabolism studies—a review. *Biotechnol Adv* **27:**16–29.
Bernhardt R (2006) Cytochromes P450 as versatile biocatalysts. *J Biotechnol* **124:**128–145.
Bernhardt R and Urlacher VB (2014) Cytochromes P450 as promising catalysts for biotechnological application: chances and limitations. *Appl Microbiol Biotechnol* **98:**6185–6203.
Caswell JM, O'Neill M, Taylor SJ, and Moody TS (2013) Engineering and application of P450 monooxygenases in pharmaceutical and metabolite synthesis. *Curr Opin Chem Biol* **17:**271–275.
Crespi CL, Langenbach R, and Penman BW (1993) Human cell lines, derived from AHH-1 TK+/- human lymphoblasts, genetically engineered for expression of cytochromes P450. *Toxicology* **82:**89–104.
Cunningham Owens, D. G.. A Guide to the Extrapyramidal Side-Effects of Antipsychotic Drugs. 2nd ed. Cambridge: Cambridge University Press, 2014. Cambridge Books Online http://dx.doi.org/10.1017/CBO9781139149112.
Daniel WA, Syrek M, Haduch A, and Wójcikowski J (2000) Pharmacokinetics and metabolism of thioridazine during co-administration of tricyclic antidepressants. *Br J Pharmacol* **131:**287–295.
Demain AL (1999) Pharmaceutically active secondary metabolites of microorganisms. *Appl Microbiol Biotechnol* **52:**455–463.
Döhmer J (2001) [Modern drug development by molecular- and cell-biological methods]. *ALTEX* **18:**9–12.
Drăgan CA, Peters FT, Bour P, Schwaninger AE, Schaan SM, Neunzig I, Widjaja M, Zapp J, Kraemer T, and Maurer HH, et al. (2011) Convenient gram-scale metabolite synthesis by engineered fission yeast strains expressing functional human P450 systems. *Appl Biochem Biotechnol* **163:**965–980.
European Medicines Agency (2009) *ICH Guidance M3(R2) on Non-Clinical Safety Studies for the Conduct of Human Clinical Trials and Marketing Authorisation for Pharmaceuticals*, European Medicines Agency, London.
Food and Drug Administration (2008) *Guidance for Industry: Safety Testing of Drug Metabolites*, U.S. Department of Health and Human Services, Food and Drug Administration, Rockville, MD.
Frederick CB and Obach RS (2010) Metabolites in safety testing: "MIST" for the clinical pharmacologist. *Clin Pharmacol Ther* **87:**345–350.
Frigerio A, Belvedere G, De Nadai F, Fanelli R, Pantarotto C, Riva E, and Morselli PL (1972) A method for the determination of imipramine in human plasma by gas-liquid chromatography-mass fragmentography. *J Chromatogr A* **74:**201–208.
Geier M, Braun A, Emmerstorfer A, Pichler H, and Glieder A (2012) Production of human cytochrome P450 2D6 drug metabolites with recombinant microbes—a comparative study. *Biotechnol J* **7:**1346–1358.
Gillam EM (2008) Engineering cytochrome p450 enzymes. *Chem Res Toxicol* **21:**220–231.
Girhard M, Klaus T, Khatri Y, Bernhardt R, and Urlacher VB (2010) Characterization of the versatile monooxygenase CYP109B1 from *Bacillus subtilis*. *Appl Microbiol Biotechnol* **87:**595–607.
Haglund J, Halldin MM, Brunnström A, Eklund G, Kautiainen A, Sandholm A, and Iverson SL (2014) Pragmatic approaches to determine the exposures of drug metabolites in preclinical and clinical subjects in the MIST evaluation of the clinical development phase. *Chem Res Toxicol* **27:**601–610.
Handa K, Nakagome I, Yamaotsu N, Gouda H, and Hirono S (2014) In silico study on the inhibitory interaction of drugs with wild-type CYP2D6.1 and the natural variant CYP2D6.17. *Drug Metab Pharmacokinet* **29:**52–60.
Hannemann F, Bichet A, Ewen KM, and Bernhardt R (2007) Cytochrome P450 systems—biological variations of electron transport chains. *Biochim Biophys Acta* **1770:**330–344.
Julsing MK, Cornelissen S, Bühler B, and Schmid A (2008) Heme-iron oxygenases: powerful industrial biocatalysts? *Curr Opin Chem Biol* **12:**177–186.
Jung ST, Lauchli R, and Arnold FH (2011) Cytochrome P450: taming a wild type enzyme. *Curr Opin Biotechnol* **22:**809–817.
Kerr BM, Thummel KE, Wurden CJ, Klein SM, Kroetz DL, Gonzalez FJ, and Levy RH (1994) Human liver carbamazepine metabolism. Role of CYP3A4 and CYP2C8 in 10,11-epoxide formation. *Biochem Pharmacol* **47:**1969–1979.
Khatri Y, Girhard M, Romankiewicz A, Ringle M, Hannemann F, Urlacher VB, Hutter MC, and Bernhardt R (2010a) Regioselective hydroxylation of norisoprenoids by CYP109D1 from *Sorangium cellulosum* So ce56. *Appl Microbiol Biotechnol* **88:**485–495.
Khatri Y, Hannemann F, Ewen KM, Pistorius D, Perlova O, Kagawa N, Brachmann AO, Müller R, and Bernhardt R (2010b) The CYPome of *Sorangium cellulosum* So ce56 and identification of CYP109D1 as a new fatty acid hydroxylase. *Chem Biol* **17:**1295–1305.
Khatri Y, Hannemann F, Girhard M, Kappl R, Hutter M, Urlacher VB, and Bernhardt R (2014) A natural heme-signature variant of CYP267A1 from *Sorangium cellulosum* So ce56 executes diverse ω-hydroxylation. *FEBS J* **10:**13104.
Khatri Y, Hannemann F, Girhard M, Kappl R, Même A, Ringle M, Janocha S, Leize-Wagner E, Urlacher VB, and Bernhardt R (2013) Novel family members of CYP109 from *Sorangium cellulosum* So ce56 exhibit characteristic biochemical and biophysical properties. *Biotechnol Appl Biochem* **60:**18–29.
Koeller KM and Wong C-H (2001) Enzymes for chemical synthesis. *Nature* **409:**232–240.
Ly TT, Khatri Y, Zapp J, Hutter MC, and Bernhardt R (2012) CYP264B1 from *Sorangium cellulosum* So ce56: a fascinating norisoprenoid and sesquiterpene hydroxylase. *Appl Microbiol Biotechnol* **95:**123–133.
Murphy CD (2015) Drug metabolism in microorganisms. *Biotechnol Lett* **37:**19–28.
Murray M (2006) Role of CYP pharmacogenetics and drug-drug interactions in the efficacy and safety of atypical and other antipsychotic agents. *J Pharm Pharmacol* **58:**871–885.

Nakamura K, Yokoi T, Inoue K, Shimada N, Ohashi N, Kume T, and Kamataki T (1996) CYP2D6 is the principal cytochrome P450 responsible for metabolism of the histamine H1 antagonist promethazine in human liver microsomes. *Pharmacogenetics* **6:**449–457.

Nelson DR (2011) Progress in tracing the evolutionary paths of cytochrome P450. *Biochim Biophys Acta* **1814:**14–18.

Nielsen KK, Flinois JP, Beaune P, and Brøsen K (1996) The biotransformation of clomipramine in vitro, identification of the cytochrome P450s responsible for the separate metabolic pathways. *J Pharmacol Exp Ther* **277:**1659–1664.

Patel RN (2002) Microbial/enzymatic synthesis of chiral intermediates for pharmaceuticals. *Enzyme Microb Technol* **31:**804–826.

Pearce RE, Vakkalagadda GR, and Leeder JS (2002) Pathways of carbamazepine bioactivation in vitro I. Characterization of human cytochromes P450 responsible for the formation of 2- and 3-hydroxylated metabolites. *Drug Metab Dispos* **30:**1170–1179.

Prox A and Breyer-Pfaff U (1987) Amitriptyline metabolites in human urine. Identification of phenols, dihydrodiols, glycols, and ketones. *Drug Metab Dispos* **15:**890–896.

Ringle M, Khatri Y, Zapp J, Hannemann F, and Bernhardt R (2013) Application of a new versatile electron transfer system for cytochrome P450-based *Escherichia coli* whole-cell bioconversions. *Appl Microbiol Biotechnol* **97:**7741–7754.

Rowland P, Blaney FE, Smyth MG, Jones JJ, Leydon VR, Oxbrow AK, Lewis CJ, Tennant MG, Modi S, and Eggleston DS, et al. (2006) Crystal structure of human cytochrome P450 2D6. *J Biol Chem* **281:**7614–7622.

Sagara Y, Wada A, Takata Y, Waterman MR, Sekimizu K, and Horiuchi T (1993) Direct expression of adrenodoxin reductase in *Escherichia coli* and the functional characterization. *Biol Pharm Bull* **16:**627–630.

Sakaki T (2012) Practical application of cytochrome P450. *Biol Pharm Bull* **35:**844–849.

Schifrin A, Ly TT, Günnewich N, Zapp J, Thiel V, Schulz S, Hannemann F, Khatri Y, and Bernhardt R (2015) Characterization of the gene cluster CYP264B1-geoA from Sorangium cellulosum So ce56: Biosynthesis of (+)-eremophilene and its hydroxylation. *ChemBioChem*, **16**:337–344

Schneiker S, Perlova O, Kaiser O, Gerth K, Alici A, Altmeyer MO, Bartels D, Bekel T, Beyer S, and Bode E, et al. (2007) Complete genome sequence of the myxobacterium *Sorangium cellulosum*. *Nat Biotechnol* **25:**1281–1289.

Shen WW (1999) A history of antipsychotic drug development. *Compr Psychiatry* **40:**407–414.

Shimkets L, Dworkin M, and Reichenbach H (2006) The myxobacteria, in *The Prokaryotes* (Dworkin M, Falkow S, Rosenberg E, Schleifer KH, and Stackebrandt E eds) pp 31–115, Springer, New York.

Singh JK, Solanki A, and Shirsath VS (2012) Comparative in-vitro intrinsic clearance of imipramine in multiple species liver microsomes: human, rat, mouse and dog. *Drug Metab Toxicol* **3:**1000126.

Sono M, Roach MP, Coulter ED, and Dawson JH (1996) Heme-containing oxygenases. *Chem Rev* **96:**2841–2888.

Tanaka E and Hisawa S (1999) Clinically significant pharmacokinetic drug interactions with psychoactive drugs: antidepressants and antipsychotics and the cytochrome P450 system. *J Clin Pharm Ther* **24:**7–16.

Uhlmann H, Kraft R, and Bernhardt R (1994) C-terminal region of adrenodoxin affects its structural integrity and determines differences in its electron transfer function to cytochrome P-450. *J Biol Chem* **269:**22557–22564.

Underberg WJ (1978) Oxidative degradation of pharmaceutically important phenothiazines I: Isolation and identification of oxidation products of promethazine. *J Pharm Sci* **67:**1128–1131.

Urlacher VB and Girhard M (2012) Cytochrome P450 monooxygenases: an update on perspectives for synthetic application. *Trends Biotechnol* **30:**26–36.

Urlacher VB, Lutz-Wahl S, and Schmid RD (2004) Microbial P450 enzymes in biotechnology. *Appl Microbiol Biotechnol* **64:**317–325.

Venkatakrishnan K, Schmider J, Harmatz JS, Ehrenberg BL, von Moltke LL, Graf JA, Mertzanis P, Corbett KE, Rodriguez MC, and Shader RI, et al. (2001) Relative contribution of CYP3A to amitriptyline clearance in humans: in vitro and in vivo studies. *J Clin Pharmacol* **41:**1043–1054.

Weissman KJ and Müller R (2010) Myxobacterial secondary metabolites: bioactivities and modes-of-action. *Nat Prod Rep* **27:**1276–1295.

Whitehouse CJC, Bell SG, and Wong L-L (2012) P450(BM3) (CYP102A1): connecting the dots. *Chem Soc Rev* **41:**1218–1260.

Wójcikowski J, Boksa J, and Daniel WA (2010) Main contribution of the cytochrome P450 isoenzyme 1A2 (CYP1A2) to *N*-demethylation and 5-sulfoxidation of the phenothiazine neuroleptic chlorpromazine in human liver—A comparison with other phenothiazines. *Biochem Pharmacol* **80:**1252–1259.

Yokono A, Morita S, Someya T, Hirokane G, Okawa M, and Shimoda K (2001) The effect of CYP2C19 and CYP2D6 genotypes on the metabolism of clomipramine in Japanese psychiatric patients. *J Clin Psychopharmacol* **21:**549–555.

Yun CH, Kim KH, Kim DH, Jung HC, and Pan JG (2007) The bacterial P450 BM3: a prototype for a biocatalyst with human P450 activities. *Trends Biotechnol* **25:**289–298.

Zanger UM and Schwab M (2013) Cytochrome P450 enzymes in drug metabolism: regulation of gene expression, enzyme activities, and impact of genetic variation. *Pharmacol Ther* **138:**103–141.

Ziegler DM (1993) Recent studies on the structure and function of multisubstrate flavin-containing monooxygenases. *Annu Rev Pharmacol Toxicol* **33:**179–199.

Address correspondence to: Rita Bernhardt, Department of Biochemistry, Saarland University, Campus B2.2, 66123 Saarbruecken, Germany. E-mail: ritabern@mx.uni-saarland.de

Drug metabolism and disposition

"Conversions of tricyclic Antidepressants and Antipsychotics with selected P450s from *Sorangium cellulosum* So ce56"

Martin Litzenburger, Fredy Kern, Yogan Khatri and Rita Bernhardt

Institut für Biochemie, Universität des Saarlandes, Campus B.2.2, 66123, Saarbruecken, Germany

1. Chromatograms of the purified products as well as the pure substrates

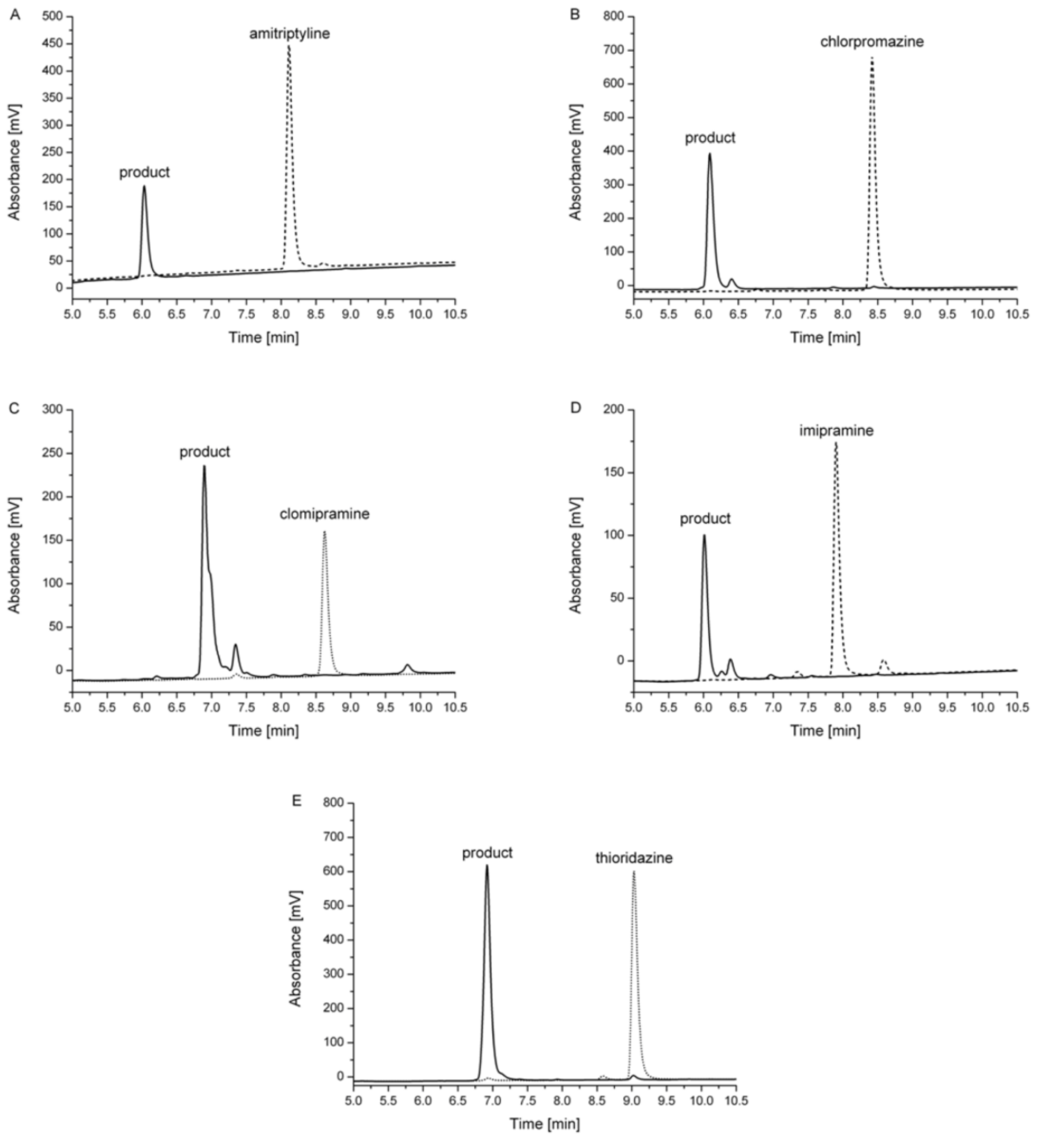

Supplemental Figure 1: Chromatograms of the purified products (solid lines) as well as the pure substrates (dashed lines): amitriptyline (A), chlorpromazine (B), clomipramine (C), imipramine (D) and thioridazine (E).

2. ^{1}H NMR, ^{13}C NMR and GC-MS data

The EI spectra showed a complete fragmentation of the molecules and the relative intensities of the fragments are shown in brackets.

Conversion of amitriptyline by CYP264A1:

NMR-data:

^{1}H NMR ($CDCl_3$, 500 MHz): δ 2.12(s, 6H, H-15 and H-16), 2.21-2.35 (m, 4H, H-13 and H-14), 3.02 (dd, 1H, H-11), 3.59 (dd, 1H, H-11), 5.05 (d, 1H, H-10), 5.89 (t, 1H, H-12), 7.12-7.44 (m, 8H, H-1, H-2, H-3, H-4, H-6, H-7, H-8 and H-9); ^{13}C NMR ($CDCl_3$, 125 MHz): δ 28.08 (C-13), 39.49 (C-11), 45.50 (C-15 and C-16), 59.60 (C-14), 70.27 (C-10), 126.82 (C-7), 127.89 (C-3), 128.12 (C-2), 128.52 (C-8), 128.72 (C-4), 130.26 (C-12), 130.79 (C-1), 131.46 (C-9), 133.99 (C-1a), 138.98 (C-9a), 140.40 (C-6a), 141.34 (C-4a), 142.98 (C-5).

EI mass spectra:

m/z 58.02 (100%), 41.98 (6%), 202.16 (5%), 215.32 (3%), 189.12 (3%), 165.13 (2%), 59.03 (2%) 42.59 (2%), 202.93 (2%), 217.21 (2%).

Conversion of chlorpromazine by CYP264A1:

^{1}H NMR ($CDCl_3$, 500 MHz): δ 1.98-2.08 (m, 2H, H-12), 2.29 (s, 6H, H14 and H15), 2.43 (dt, 2H, H-13), 4.29 (t, 2H, H-11), 7.19 (dd, 1H, H-3), 7.26 (dd, 1H, H-7), 7.50 (d, 1H, H-9), 7.59 (d, 1H, H-1), 7.61 (m, 1H, H-8), 7.84 (d, 1H, H-8), 7.91 (dd, 1H, H-6); ^{13}C NMR ($CDCl_3$, 125 MHz): δ 24.62 (C-12), 45.73 (C-14 and C15), 46.07 (C-11), 56.53 (C-13), 115.98 (C-1), 116.10 (C-9), 121.95 (C-3), 122.28 (C-7), 131.71 (C-6), 132.84 (C-4), 133.04 (C-8), 137.90 (C-9a), 139.02 (C-1a), 142.28 (C-4a), 142.84 (C-6a).

EI mass spectra:

m/z 58.00 (100%), 245.99 (97%), 248.11 (33%), 42.02 (28%), 214.13 (22%), 233.08 (19%), 247.19 (19%), 83.89 (12%), 44.07 (9%), 232.24 (9%).

Conversion of clomipramine by CYP264A1:

^{1}H NMR ($CDCl_3$, 500 MHz): δ 1.67-1.74 (m, 2H, H-13), 2.10 (s, 6H, H-13 and H-14), 2.27 (t, 2H, H-14), 3.15 (dd, 1H, H-11), 3.41 (dd, 1H, H11), 3.75 (t, 2H, C-12), 4.96-5.09 (m, 1H, H-10), 6.89-7.39 (m, 7H, H-1, H-2, H-4, H-6, H-7, H-8, H-9); ^{13}C NMR ($CDCl_3$, 125 MHz): δ 25.95 (C-13), 39.36 (C-11), 45.42 (C-15 and C-16), 48.74 (C-12), 57.49 (C-14), 69.96 (C-10), 118.86 (C-4), 121.02 (C-8), 121.94 (C-2), 123.94 (C-6), 127.12 (C-9), 130.54 (C-7), 132.15 (C-9a), 132.47 (C-1), 133.43 (C-1a), 147.65 (C-6a), 148.48 (C-4a).

EI mass spectra:

m/z 58.09 (100%), 84.78 (26%), 180.21 (20%), 85.32 (19%), 285.02 (18%), 57.45 (17%), 42.22 (15%), 226.92 (14%), 253.71 (14%), 83.90 (12%).

Conversion of imipramine by CYP264A1:

^{1}H NMR ($CDCl_3$, 500 MHz): δ 1.69-1.77 (m, 2H, H-11), 2.11 (s, 6H, H-15 and H-16), 2.29 (t, 2H, H-14), 3.19 (dd, 1H, H-11), 3.45 (dd, 1H, H-11), 3.73-3.84 (m, 2H, H-12), 5.06 (dd, 1H, H-10), 6.94- 7.21 (m, 8H, H-1, H-2, H-3, H-4, H-6,H-7, H-8, H-9); ^{13}C NMR ($CDCl_3$, 125 MHz): δ 26.03 (C-13), 39.81 (C-11), 45.41 (C-15 and C-16), 48.57 (C-12), 57.63 (C-14), 70.48 (C-10), 118.90 (C-8), 120.54 (C-2), 122.25 (C-4), 123.33 (C-6), 126.89 (C-3), 128.04 (C-7), 130.57 (C-9), 130.69 (C-1), 131.97 (C-1a), 134.33 (C-9a), 146.76 (C-6a), 148.76 (C-4a).

EI mass spectra:

m/z 58.00 (100%), 85.10 (29%), 180.09 (27%), 193.11 (27%), 42.02 (23%), 251.22 (19%), 194.14 (16%) 232.22 (15%), 206.23 (12%), 84.04 (12%)

Conversion of thioridazine by CYP267A1:

The use of the racemic mixture of (*R*)- and (*S*)-thioridazine as substrate leads to their respective enantiomeric products. As a consequence, the NMR-signals are duplicated. The enantiomeric signals are labeled as a and b.

^{1}H NMR ($CDCl_3$, 500 MHz): δ 1.33 (m, 2H, H-16a), 1.76 (m, 2H, H-16b), 1.52 (m, 2H, H-15a), 1.65 (m, 2H, H-15b), 1.93 (d, 2H, H-12a), 2.19 (d, 2H, H-12b), 2.11 (m, 2H, H-14a), 2.28 (m, 2H, H-14b), 2.20 (m, 2H, H-17a), 2.27 (s, 2H, H-19a and H-19b), 2.25 (m, 2H, H-13a and H-13b), 2.37 (s, 2H, H-19a and H-19b), 2.72(s, 2H, H-19a and H-19b) 2.91 (m, 2H, H-17b), 2.58 (s, 3H, H-21a), 2.59 (s, 3H, H-21b) 3.96 (m, 2H, H-11a), 4.05 (m, 2H, H-11b), 6.94 (d, 1H, H-4a), 6.98 (t, 1H, H-4b), 7.07 (dd, 1H, H-7a), 7.11 (dt, 1H, H-7b), 7.17 (d, 1H, H-3a), 7.22 (t, 2H, H-3b), 7.24 (d, 1H, H-1a), 7.26 (d, 1H, H-1b), 7.25 (m, 1H, H-9a), 7.28 (m, 1H, H-9b), 7.45 (m, 1H, H-6a), 7.63 (m, 1H, H-6b), 7.83 (m, 1H, H-8a), 7.93 (m, 1H, H-8b); ^{13}C NMR ($CDCl_3$, 125 MHz): δ 15.37 (C-21), 23.85 (C-16a), 30.33 (C-16b), 25.07 (C-15a), 25.10 (C-15b), 29.13 (C-14a), 29.16 (C-14b), 29.61 (C-12a), 29.64 (C-12b), 44.04 (C-11a), 44.70 (C-11b), 56.66 (C-17a), 56.70 (C-17b), 61.95 (C-13a), 62.20 (C-13b), 109.76 (C-9a), 109.83 (C-9b), 115.95 (C-4a and C-4b), 117.25 (C-7a), 119.05 (C-7b), 124.44 (C-2a and C-2b), 127.62 (C-3a), 127.66 (C-3b), 127.85 (C-1a), 127.89 (C-1b), 129.14 (C-6a-a), 129.17 (C-6a-b), 144.35 (C-4a-a and C-4a-b), 144.94 (C-1a-a), 144.96 (C-1a-b), 145.55 (C-9a-a), 145.64 (C-9a-b).

EI mass spectra:

m/z 98.08 (100%), 97.13 (14%), 244.94 (13%), 206.88 (12%), 42.03 (12%), 195.93 (11%), 223.07 (11%), 196.79 (10%), 211.20 (10%), 386.06 (9%)

3. Comparison of CYP264A1 and 267A1 with human CYP2D6

```
CYP264A1        ---------------------------------------MSERVDIMTPAFRADPYTPYA 21
CYP267A1        ------------------MNSPDAPKPDAPPAANPAADADLDPFRLQSPETLANPYPVYA 42
CYP2D6          MGLEALVPLAVIVAIFLLLVDLMHRRQRWAARYPPGPLPLPGLGNLLHVDFQNTPYCFDQ 60

CYP264A1        AMRREAPVC-------------QVDPGGMWAVSRYADVATVLRSP-------ERFSSQGF 61
CYP267A1        RLRQEAPVY-------------FSAAYNGWLITRYDQVAAGFRDPRLSAKRSSAFVTKLP 89
CYP2D6          LRRRFGDVFSLQLAWTPVVVLNGLAAVREALVTHGEDTADRPPVPITQILGFGPRSQGVF 120

CYP264A1        RAAWQPAWVGHNPLASSILAMDGPDHARLRGLVSRAFGAPAIARIEQ-----RARDLCER 116
CYP267A1        DEVRQRLEPLRRNLASWALLLDPPEHTRIRSLINKAFVPRLVEGLRS-----RVETLVNE 144
CYP2D6          LARYGPAWREQRRFSVSTLRNLGLGKKSLEQWVTEEAACLCAAFANHSGRPFRPNGLLDK 180

CYP264A1        LAGRLD--GEVDFIAAAAAPLPAFVISELLGLDHALEPHFKRWMDDLLSVT-PEPASAEH 173
CYP267A1        LLDAVAPAGRMDVLRDLGDLLPLLVIGEVLGVPAEDRHRLKGWSNALSGFLGAGRPTLEI 204
CYP2D6          AVSNVIASLTCGRRFEYDDPRFLRLLDLAQEGLKEESGFLREVLNAVPVLLHIPALAGKV 240


CYP264A1        AARVRATIAELDRYMADVIAARR-----RSPSDDLVSELARA----GELLGDREIIDLLV 224
CYP267A1        AGGALSAVAELEDYFRGVIAARR-----QSPGNDLLSQLILAE-EQGMILGEQELLSTCC 258
CYP2D6          LRFQKAFLTQLDELLTEHRMTWDPAQPPRDLTEAFLAEMEKAKGNPESSFNDENLRIVVA 300

CYP264A1        SILGGGLETTTHFLGSSMLLLAERPAELERLR------------------ASPQLIPRFI 266
CYP267A1        MLLFGGHETTKNLIGNGLLALLLHRSEREALR------------------ATPSLIGPAV 300
CYP2D6          DLFSAGMVTTSTTLAWGLLLMILHPDVQRRVQQEIDDVIGQVRRPEMGDQAHMPYTTAVI 360

CYP264A1        EEMMRYDGPTQS-VPRLTTSDVALAGVTIPAGSLVLALVGSANRDEVRFTDPDRFD---- 321
CYP267A1        EELLRYDSPVQW-MSRVALDDIELDGVRIPKGDRAFLVLGAANRDPAQFPDPDKLD---- 355
CYP2D6          HEVQRFGDIVPLGVTHMTSRDIEVQGFRIPKGTTLITNLSSVLKDEAVWEKPFRFHPEHF 420

CYP264A1        -----LHRGQP-SLTFGHGAHFCLGAALARMEAKVALEVLVPRIGEVTRAPGEIPYNRTL 375
CYP267A1        -----FRRTDIRHISLGLGVHYCAGSALARVEAQAAISTFLRRFPDAELSPGPLTWRMNP 410
CYP2D6          LDAQGHFVKPEAFLPFSAGRRACLGEPLARMELFLFFTSLLQHFSFSVPTGQPRPSHHGV 480

CYP264A1        TVRGPVSLPLRFRPA---- 390
CYP267A1        GMRGVTALPIELGPQSSAS 429
CYP2D6          FAFLVSPSPYELCAVPR-- 497
```

Supplemental Figure 2: Multiple sequence alignment of human CYP2D6 (AFX95842.1), and the S. cellulosum So ce56 CYP264A1 (YP_001616970.1) and CYP267A1 (YP_001611312.1). The amino acid sequences of CYP2D6, CYP264A1 and CYP267A1 were retrieved from EMBL database (http://www.ebi.ac.uk/embl/) and aligned by Clustal W2 (http://www.ebi.ac.uk/Tools/msa/clustalw2/). The absolutely conserved amino-acid residues are highlighted in grey, and the yellow highlight indicates the interacting residues during docking of imipramine as described (Handa et al., 2014).

Handa K, Nakagome I, Yamaotsu N, Gouda H, and Hirono S (2014) In Silico Study on the Inhibitory Interaction of Drugs with Wild-type CYP2D6.1 and the Natural Variant CYP2D6.17. *Drug Metabolism and Pharmacokinetics* 29:52-60.

4 General discussion

In this Thesis, the myxobacterial P450 CYP167A1 (EpoK) from *S. cellulosum* So ce90 was investigated with respect to different hetero- and autologous redox partners. Furthermore, the CYP109, CYP260, CYP264 and CYP267 families and the individual CYP265A1 and CYP266A1 from *S. cellulosum* So ce56 were investigated toward a conversion of epothilone D, the natural substrate of EpoK. Since the CYP267 family, and especially CYP267B1, turned out to be related to drug metabolizing bacterial P450s, their potential application as drug metabolizers was investigated *in vitro* and in a whole-cell system by testing a broad spectrum of drug compounds.

4.1 CYP167A1 (EpoK): the search for efficient redox partners

The substrates of EpoK, epothilone C and D, are 16-membered macrolides with the ability to block the mitosis rate by targeting microtubules (Mulzer *et al.*, 2008). This characteristic makes this compound class to one of the most efficient anticancer drugs to date (Mukhtar *et al.*, 2014). The products of EpoK, epothilone A and B were first discovered in 1987 as antifungal compounds in the fermentation broth of *S. cellulosum* and later in 1995, their cytotoxic activity was found (Gerth *et al.*, 1996; Hofle *et al.*, 1996). In fact, epothilone B turned out to be the most promising and active anticancer drug candidate and is approved for the treatment of breast cancer in the U.S. by substituting the lactone with an amide functionality (Brogdon *et al.*, 2014).

Since the epothilones are secondary metabolites and naturally produced in the myxobacterium *S. cellulosum* (Wenzel and Müller, 2009), the large-scale isolation of these compounds is hindered by their low production in this organism and by their extraction and purification afterwards. Even though the biosynthetic pathway of epothilones (Figure 12) was elucidated (Tang, 2000) and, by now, the purification of nearly 40 mg epothilone B out of a crude extract of *S. cellulosum* fermentation broth is possible, the required effort of using complex methods like high-speed counter-current chromatography in combination with a two-phase purification system is extraordinary high (Yang *et al.*, 2014). To overcome these fermentation-dependent limitations, several other approaches are of in-terest to enable a sufficient production of epothilones.

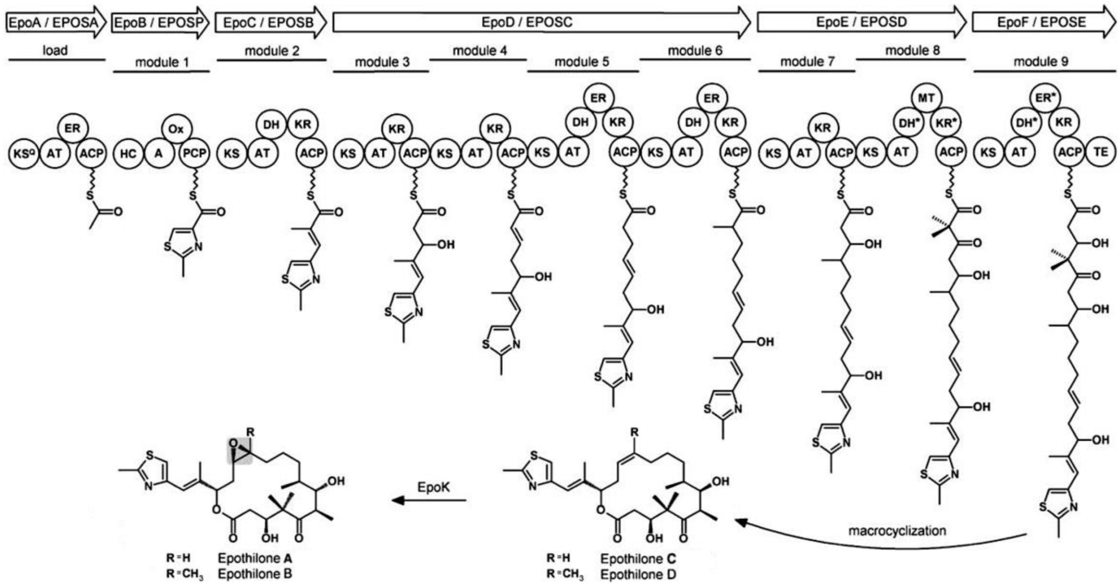

Figure 12. Epothilone biosynthesis in *S. cellulosum* So ce90 (modified and taken from (Mulzer *et al.*, 2008)).

The expression of the epothilone biosynthetic gene cluster in *E. coli* led to the successful implementation and heterologous production of epothilones C and D (Mutka *et al.*, 2006). Analogous experiments were also performed in *Myxococcus xanthus* (Julien and Shah, 2002). With the specific optimization of the individual polyketide synthases leading to high production of intermediates of the epothilone biosynthesis (Lau *et al.*, 2004) or a precursor-directed approach (Boddy *et al.*, 2004), a complete heterologous production of the desired epothilone B is conceivable. Nevertheless, the lack of studies heading toward such an approach might be attributed to the missing electron transfer system for EpoK and its involvement in the important last-step epoxidation of epothilone D to B. The only successful enhancement of epothilone B formation in the fermentation broth was achieved by bypassing the use of EpoK. The insertion of the genes of *Vitreoscilla* hemoglobin (to improve secondary metabolite production) and the P450 epoxidase EpoF in *S. cellulosum* So ce M4 shifted the epothilone production to the desired epothilone B product (Ye *et al.*, 2016).

However, the opportunity for a direct implementation of the natural epothilone epoxidase EpoK might be more beneficial. Within this study, a novel and highly efficient redox system for EpoK was found and characterized. The usage of SynFdx from *Synechocystis* and FNR from *C. reinhardtii* with EpoK resulted in the most efficient epothilone B formation described to date. The experimental determination of the kinetics resulted in a v_{max} value which is remarkably more than seven orders of magnitude higher than the one described for EpoK supported by the spinach redox partners (Kern *et al.*, 2015). The insertion of their genes into the organism of *S. cellulosum* or into a heterologous production host like *E. coli* might lead to a sufficient production of the epoxidized products of interest, epothilone A and B. Furthermore, the search for the unknown natural redox partners of EpoK for the biosynthesis of the products would be promoted by a further investigation of the *S. cellulosum* So ce90 genome. Since the autologous Fdx8 and FdR_B from *S. cellulosum* So ce56 were shown to transfer electrons to EpoK *in vitro* (Kern *et al.*, 2015), a bioinformatics study could elucidate homologs of them as natural redox partners and provide the opportunity for an alternative redox system for EpoK and its epoxidation of epothilone D to B.

4.2 Derivatization of epothilone D with myxobacterial P450s

As mentioned previously, epothilones are promising anticancer compounds and offer further conceivable application possibilities, which makes them interesting targets for drug design. Novel epothilone derivatives are, therefore, desirable compounds and of great interest for pharmaceutical research (Brogdon *et al.*, 2014). The efforts for a derivatization of epothilones by means of total chemical synthesis (Mulzer *et al.*, 2008), chemical modifications (Zhang *et al.*, 2014) or additional biotransformation steps (Basch and Chiang, 2007) are numerous and show the demand for new epothilone compounds. Although there was so far no epothilone derivative found with a higher activity toward cancer treatment compared to epothilone B (Table 1, chemical structures can be found in Figure S 1), the altered compounds might be also interesting with respect to investigations concerning their use in the treatment of Alzheimer’s or Parkinson’s diseases, since epothilone D has been shown to decrease the accumulation of tau protein and to rescue microtubule defects (Zhang *et al.*, 2012; Cartelli *et al.*, 2013). However, the derivatives 26-fluoro epothilone B or sagopilone, an epothilone B analog with an additional propenyl group, showed IC_{50} values comparable to epothilone B. The alteration of the epothilone B structure usually results in an increased IC_{50} value as observed for ixabepilone, a lactam epothilone B analogue, or KOS-1584, an epothilone B analog with an additional double bond between C9 and C10. Epothilone D also features low IC_{50} values for different cell lines like MCF7 or KB-31, whereas hydroxylated epothilone D derivatives exhibit higher IC_{50} values as shown for 14-, 21- or 26-hydroxy epothilone D, respectively (Table 1).

Table 1. Overview of selected epothilone derivatives and their activity against cancer cell lines. (a: (Altmann *et al.*, 2000), b: (Chou *et al.*, 1998), c: (Tang *et al.*, 2003), d: (Lee *et al.*, 2001), e: (Chen *et al.*, 2008), 'alt. name' = alternative name)

Compound (alt. name)	**IC_{50} [nM] (cell line)**	**Further references and comments**
Epothilone B	0.18[a] (KB-31), 0.5[b] (MCF7)	(Kowalski *et al.*, 1997; Meier *et al.*, 2013)
26-Fluoro epothilone B	0.26[a] (KB-31)	(Nicolaou *et al.*, 1998; Newman *et al.*, 2001; Koch *et al.*, 2004)
Ixabepilone (BMS-247550)	2.7[d] (MCF7)	(Goodin, 2008; Pishvaian and Smaglo, 2014)
Sagopilone (ZK-EPO)	<1[d]	(Galmarini, 2009; Stupp *et al.*, 2011)
KOS-1584	6 (MCF7)	(Zhou *et al.*, 2005)
Epothilone D (KOS-682)	2.7[a] (KB-31), 2.9[b] (MCF7), 9[c] (MCF7), 16[e] (PC3)	(Monk *et al.*, 2012)
9-Hydroxy epothilone D	280[c] (MCF7)	
11-Hydroxy epothilone D	21[c] (MCF7)	
14-Hydroxy epothilone D	29[c] (MCF7)	
S-14-Methoxy epothilone D	3.7 (MCF7)	(Frein *et al.*, 2009)
21-Hydroxy epothilone D (Epothilone F)	23[c] (MCF7)	(Basch and Chiang, 2007)
26-Hydroxy epothilone D	95[c] (MCF7)	(Nicolaou *et al.*, 1998)
26-Fluoro epothilone D	7.5[a] (KB-31)	(Koch *et al.*, 2004)
EPO490	25[c] (MCF7)	(Njardarson *et al.*, 2002)
Bridged epothilone D	77[e] (PC3)	IC_{50} value taken from compound 30

In contrast to the majority of the described attempts toward a derivatization of epothilones via chemical synthesis or biotransformation in different microorganisms, in this study, the derivatization of epothilone D was achieved with the use of myxobacterial P450s of *S. cellulosum* So ce56. The P450s tested were selected by their relatedness to EpoK from *S. cellulosum* So ce90, whereby the CYP109, CYP260, CYP264 and CYP267 families and the individual CYP265A1 and CYP266A1 were selected for an epothilone D conversion. In contrast to the CYP109, CYP260 and CYP264 families of *S. cellulosum* So ce56 showing no activity, CYP265A1 and CYP266A1 were found to convert epothilone D to 14-hydroxy epothilone D (Kern *et al.*, 2015). Besides the fact that epothilone D is the first substrate found for these P450s, the autologous redox systems from *S. cellulosum* So ce56 were also found to be more efficient for the required electron supply than *bovine* $Adx_{4\text{-}108}$/AdR. For CYP265A1, each of the tested redox systems (*bovine* $Adx_{4\text{-}108}$/AdR and the autologous Fdx2/FdR_B and Fdx8/FdR_B) showed the ability to support this P450 with electrons, with Fdx8/FdR_B showing highest conversion of epothilone D yielding 6% 14-hydroxy epothilone D (Kern *et al.*, 2015). In case of CYP266A1, attempts of using the spinach redox system or bovine Adx_{4-108}/AdR for its reduction have been previously shown to be unsuccessful (Khatri, Hannemann, *et al.*, 2010). In this study, the ineffective use of the heterologous Adx_{4-108}/AdR confirmed these earlier studies of CYP266A1. However, the conversion of epothilone D by CYP266A1 was achieved using autologous redox partners, where the highest activity was observed with Fdx2/FdR_B yielding 6.9% 14-hydroxy epothilone D (Kern *et al.*, 2015). In addition, these results open the possibility to further investigate the substrate spectrum of CYP265A1 and CYP266A1. CYP266A1 owns an interesting solitary and distant position within the phylogenetic tree of the CYPome of *S. cellulosum* So ce56, which might be an indication for a special or extraordinary substrate acceptance. Moreover, the expression yield of CYP266A1 is very high (1400 nmol/l, (Khatri, Hannemann, *et al.*, 2010)), which would be a supporting and encouraging basis toward further *in vitro* and potential whole-cell experiments.

Epothilone D was also converted by CYP267B1, which showed the remarkable ability to convert epothilone D into 5 different products. Thereby, the highest yields were also observed when using the autologous redox partners Fdx8/FdR_B from *S. cellulosum* So ce56. Among epothilone B, also 14-, 21- and 26-hydroxy epothilone D were found. The products epothilone B and 26-hydroxy epothilone D showed a combined yield of 11.7% and with a yield of 4.8% and 5.5%, 14-hydroxy and 21-hydroxy epothilone D were also found to be side products of the epothilone D conversion by CYP267B1 (Kern *et al.*, 2015). However, in case of these hydroxylated epothilone D derivatives, their usage as precursors for a subsequent chemical modification might be of interest. Therefore, chemical modifications at position 14 (etherification with methanol, (Frein *et al.*, 2009)), position 21 (oxidation to ketone functionality, (Nicolaou *et al.*, 1998)) and position 26 (fluorination, (Koch *et al.*, 2004)) might be feasible by using the corresponding hydroxylated epothilone D derivatives as precursor instead of their complex bottom-up chemical synthesis. These functionalized derivatives would be accessible more easily using a chemo-enzymatic production. Most interestingly, the fifth epothilone derivative formed by CYP267B1 turned out to be a novel und unknown epothilone derivative, 7-ketone epothilone D. In fact, this epothilone derivative was found to be the main product of the epothilone D conversion by CYP267B1 with a 8.7% yield (Kern *et al.*, 2015). An oxidation of the hydroxyl group at position 7 was not described yet and the effect of this modification on the pharmacological activity of epothilone D is, therefore, unexplored. This product is an interesting candidate for further pharmacological testing both for potential antitumor activity and for the treatment of Alzheimer's or Parkinson's disease.

4.3 Selection of drugs as potential substrates for myxobacterial P450s

In order to investigate the substrate spectrum of myxobacterial P450s from *S. cellulosum* So ce56 toward pharmaceutical drugs and their ability to produce respective drug metabolites, a substrate library of different chemical structures was established. To increase the relevance of this substrate library, 14 of the selected drugs (amitriptyline, amodiaquine, carbamazepine, chlorpromazine, clomipramine, dexamethasone, haloperidol, ibuprofen, nifedipine, omeprazole, ritonavir, tamoxifen, testosterone, verapamil) are representatives of the World Health Organizations List of Essential Medicines, the most important medications needed in a basic health system (World Health Organization, 2013). The usage of this library should lead to a general impression of the substrate acceptance as well as potential fields of application for myxobacterial P450s. An overview of the tested drug molecules is presented in Figure 13 and Figure 14, where the compounds are clustered according to similar basic chemical motifs.

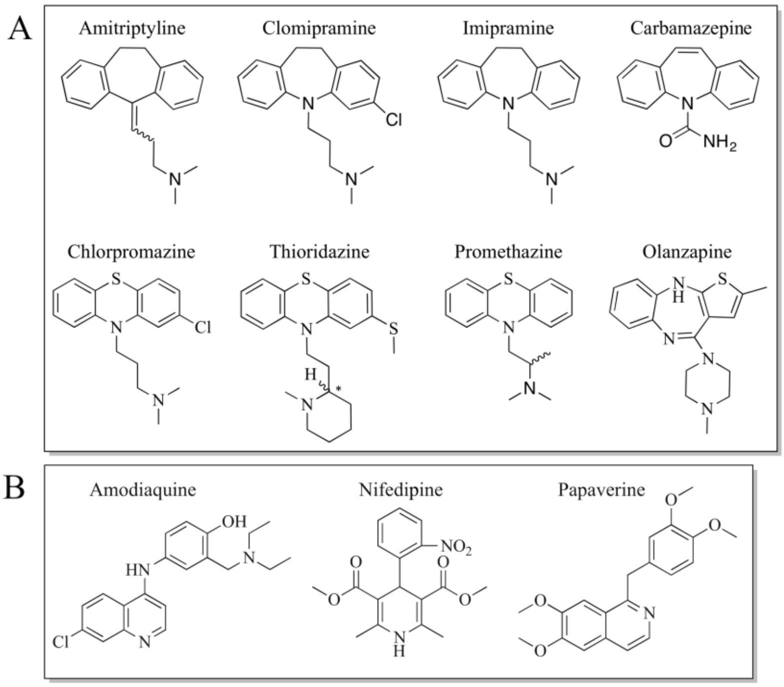

Figure 13. Part I: Substrates investigated in this study clustered after their structure as tricyclic (A) and pyridine compounds (B).

The first group of the tested substrates belong to tricyclic compounds as shown in Figure 13 A. This substance class acts as inhibitor for serotonin and norepinephrine transporters (Gillman, 2007). The down-regulation of these transporters has a beneficial effect on mental disorders like depression and anxiety (Rénéric and Lucki, 1998). The second group tested consist of pyridine analogs as presented in Figure 13 B. Although amodiaquine and papaverine share a similar overall structure, their field of application is different. While amodiaquine is used for the treatment of malaria since the 1950s (Li *et al.*, 2002), papaverine is predominantly used for the treatment of cerebral vasospasm (Liu and Couldwell, 2005). The third substrate listed in this group is nifedipine, an antihypertensive drug also used in the therapy of the Raynaud-syndrome (Varon and Marik, 2003; Anderson *et al.*, 2004).

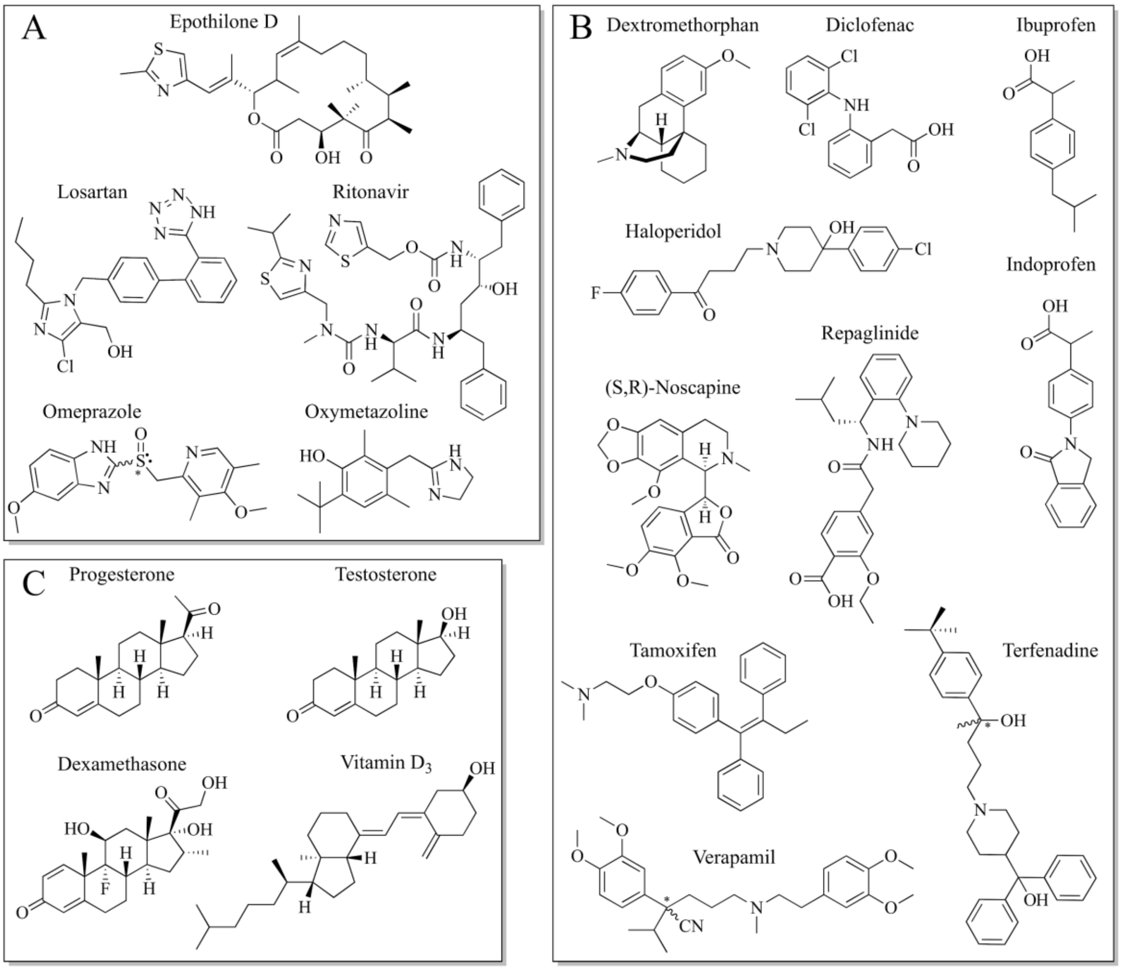

Figure 14. Part II: Substrates investigated in this study clustered after their structure as azole (A), benzene (B) and (seco-)steroid (C) compounds.

The second overview of the tested substrates starts with the clustering of compounds containing an azole group (Figure 14 A). Apart from the macrolide epothilone D, which was already discussed in previous sections, four more drug compounds with azole residues were investigated. Analogous to nifedipine, losartan is also an antihypertensive compound, but with a much more specific mechanism and higher affinity to block the angiotensin-I receptor (McIntyre *et al.*, 1997). Together with lopinavir, the third compound, ritonavir, is the first and only co-formulated HIV-1 protease inhibitor and is effectively used in the treatment of HIV-1 infection (Chandwani and Shuter, 2008). The next two substrates are omeprazole and oxymetazoline, both smaller compounds as the previously mentioned azole derivatives. Omeprazole is a prodrug which is converted to its active form only at the desired site of action, the parietal cell, to reduce gastric acid secretion (Oosterhuis and Jonkman, 1989). On the other hand, due to vasoconstricting properties, the latter drug, oxymetazoline, is used in nasal sprays for the treatment of nasal congestion (Krempl and Noorily, 1995).

In Figure 14 B, the ten compounds with benzene functionality are clustered and provide a high structural variety. Dextromethorphan as well as noscapine are the active ingredients in a variety of widely used cough remedies (Church *et al.*, 1989). Although dextromethorphan exhibits a tricyclic basic structure, it belongs to the morphinan class. However, this compound was clustered within the benzene group with respect to its pharmacological effect together with noscapine and other non-steroidal analgesics, namely diclofenac, ibuprofen and indoprofen. The latter three compounds are also considered as anti-inflammatory and share the common mechanism of inhibiting cyclooxygenase activity (FitzGerald and Patrono, 2001). Another compound listed in this class is haloperidol, an effective antipsychotic for the treatment of schizophrenia or Tourette syndrome, respectively (Irving *et al.*, 2006). Analogous to the linear structure of haloperidol, terfenadine and verapamil are also clustered within this group. Terfenadine is an antihistamine and effectively used as antiallergic drug (Thompson and Oster, 1996) and verapamil is the third drug for the treatment of hypertension used as substrate in this study (Chen *et al.*, 2010). The last two compounds in this group are repaglinide and tamoxifen. The first one is used for the treatment of type 2 diabetes mellitus (Scott, 2012) and tamoxifen is another anticancer compound (EBCTCG, 1998).

The last clustered compounds tested are (seco-)steroidal structures (Figure 14 C). To test the activity of myxobacterial P450s toward steroids, testosterone, progesterone and dexamethasone were selected. Testosterone is used in replacement therapy to treat hypogonadism in males (Kumar *et al.*, 2010) and progesterone is the most important progestogen in the body involved in the biosynthesis of major hormones and corticosteroids (Yamazaki and Shimada, 1997) and is also used in the treatment of various diseases. The last steroidal compound is dexamethasone, a multifaceted drug with a broad spectrum of anti-inflammatory and anti-allergic benefits (Gao *et al.*, 2003). Additionally, vitamin D_3 was also investigated during this study to extend the steroidal basic structure with one representative of secosteroids. Vitamin D_3 is important for muscle and bone health and can be used as a supplement to treat deficiencies (Stroud *et al.*, 2008).

In terms of experimental procedures, the diverse chemical structures and functional groups required additional consideration. To ensure an optimal extraction and HPLC analysis, substrate-dependent protocols and methods were established. The extraction protocol was optimized by comparing the solvents ethyl acetate and chloroform as extraction agents in control experiments (only 100 µM substrate in reaction buffer, 3 hours at 30°C). In general, the presence of a nitrogen in the chemical structure of the substrate resulted in additional peaks in the chromatogram. To prevent these interference factors, an additional step of increasing or decreasing the pH before extraction was established using glycine (pH 11) or acetic acid/acetate buffer (pH 4). The resulting deprotonated or protonated drug molecule enabled a reproducible and distinct HPLC analysis. The absorption maxima of the substrates were determined in the spectrophotometer (reaction buffer, 200 µM) and used in the respective HPLC methods. As a result, a favorable and reproducible analysis procedure was found for all drug compounds, both for *in vitro* and whole-cell experiments and a substrate-dependent protocol was established. This provided access to an interesting and diverse drug library to investigate and enlarge the known substrate spectrum of myxobacterial P450s from *S. cellulosum* So ce56.

4.4 Investigation of the substrate spectrum of CYP267A1 and CYP267B1

Bioinformatics studies showed a high relatedness of the CYP267 family to distinct bacterial drug metabolizers in comparison to the other P450s of *S. cellulosum* So ce56 (Kern *et al.*, 2016). The phylogenetic relatedness to drug metabolizing P450s proved to be a good indication for testing different drug molecules as substrates. This novel P450 family consists of two members, of which the first, CYP267A1, was previously found to convert fatty acids to their respective hydroxylated products (Khatri *et al.*, 2015). Since the second member, CYP267B1, was shown to convert the anticancer drug epothilone D in this study, both members of the CYP267 family, CYP267A1 and CYP267B1, were selected for a comprehensive investigation toward their ability to convert drug compounds. Concerning this, *in vitro* conversions of the structurally diverse drug library were performed with CYP267A1 and CYP267B1. Out of the established library, seven and 14 new substrates were found for CYP267A1 and CYP267B1, respectively. The activity of CYP267B1 towards steroidal compounds like testosterone and progesterone (Ziska, 2011) was also confirmed. In general, the usage of the autologous Fdx8/FdR_B as redox partners for the CYP267 family turned out to be more favorable compared to the *bovine* Adx_{4-108}/AdR and resulted in higher yields within the *in vitro* conversion of drug molecules as demonstrated for the increased *in vitro* conversion of amitriptyline by

CYP267B1, respectively (from 15% to 60% 10-hydroxy amitriptyline, when using CYP267B1-Fdx8-FdR_B (Kern *et al.*, 2016)).

The rough clustering of the compounds in different groups of basic chemical motifs was primarily performed to screen associated substrates with different sizes and topology. The second motive was to find and clarify potentially favored substance classes or chemical motifs as distinctive feature for the acceptance as a substrate for the CYP267 family. Indeed, a high number of hits was observed for the tricyclic compounds (Figure 13 A), with seven out of eight compounds showing an *in vitro* conversion with CYP267B1. In comparison, CYP267A1 is able to convert only thioridazine. In the group of pyridine analogs (Figure 13 B), only the structurally similar amodiaquine and papaverine are converted by CYP267B1, whereby CYP267A1 showed no activity. All five compounds containing azole functionalities (Figure 14 A) are accepted as a substrate for CYP267B1 only, although their chemical structures range from 15-membered macrolides like epothilone D to small phenol derivatives like oxymetazoline. The members of the CYP267 family showed similar and complementary substrate acceptance for eight out of the ten compounds of the second last group (benzene derivatives, Figure 14 B). While dextromethorphan and haloperidol are only converted by CYP267A1, ibuprofen, tamoxifen and terfenadine are converted by both, CYP267A1 and CYP267B1. Diclofenac and noscapine are only converted by CYP267B1. The two compounds showing no conversion are indoprofen and verapamil. The substitution of the isobutyl group of ibuprofen with an isoindolin-1-one residue seems to have a significant influence on the binding of the resulting derivative indoprofen in the active site of CYP267B1. Only for CYP267B1, the steroids testosterone and progesterone of the (seco-)steroidal group in Figure 14 C are accepted as a substrate with an *in vitro* conversion of 7% and 18% by CYP267B1-Fdx8-FdR_B, respectively. These results confirm steroids as a potential substrate class for CYP267B1.

The diverse catalytic activities, which were observed here for CYP267A1 and especially CYP267B1, are known only for human CYP3A4 (Park *et al.*, 2005), but very uncommon for bacterial P450s (Yin *et al.*, 2014). The most studied bacterial P450, CYP102A1 (BM3) from *B. megaterium*, was genetically modified toward a broader substrate range by rational protein design (Whitehouse *et al.*, 2012; Ren *et al.*, 2015). However, native bacterial P450s featuring a broad substrate range are rare. CYP105D1 from *S. griseus* has been demonstrated to feature an unusually wide substrate range and was long known for being the only bacterial P450 comparable to human CYP3A4 in terms of substrate range (Taylor *et al.*, 1999). Likewise, CYP116B4 ($P450_{LaMO}$) from *L. aggregata* was recently shown to be a versatile bacterial P450, which couples its self-sufficient nature with a broad substrate range toward different compounds like sulfide derivatives, aromatic and bicyclic hydrocarbons and olefins (Yin *et al.*, 2014).

4.5 Production of drug metabolites with CYP267A1 and CYP267B1

As a consequence of the previously mentioned guideline for the detection of drug metabolites during drug development and clinical phases (chapter 1.3), the availability of human drug metabolites for toxicological tests or as authentic reference standards is desired by the pharmaceutical industry. Genetic polymorphisms, especially in human P450s, have been linked to interindividual differences in the efficacy and toxicity of many medications (Evans and Relling, 1999). The altered metabolism of drugs by poor metabolizers and the resulting drug-drug interaction require authentic human drug metabolites for toxicological studies. Another application of reference standards arises from the increased and self-evidently use of drugs in every day life. Excreted by humans, drug compounds and their metabolites reach our groundwater. An enhanced surveillance of water quality and detailed information on the concentration and fate of drugs in the environment or wastewater treatment plants is, therefore, of high interest. The whole-cell system established in this work is able to produce the human drug metabolites 4'-hydroxydiclofenac and 2-hydroxyibuprofen, which could be applied as authentic reference standards in aquatic environmental studies (Tixier *et al.*, 2003). Another important application of the drug metabolites produced by the CYP267-Fdx8-FdR_B system are investigations on altered pharmacological effects. The oxidized metabolite of losartan, E 3174 (losartan carboxylic acid), shows a higher metabolic half-life and activity (Stearns *et al.*, 1995).

Concerning the multifaceted use of drug metabolites, an efficient production of them is of great interest. To this day, the application of bacterial P450s with a wide substrate acceptance for a large-scale production of drug metabolites remained unexplored. With CYP267B1 from *S. cellulosum* So ce56, a new bacterial P450 was found with the remarkable ability to convert 20 out of 31 tested drugs *in vitro*. Together with the other member of the CYP267 family, CYP267A1, the application of this interesting P450 family in an *E. coli* based whole-cell system was the first approach of employing wild-type bacterial P450 for a large-scale production of different drug metabolites. Out of the 20 positive *in vitro* hits, the established whole-cell system with CYP267B1, Fdx8 and FdR_B from *S. cellulosum* So ce56 was able to convert 12 drugs within the corresponding whole-cell experiment in a 200 mL scale (Kern *et al.*, 2016). Moderate whole-cell conversions (<10%) were observed for amodiaquine, noscapine, papaverine, repaglinide, tamoxifen and terfenadine. The high yields of the whole-cell conversions of chlorpromazine (30.3%), diclofenac (38%), ibuprofen (44.1%) and omeprazole (78.1%) allowed an upscaling to 2.5 L with no significant change in the yields of the corresponding drug metabolites. After purification by preparative HPLC, 5-20 mg of these metabolites were obtained in high purity. Although CYP267A1 showed a restricted substrate acceptance, the CYP267A1-Fdx8-FdR_B whole-cell system was successfully established for a large-scale conversion of thioridazine (44.7% yield) and, likewise, 5 mg of the respective metabolite was obtained in high purity.

Most interestingly, the drug metabolites of chlorpromazine, diclofenac, ibuprofen, omeprazole and thioridazine, which are produced by the CYP267 family, are the corresponding drug metabolites produced by human liver P450s (Table 2 and Supplemental Figure 6 of (Kern *et al.*, 2016)). This result makes the members of the CYP267 family, CYP267A1 and CYP267B1, perfect candidates for an application in the pharmaceutical industry. In case of the *in vitro* experiments, the low formation of side-products for a few substrates was once again reduced within the corresponding whole-cell system (Kern *et al.*, 2016). The connection of an unusual broad substrate range with a high selectivity of the conversion of drug molecules allows the usage of one whole-cell system to selectively produce defined human drug metabolites for different fields of application. Due to the frequently upcoming new structures of drugs and drug candidates, the pharmaceutical industry might benefit from an established and highly versatile *E. coli*-based biocatalyst like the investigated CYP267B1-Fdx8-FdR_B system able to metabolize structurally diverse compounds. In particular, this would enable a cost-efficient and simplified production procedure to accommodate the demand of authentic drug metabolites.

5 Conclusion and future prospects

Myxobacterial P450s from *S. cellulosum* are promising biocatalysts with a high potential for biotechnological application. In *S. cellulosum* So ce90, the P450 EpoK is responsible for the epoxidation of epothilone C/D and produces the much more active antitumor compounds epothilone A/B. With the novel hybrid system Fdx from *Synechocystis* and FNR from *C. reinhardtii* found in this study, the most efficient electron transfer system to date has been established. This opens the possibility to express this highly efficient hybrid system for an increased heterologous and autologous production of epothilone A/B in *E. coli* and *S. cellulosum*, respectively. In *S. cellulosum* So ce56, the physiological role of the 21 P450s is still not known. Recent studies revealed their ability to convert different terpenes, terpenoids and fatty acids and showed the capability for an industrial and biotechnological application (Khatri, Girhard, *et al.*, 2010; Khatri, Hannemann, *et al.*, 2010; Khatri *et al.*, 2015; Schifrin, Litzenburger, *et al.*, 2015b; Schifrin, Ly, *et al.*, 2015). However, their potential as biocatalysts for the conversion and production of pharmaceutically interesting compounds has not been discovered until now. Within this study, the myxobacterial P450s CYP265A1, CYP266A1 and CYP267B1 were found to be capable of derivatizing the antitumor drug epothilone D to the respective hydroxylated products 14-, 21- and 26-hydroxy epothilone D. Furthermore, a novel epothilone derivative, 7-ketone epothilone D, was found as the main product of the CYP267B1-dependent epothilone D conversion, which opens access to a novel epothilone derivate with potential antitumor activity. The oxidation of the 7-hydroxy group of epothilone D by CYP267B1 enables the production of 7-ketone epothilone D by the use of an enzymatic approach. A large-scale production of this interesting derivative might be feasible when expressing CYP267B1, its efficient autologous redox system Fdx8/FdR_B from *S. cellulosum* So ce56 and the biosynthetic gene cluster of epothilones from *S. cellulosum* So ce90 in *E. coli* (exclusive EpoK, (Mutka *et al.*, 2006)). This should result in the heterologous biosynthesis of epothilone C/D and the subsequent oxidation to 7-ketone epothilone D by CYP267B1/Fdx8/FdR_B.

With respect to the production of human drug metabolites, the CYP267 family, especially CYP267B1, from *S. cellulosum* So ce56 were found to be highly versatile drug metabolizers with the ability to produce human drug metabolites with high selectivity. Together with the ability to catalyze three different reaction types (hydroxylation, epoxidation and sulfoxidation), CYP267B1 from *S. cellulosum* So ce56 was found to be an exceptional bacterial wild-type P450 with a great potential for further biotechnological application. In combination with the established co-expression of the autologous redox partners Fdx8 and FdR_B in *E. coli*, a multi-milligram (5-20 mg) production of the human drug metabolites chlorpromazine sulfoxide, 4'-hydroxydiclofenac, 2-hydroxy-ibuprofen, omeprazole sulfone and thioridazine-5-sulfoxide was achieved.

An enzymatic production of drug derivatives and human metabolites with the usage of microbial P450s in a whole-cell system benefits from many advantages. First of all, microbial P450s are easy to handle and usually hold higher expression levels and activities than human P450s (Bernhardt, 2006). Secondly, in comparison with the utilization of drug metabolizing model microorganisms like *Cunninghamella* sp. (Asha and Vidyavathi, 2009), a whole-cell application with one P450 expressed would result in a defined process and a selective production of a desired metabolite. The established CYP267B1-Fdx8-FdR_B system is a great starting point for an application in the pharmaceutical industry. On one hand, the high tolerance toward different chemical structures opens up the possibility to investigate a broad variety of drug compounds. On the other hand, the established whole-cell systems are an excellent starting point toward further optimizations in view of biotechnological upscaling and applicability. To overcome the substrate uptake by *E. coli*, EDTA and polymyxin B were successfully used to enhance metabolite formation. However, other permeabilizing detergents like TritonX100 are potential topics of interest, due to the recently shown increased product formation in related whole-cell experiments when expressing the human UDP-glucose 6-dehydrogenase (UGDH, EC 1.1.1.22) in *S. pombe* (Weyler *et al.*, 2015). Instead of using a minimal medium to avoid indole production by tryptophanase TnaA of *E. coli* (Li and Young, 2013), the recently published indole deficient *E. coli* strain showed promising biotechnological potential (Brixius-Anderko *et al.*, 2016) and could be used as an alternative host for the established CYP267B1-Fdx8-FdR_B whole-cell system. Since the basic requirement of a whole-cell system can also be the NADPH availability of the host, a modification of the pentose phosphate pathway (Siedler *et al.*, 2011) or a co-expression of NADPH regenerating systems (Janocha and Bernhardt, 2013) could also lead to an increased P450-dependent conversion of the substrates of interest.

Due to the broad substrate range of the CYP267B1 biocatalyst and the moderate to high conversion yields, the potential fields of application are widespread. Not only the formation of drug metabolites can be performed in a multi-milligram scale, also the conversion of building blocks for further chemical syntheses and the derivatization of non-drug compounds for further chemical modification are conceivable biotechnological approaches of this remarkable P450 from *S. cellulosum* So ce56.

6 Attachments

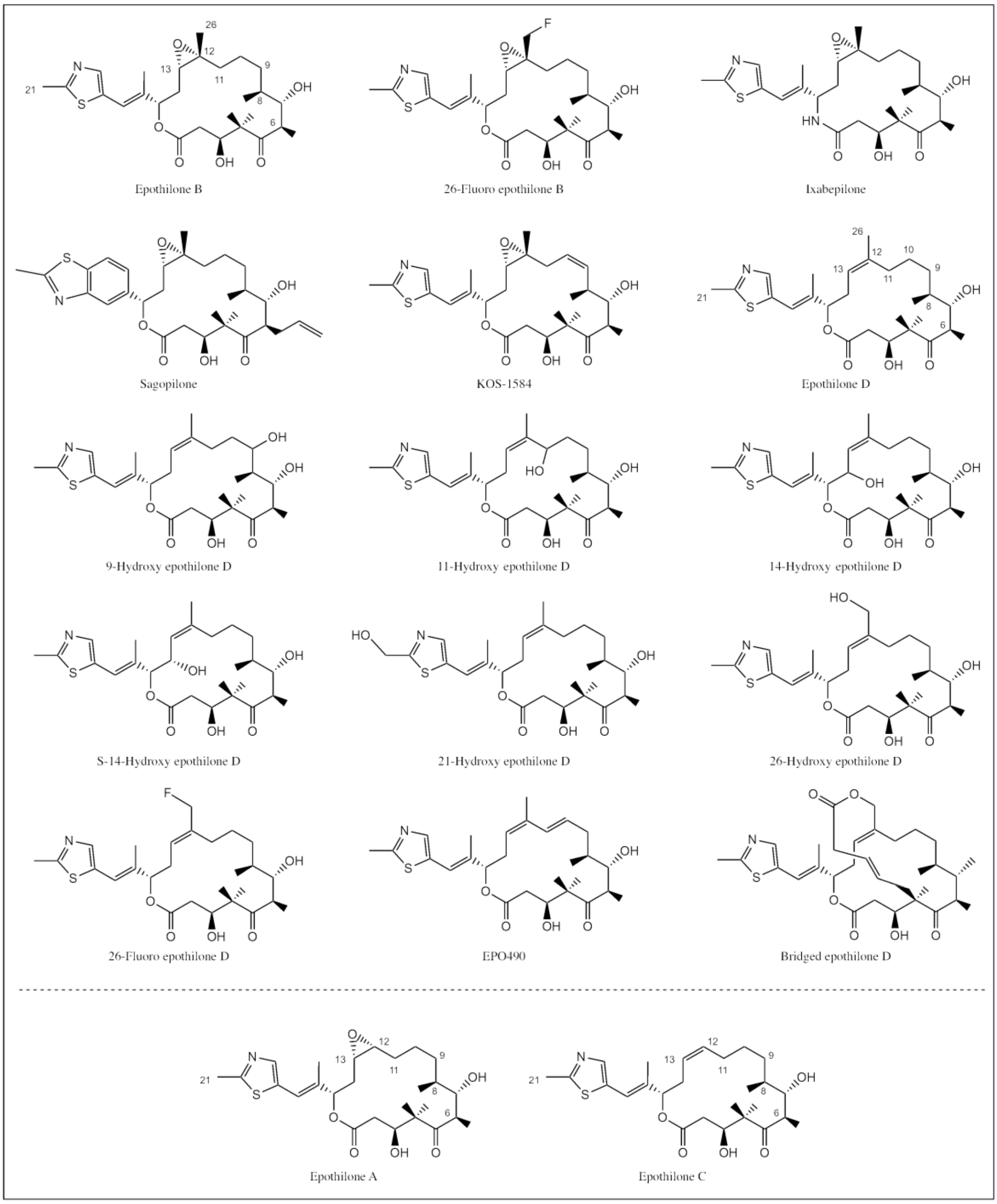

Figure S 1. Overview of relevant epothilone derivatives in this Thesis.

Table S 1. Cytochromes P450 used for bioinformatics studies.

Organism	P450	UniProtKB	Organism	P450	UniProtKB
Homo sapiens	CYP1A1	P04798	***S. cellulosum* So ce56**	CYP109C1	A9GLI3
	CYP1A2	P05177		CYP109C2	A9G8X8
	CYP1B1	Q16678		CYP109D1	A9F9S4
	CYP2A6	P11509		CYP110H1	A9GI66
	CYP2A7	P20853		CYP110J1	A9GKJ2
	CYP2A13	Q16696		CYP117B1	A9G2V2
	CYP2B6	P20813		CYP124E1	A9FBP8
	CYP2C8	P10632		CYP259A1	A9F9S8
	CYP2C9	P11712		CYP260A1	A9FDB7
	CYP2C18	P33260		CYP260B1	A9FFA1
	CYP2C19	P33261		CYP261A1	A9GM12
	CYP2D6	P10635		CYP261B1	A9G7P4
	CYP2E1	P05181		CYP262A1	A9FW73
	CYP2F1	P24903		CYP262B1	A9FP31
	CYP2J2	P51589		CYP263A1	A9FJV1
	CYP2R1	Q6VVX0		CYP264A1	A9GJU5
	CYP2S1	Q96SQ9		CYP264B1	A9FZ85
	CYP2U1	Q7Z449		CYP265A1	A9FN58
	CYP2W1	Q8TAV3		CYP266A1	A9G3Q4
	CYP3A4	P08684		CYP267A1	A9EN90
	CYP3A5	P20815		CYP267B1	A9ERX9
	CYP3A7	P24462	***S. cellulosum* So ce90**	CYP167A1	Q9KIZ4
	CYP3A43	Q9HB55	***Streptomyces griseus***	P450-SOY	P26911
	CYP4A11	Q02928	***Actinoplanes* sp. ATCC**	CYP107E4	ACN71221
	CYP4A22	Q5TCH4	***Labrenzia aggregate***	CYP116B4	EAV41564
	CYP4B1	P13584	***Bacillus cereus***	CYP102A5	Q81BF4
	CYP4F2	P78329	***Rhodococcus jostii* RHA1**	CYP51_RHA1	Q0S7M9
	CYP4F3	Q08477		CYP105_RHA1	Q0SDH7
	CYP4F8	P98187		CYP116_RHA1	Q0RUR9
	CYP4F11	Q9HBI6		CYP125_RHA1	Q0S7N3
	CYP4F12	Q9HCS2		CYP256_RHA1	Q0RXF8
	CYP4F22	Q6NT55		CYP257_RHA1	Q0RVH0
	CYP4V2	Q6ZWL3		CYP258_RHA1	Q0RUW2
	CYP4X1	Q8N118			
	CYP4Z1	Q86W10			
	CYP5A1	P24557			
	CYP7A1	P22680			
	CYP7B1	O75881			
	CYP8A1	Q16647			

	CYP8B1	Q9UNU6			
	CYP11A1	P05108			
	CYP11B1	P15538			
	CYP11B2	P19099			
	CYP17A1	P05093			
	CYP19A1	P11511			
	CYP20A1	Q6UW02			
	CYP21A2	P08686			
	CYP24A1	Q07973			
	CYP26A1	O43174			
	CYP26B1	Q9NR63			
	CYP26C1	Q6V0L0			
	CYP27A1	Q02318			
	CYP27B1	O15528			
	CYP27C1	Q4G0S4			
	CYP39A1	Q9NYL5			
	CYP46A1	Q9Y6A2			
	CYP51A1	Q16850			

7 References

Altmann K-H, Wartmann M, and O'Reilly T (2000) Epothilones and related structures – a new class of microtubule inhibitors with potent in vivo antitumor activity. *Biochim Biophys Acta - Rev Cancer* **1470**:M79–M91.

Anderson JE, Held N, and Wright K (2004) Raynaud's phenomenon of the nipple: a treatable cause of painful breastfeeding. *Pediatrics* **113**:360–4.

Anderson S (2005) *Making medicine: A brief history of pharmacy and pharmaceuticals*, Pharmaceutical Press.

Andrew Williams J, Ring BJ, Cantrell VE, Jones DR, Eckstein J, Ruterbories K, Hamman M a., Hall SD, and Wrighton S a. (2002) Comparative metabolic capabilities of CYP3A4, CYP3A5, and CYP3A7. *Drug Metab Dispos* **30**:883–891.

Asha S, and Vidyavathi M (2009) Cunninghamella – A microbial model for drug metabolism studies – A review. *Biotechnol Adv* **27**:16–29.

Bak S, Beisson F, Bishop G, Hamberger B, Höfer R, Paquette S, and Werck-Reichhart D (2011) Cytochromes P450. *Arab B* **9**:e0144.

Basch J, and Chiang SJ (2007) Cloning and expression of a cytochrome P450 hydroxylase gene from Amycolatopsis orientalis: Hydroxylation of epothilone B for the production of epothilone F. *J Ind Microbiol Biotechnol* **34**:171–176.

Bernhardt R (2006) Cytochromes P450 as versatile biocatalysts. *J Biotechnol* **124**:128–145.

Bernhardt R, and Urlacher VB (2014) Cytochromes P450 as promising catalysts for biotechnological application: Chances and limitations. *Appl Microbiol Biotechnol* **98**:6185–6203.

Boddy CN, Hotta K, Tse ML, Watts RE, and Khosla C (2004) Precursor-directed biosynthesis of epothilone in Escherichia coil. *J Am Chem Soc* **126**:7436–7437.

Bohren KM, Bullock B, Wermuth B, and Gabbay KH (1989) The aldo-keto reductase superfamily. cDNAs and deduced amino acid sequences of human aldehyde and aldose reductases. *J Biol Chem* **264**:9547–9551.

Bollag DM, McQueney P a, Zhu J, Hensens O, Koupal L, Liesch J, Goetz M, Lazarides E, and Woods CM (1995) Epothilones, a new class of microtubule-stabilizing agents with a taxol-like mechanism of action. *Cancer Res* **55**:2325–2333.

Braenden OJ, Eddy NB, and Halbach H (1955) Synthetic substances with morphine-like effect: Relationship between chemical structure and analgesic action. *Bull World Health Organ* **13**:937–998.

Bright T V, Clark BR, O'Brien E, and Murphy CD (2011) Bacterial production of hydroxylated and amidated metabolites of flurbiprofen. *J Mol Catal B Enzym* **72**:116–121.

Brixius-Anderko S, Hannemann F, Ringle M, Khatri Y, and Bernhardt R (2016) An indole deficient Escherichia coli strain improves screening of cytochromes P450 for biotechnological applications. *Biotechnol Appl Biochem* **in press**.

Brogdon CF, Lee FY, and Canetta RM (2014) Development of other microtubule-stabilizer families. *Anticancer Drugs* **25**:599–609.

Butler MS, and Newman DJ (2008) Natural Compounds as Drugs Volume I, in (Petersen F, and Amstutz R eds) pp 1–44.

Cabana H, Jones JP, and Agathos SN (2007) Elimination of Endocrine Disrupting Chemicals using White Rot Fungi and their Lignin Modifying Enzymes: A Review. *Eng Life Sci* **7**:429–456.

Cartelli D, Casagrande F, Busceti CL, Bucci D, Molinaro G, Traficante A, Passarella D, Giavini E, Pezzoli G, Battaglia G, and Cappelletti G (2013) Microtubule alterations occur early in experimental parkinsonism and the microtubule stabilizer epothilone D is neuroprotective. *Sci Rep* **3**:1837.

Cavero I (2009) Exploratory safety pharmacology: a new safety paradigm to de-risk drug candidates prior to selection for regulatory science investigations. *Expert Opin Drug Saf* **8**:627–47.

Chandwani A, and Shuter J (2008) Lopinavir/ritonavir in the treatment of HIV-1 infection: a review. *Ther Clin Risk Manag* **4**:1023–1033.

Chen N, Zhou M, Yang M, Guo J, Zhu C, Yang J, Wang Y, Yang X, and He L (2010) Calcium channel blockers versus other classes of drugs for hypertension, in *Cochrane Database of Systematic Reviews* (He L ed), John Wiley & Sons, Ltd, Chichester, UK.

Chen Q-H, Ganesh T, Brodie P, Slebodnick C, Jiang Y, Banerjee A, Bane S, Snyder JP, and Kingston DGI (2008) Design, synthesis and biological evaluation of bridged epothilone D analogues. *Org Biomol Chem* **6**:4542, Royal Society of Chemistry.

Chou TC, Zhang XG, Harris CR, Kuduk SD, Balog A, Savin KA, Bertino JR, and Danishefsky SJ (1998) Desoxyepothilone B is curative against human tumor xenografts that are refractory to paclitaxel. *Proc Natl Acad Sci U S A* **95**:15798–15802.

Church J, Jones MG, Davies SN, and Lodge D (1989) Antitussive agents as N-methylaspartate antagonists: further studies. *Can J Physiol Pharmacol* **67**:561–567.

Clark AM, and Hufford CD (1991) Use of microorganisms for the study of drug metabolism: An update. *Med Res Rev* **11**:473–501.

Degtyarenko KN, and Kulikova T a (2001) Evolution of bioinorganic motifs in P450-containing systems. *Biochem Soc Trans* **29**:139–147.

Delprat GD, and Whipple GH (1921) STUDIES OF LIVER FUNCTION: BENZOATE ADMINISTRATION AND HIPPURIC ACID SYNTHESIS. *J Biol Chem* **49**:229–246.

Denisov IG, Makris TM, Sligar SG, and Schlichting I (2005) Structure and chemistry of cytochrome P450. *Chem Rev* **105**:2253–2277.

Di Nardo G, and Gilardi G (2012) Optimization of the bacterial cytochrome P450 BM3 system for the production of human drug metabolites. *Int J Mol Sci* **13**:15901–15924.

Drews J (2000) Drug discovery: a historical perspective. *Science* **287**:1960–1964.

EBCTCG (1998) Tamoxifen for early breast cancer: an overview of the randomised trials. Early Breast Cancer Trialists' Collaborative Group. *Lancet (London, England)* **351**:1451–1467.

Edmondson DE, Mattevi A, Binda C, Li M, and Hubalek F (2004) Structure and Mechanism of Monoamine Oxidase.

Evans WE, and Relling M V (1999) Pharmacogenomics: Translating Functional Genomics into Rational Therapeutics. *Science (80-)* **286**:487–491.

Ewen KM, Hannemann F, Khatri Y, Perlova O, Kappl R, Krug D, Hütterman J, Müller R, and Bernhardt R (2009) Genome mining in Sorangium cellulosum So ce56: Indentification characterization of the homologous electron transfer proteins of a Myxobacterial cytochrome P450. *J Biol Chem* **284**:28590–28598.

FDA (2008) *Guidance for Industry Safety Testing of Drug Metabolites* (FDA MD R ed).

FitzGerald GA, and Patrono C (2001) Drug therapy: The coxibs, selective inhibitors of cyclooxygenase-2. *N Engl J Med* **345**:433–442.

Frein JD, Taylor RE, and Sackett DL (2009) New Sources of Chemical Diversity Inspired by Biosynthesis: Rational Design of a Potent Epothilone Analogue. *Org Lett* **11**:3186–3189.

Galmarini CM (2009) Sagopilone, a microtubule stabilizer for the potential treatment of cancer. *Curr Opin Investig Drugs* **10**:1359–1371.

Gao H-M, Liu B, Zhang W, and Hong J-S (2003) Novel anti-inflammatory therapy for Parkinson's disease. *Trends Pharmacol Sci* **24**:395–401, Elsevier.

Gao R, Li L, Xie C, Diao X, Zhong D, and Chen X (2012) Metabolism and pharmacokinetics of morinidazole in humans: Identification of diastereoisomeric morpholine N +-glucuronides catalyzed by UDP glucuronosyltransferase 1A9. *Drug Metab Dispos* **40**:556–567.

Geier M, Bachler T, Hanlon SP, Eggimann FK, Kittelmann M, Weber H, Lütz S, Wirz B, and Winkler M (2015) Human FMO2-based microbial whole-cell catalysts for drug metabolite synthesis. *Microb Cell Fact* **14**:82.

Gerth K, Bedorf N, Höfle G, Irschik H, and Reichenbach H (1996) Epothilons A and B: antifungal and cytotoxic compounds from Sorangium cellulosum (Myxobacteria). Production, physico-chemical and biological properties. *J Antibiot (Tokyo)* **49**:560–563.

Gerth K, Pradella S, Perlova O, Beyer S, and Müller R (2003) Myxobacteria: Proficient producers of novel natural products with various biological activities - Past and future biotechnological aspects with the focus on the genus Sorangium. *J Biotechnol* **106**:233–253.

Gillman PK (2007) Tricyclic antidepressant pharmacology and therapeutic drug interactions updated. *Br J Pharmacol* **151**:737–748.

Goodin S (2008) Ixabepilone: A novel microtubule-stabilizing agent for the treatment of metastatic breast cancer. *Am J Heal Pharm* **65** :2017–2026.

Guengerich FP (1990) Enzymatic oxidation of xenobiotic chemicals. *Crit Rev Biochem Mol Biol* **25**:97–153.

Hannemann F, Bichet A, Ewen KM, and Bernhardt R (2007) Cytochrome P450 systems-biological variations of electron transport chains. *Biochim Biophys Acta* **1770**:330–344.

Hasemann CA, Kurumbail RG, Boddupalli SS, Peterson JA, and Deisenhofer J (1995) Structure and function of cytochromes P450:a comparative analysis of three crystal structures. *Structure* **3**:41–62.

Hirsch BR, Reed SD, and Lyman GH (2013) Update on the role of epothilones in metastatic breast cancer. *Curr Breast Cancer Rep* **5**:51–56.

Hofle GH, Bedorf N, Steinmetz H, Schomburg D, Gerth K, and Reichenbach H (1996) Epothilone A and B - Novel 16-membered macrolides with cytotoxic activity: Isolation, crystal structure, and conformation in solution. *Angew Chemie-International Ed English* **35**:1567–1569.

ICH (2009) Guidance of Nonclinical safety studies for the conduct of human clinical trials and marketing authorization for pharmaceuticals M3 (R2).

ICH (2012) ICH guideline M3 (R2) - questions and answers.

Irving CB, Adams CE, and Lawrie S (2006) Haloperidol versus placebo for schizophrenia, in *Cochrane Database of Systematic Reviews* (Irving CB ed), John Wiley & Sons, Ltd, Chichester, UK.

Janocha S, and Bernhardt R (2013) Design and characterization of an efficient CYP105A1-based whole-cell biocatalyst for the conversion of resin acid diterpenoids in permeabilized Escherichia coli. *Appl Microbiol Biotechnol* **97**:7639–7649.

Jones SFA (1996) Herbs - useful plants. Their role in history and today. *Eur J Gastroenterol Hepatol* **8**.

Julien B, and Shah S (2002) Heterologous expression of epothilone biosynthetic genes in Myxococcus xanthus. *Antimicrob Agents Chemother* **46**:2772–2778.

Kern F, Dier TKF, Khatri Y, Ewen KM, Jacquot J-P, Volmer DA, and Bernhardt R (2015) Highly Efficient CYP167A1 (EpoK) dependent Epothilone B Formation and Production of 7-Ketone Epothilone D as a New Epothilone Derivative. *Sci Rep* **5**:14881.

Kern F, Khatri Y, Litzenburger M, and Bernhardt R (2016) CYP267A1 and CYP267B1 from Sorangium cellulosum So ce56 are Highly Versatile Drug Metabolizers. *Drug Metab Dispos* **44**(4):495-504.

Khatri Y (2009) The cytochrome P450 complement of the myxobacterium Sorangium cellulosum So ce56 and characterization of two members , CYP109D1 and CYP260A1, Universität des Saarlandes, Saarbrücken.

Khatri Y, Girhard M, Romankiewicz A, Ringle M, Hannemann F, Urlacher VB, Hutter MC, and Bernhardt R (2010) Regioselective hydroxylation of norisoprenoids by CYP109D1 from Sorangium cellulosum So ce56. *Appl Microbiol Biotechnol* **88**:485–495.

Khatri Y, Hannemann F, Ewen KM, Pistorius D, Perlova O, Kagawa N, Brachmann AO, Müller R, and Bernhardt R (2010) The CYPome of sorangium cellulosum so ce56 and identification of CYP109D1 as a new fatty acid hydroxylase. *Chem Biol* **17**:1295–1305.

Khatri Y, Hannemann F, Girhard M, Kappl R, Hutter M, Urlacher VB, and Bernhardt R (2015) A natural heme-signature variant of CYP267A1 from Sorangium cellulosum So ce56 executes diverse ω-hydroxylation. *FEBS J* **282**:74–88.

Khatri Y, Hannemann F, Girhard M, Kappl R, Même A, Ringle M, Janocha S, Leize-Wagner E, Urlacher VB, and Bernhardt R (2013) Novel family members of CYP109 from Sorangium cellulosum so ce56 exhibit characteristic biochemical and biophysical properties. *Biotechnol Appl Biochem* **60**:18–29.

Khatri Y, Ringle M, Lisurek M, von Kries JP, Zapp J, and Bernhardt R (2016) Substrate Hunting for the Myxobacterial CYP260A1 Revealed New 1alpha-Hydroxylated Products from C-19 Steroids. *Chembiochem* **17**:90–101.

Kim Y, and Kang K (2011) Application of drug metabolism and pharmacokinetics for new drug development. *Arch Pharm Res* **34**:1769–1771, Pharmaceutical Society of Korea.

Kiss FM, Lundemo MT, Zapp J, Woodley JM, and Bernhardt R (2015) Process development for the production of 15β-hydroxycyproterone acetate using Bacillus megaterium expressing CYP106A2 as whole-cell biocatalyst. *Microb Cell Fact* **14**:1–13.

Klingenberg M (1958) Pigments of rat liver microsomes. *Arch Biochem Biophys* **75**:376–386.

Koch G, Loiseleur O, and Altmann K-H (2004) Total Synthesis of 26-Fluoro-epothilone B. *Synlett* **2004**:693–697.

Kowalski RJ, Giannakakous P, and Hamel E (1997) Activities of the Microtubule-stabilizing Agents Epothilone A and B with Purified and in Cells Resistant to Paclitaxel (Taxol). *J Biol Chem* **272**:2534–2541.

Kremers E (1976) *Kremers and Urdang's History of Pharmacy*, 4. ed. (Sonnendecker G ed).

Krempl GA, and Noorily AD (1995) Use of oxymetazoline in the management of epistaxis. *Ann Otol Rhinol Laryngol* **104**:704–706.

Kubinyi H (2003) Drug research: myths, hype and reality. *Nat Rev Drug Discov* **2**:665–668.

Kulig JK, Spandolf C, Hyde R, Ruzzini AC, Eltis LD, Grönberg G, Hayes M a., and Grogan G (2015) A P450 fusion library of heme domains from Rhodococcus jostii RHA1 and its evaluation for the biotransformation of drug molecules. *Bioorg Med Chem* **23**:5603–5609.

Kumar P, Kumar N, Thakur DS, and Patidar A (2010) Male hypogonadism: Symptoms and treatment. *J Adv Pharm Technol Res* **1**:297–301.

Lau J, Tran C, Licari P, and Galazzo J (2004) Development of a high cell-density fed-batch bioprocess for the heterologous production of 6-deoxyerythronolide B in Escherichia coli. *J Biotechnol* **110**:95–103.

Lee FY, Borzilleri R, Fairchild CR, Kim SH, Long BH, Reventos-Suarez C, Vite GD, Rose WC, and Kramer RA (2001) BMS-247550: a novel epothilone analog with a mode of action similar to paclitaxel but possessing superior antitumor efficacy. *Clin*

Cancer Res **7**:1429–1437.

Li G, and Young KD (2013) Indole production by the tryptophanase TnaA in Escherichia coli is determined by the amount of exogenous tryptophan. *Microbiology* **159**:402–10.

Li X-Q, Björkman A, Andersson TB, Ridderström M, and Masimirembwa CM (2002) Amodiaquine clearance and its metabolism to N-desethylamodiaquine is mediated by CYP2C8: a new high affinity and turnover enzyme-specific probe substrate. *J Pharmacol Exp Ther* **300**:399–407.

Litzenburger M, and Bernhardt R (2016) Selective oxidation of carotenoid-derived aroma compounds by CYP260B1 and CYP267B1 from Sorangium cellulosum So ce56. *Appl Microbiol Biotechnol* **in press**.

Liu JK, and Couldwell WT (2005) Intra-Arterial Papaverine Infusions for the Treatment of Cerebral Vasospasm Induced by Aneurysmal Subarachnoid Hemorrhage. *Neurocrit Care* **2**:124–132.

Ly TTB, Khatri Y, Zapp J, Hutter MC, and Bernhardt R (2012) CYP264B1 from Sorangium cellulosum so ce56: A fascinating norisoprenoid and sesquiterpene hydroxylase. *Appl Microbiol Biotechnol* **95**:123–133.

Macherey AC, and Dansette PM (2008) Biotransformations Leading to Toxic Metabolites. Chemical Aspect, in *The Practice of Medicinal Chemistry* pp 674–696.

McIntyre M, Caffe SE, Michalak RA, and Reid JL (1997) Losartan, an orally active angiotensin (AT1) receptor antagonist: a review of its efficacy and safety in essential hypertension. *Pharmacol Ther* **74**:181–194.

Meier V, Geigy C, Grosse N, McSheehy P, and Rohrer Bley C (2013) Use of Epothilone B (Patupilone) in Refractory Lymphoma and Advanced Solid Tumors in Dogs. *J Vet Intern Med* **27**:120–125.

Meyer U a. (1996) Overview of enzymes of drug metabolism. *J Pharmacokinet Biopharm* **24**:449–459.

Molnár I, Schupp T, Ono M, Zirkle R, Milnamow M, Nowak-Thompson B, Engel N, Toupet C, Stratmann A, Cyr D, Gorlach J, Mayo J, Hu A, Goff S, Schmid J, and Ligon J (2000) The biosynthetic gene cluster for the microtubule-stabilizing agents epothilones A and B from Sorangium cellulosum So ce90. *Chem Biol* **7**:97–109.

Monk JP, Villalona-Calero M, Larkin J, Otterson G, Spriggs DS, Hannah AL, Cropp GF, Johnson RG, and Hensley ML (2012) A phase 1 study of KOS-862 (Epothilone D) co-administered with carboplatin (Paraplatin®) in patients with advanced solid tumors. *Invest New Drugs* **30**:1676–1683.

Monostory K, and Dvorak Z (2011) Steroid regulation of drug-metabolizing cytochromes P450. *Curr Drug Metab* **12**:154–172.

Mukhtar E, Adhami VM, and Mukhtar H (2014) Targeting microtubules by natural agents for cancer therapy. *Mol Cancer Ther* **13**:275–84.

Müller-Jahncke W-D, and Friedrich C (1996) *Geschichte der Arzneimitteltherapie*.

Mulzer J, Altmann K-H, Höfle G, Müller R, and Prantz K (2008) Epothilones – A fascinating family of microtubule stabilizing antitumor agents. *Comptes Rendus Chim* **11**:1336–1368.

Murphy CD, and Sandford G (2012) Fluorinated drug metabolism in microorganisms. *Chim Oggi/Chemistry Today* **30**:16–19.

Mutka SC, Carney JR, Liu Y, and Kennedy J (2006) Heterologous production of epothilone C and D in Escherichia coli. *Biochemistry* **45**:1321–1330.

Nelson DR (2011) Progress in tracing the evolutionary paths of cytochrome P450. *Biochim Biophys Acta* **1814**:14–8.

Nelson DR (2009) The cytochrome p450 homepage. *Hum Genomics* **4**:59–65.

Nelson DR, Koymans L, Kamataki T, Stegeman JJ, Feyereisen R, Waxman DJ, Waterman MR, Gotoh O, Coon MJ, Estabrook RW, Gunsalus IC, and Nebert DW (1996) P450 superfamily: update on new sequences, gene mapping, accession numbers and nomenclature.

Newman RA, Yang J, Finlay RM, Cabral F, Vourloumis D, Stephens CL, Troncoso P, Wu X, Logothetis CJ, and Nicolaou K (2001) Antitumor efficacy of 26-fluoroepothilone B against human prostate cancer xenografts. *Cancer Chemother Pharmacol* **48**:319–326.

Nicolaou KC, Finlay MR V, Ninkovic S, and Sarabia F (1998) Total synthesis of 26-hydroxy-epothilone B and related analogs via a macrolactonization based strategy. *Tetrahedron* **54**:7127–7166.

Njardarson JT, Biswas K, and Danishefsky SJ (2002) Application of hitherto unexplored macrocyclization strategies in the epothilone series: novel epothilone analogs by total synthesis. *Chem Commun* 2759–2761, The Royal Society of Chemistry.

Odontuya G, Hoult JRS, and Houghton PJ (2005) Structure-activity relationship for antiinflammatory effect of luteolin and its derived glycosides. *Phyther Res* **19**:782–786.

Ogura H, Nishida CR, Hoch UR, Perera R, Dawson JH, and Ortiz De Montellano PR (2004) EpoK, a cytochrome P450 involved in biosynthesis of the anticancer agents epothilones A and B. Substrate-mediated rescue of a P450 enzyme. *Biochemistry* **43**:14712–14721.

Oosterhuis B, and Jonkman JH (1989) Omeprazole: pharmacology, pharmacokinetics and interactions. *Digestion* **44 Suppl 1**:9–17.

Park H, Lee S, and Suh J (2005) Structural and Dynamical Basis of Broad Substrate Specificity, Catalytic Mechanism, and Inhibition of Cytochrome P450 3A4. *J Am Chem Soc* **127**:13634–13642.

Pishvaian M, and Smaglo B (2014) Profile and potential of ixabepilone in the treatment of pancreatic cancer. *Drug Des Devel Ther* **8**:923.

Reinen J, Van Leeuwen JS, Li Y, Sun L, Grootenhuis PDJ, Decker CJ, Saunders J, Vermeulen NPE, and Commandeur JNM (2011) Efficient screening of cytochrome P450 BM3 mutants for their metabolic activity and diversity toward a wide set of drug-like molecules in chemical space. *Drug Metab Dispos* **39**:1568–1576.

Ren X, Yorke J a., Taylor E, Zhang T, Zhou W, and Wong LL (2015) Drug Oxidation by Cytochrome P450 $_{BM3}$: Metabolite Synthesis and Discovering New P450 Reaction Types. *Chem - A Eur J* n/a–n/a.

Rendic S, and Guengerich FP (2015) Survey of Human Oxidoreductases and Cytochrome P450 Enzymes Involved in the Metabolism of Xenobiotic and Natural

Chemicals. *Chem Res Toxicol* **28**:38–42.

Rénéric J-P, and Lucki I (1998) Antidepressant behavioral effects by dual inhibition of monoamine reuptake in the rat forced swimming test. *Psychopharmacology (Berl)* **136**:190–197.

Ringle M, Khatri Y, Zapp J, Hannemann F, and Bernhardt R (2013) Application of a new versatile electron transfer system for cytochrome P450-based Escherichia coli whole-cell bioconversions. *Appl Microbiol Biotechnol* **97**:7741–7754.

Rosano GL, and Ceccarelli EA (2014) Recombinant protein expression in Escherichia coli: advances and challenges. *Front Microbiol* **5**:172, Frontiers Media S.A.

Roses AD (2008) Pharmacogenetics in drug discovery and development: a translational perspective. *Nat Rev Drug Discov* **7**:807–817, Nature Publishing Group.

Rushmore TH, Reider PJ, Slaughter D, Assang C, and Shou M (2000) Bioreactor systems in drug metabolism: synthesis of cytochrome P450-generated metabolites. *Metab Eng* **2**:115–125.

Sahoo N, Manchikanti P, and Dey S (2010) Herbal drugs: standards and regulation. *Fitoterapia* **81**:462–71.

Schifrin A, Litzenburger M, Ringle M, Ly TTB, and Bernhardt R (2015a) Inside Cover: New Sesquiterpene Oxidations with CYP260A1 and CYP264B1 from Sorangium cellulosum So ce56 (ChemBioChem 18/2015). *ChemBioChem* **16**:2542.

Schifrin A, Litzenburger M, Ringle M, Ly TTB, and Bernhardt R (2015b) New Sesquiterpene Oxidations with CYP260A1 and CYP264B1 from Sorangium cellulosum So ce56. *ChemBioChem* **16**:2624–2632.

Schifrin A, Ly TTB, Günnewich N, Zapp J, Thiel V, Schulz S, Hannemann F, Khatri Y, and Bernhardt R (2015) Characterization of the Gene Cluster CYP264B1- geo A from Sorangium cellulosum So ce56: Biosynthesis of (+)-Eremophilene and Its Hydroxylation. *ChemBioChem* **16**:337–344.

Schneiker S, Perlova O, Kaiser O, Gerth K, Alici A, Altmeyer MO, Bartels D, Bekel T, Beyer S, Bode E, Bode HB, Bolten CJ, Choudhuri J V, Doss S, Elnakady Y a, Frank B, Gaigalat L, Goesmann A, Groeger C, Gross F, Jelsbak L, Jelsbak L, Kalinowski J, Kegler C, Knauber T, Konietzny S, Kopp M, Krause L, Krug D, Linke B, Mahmud T, Martinez-Arias R, McHardy AC, Merai M, Meyer F, Mormann S, Muñoz-Dorado J, Perez J, Pradella S, Rachid S, Raddatz G, Rosenau F, Rückert C, Sasse F, Scharfe M, Schuster SC, Suen G, Treuner-Lange A, Velicer GJ, Vorhölter F-J, Weissman KJ, Welch RD, Wenzel SC, Whitworth DE, Wilhelm S, Wittmann C, Blöcker H, Pühler A, and Müller R (2007) Complete genome sequence of the myxobacterium Sorangium cellulosum. *Nat Biotechnol* **25**:1281–1289.

Scott EE, and Halpert JR (2005) Structures of cytochrome P450 3A4. *Trends Biochem Sci* **30**:5–7.

Scott LJ (2012) Repaglinide: a review of its use in type 2 diabetes mellitus. *Drugs* **72**:249–272.

Shumyantseva VV, Kuzikov AV, Masamrekh RA, Khatri Y, Zavialova MG, Bernhardt R, and Archakov AI (2016) Direct electrochemistry of CYP109C1, CYP109C2 and CYP109D1 from Sorangium cellulosum So ce56. *Electrochim Acta* **192**:72-79.

Siedler S, Bringer S, and Bott M (2011) Increased NADPH availability in Escherichia coli: improvement of the product per glucose ratio in reductive whole-cell biotransformation. *Appl Microbiol Biotechnol* **92**:929–937.

Sirim D, Widmann M, Wagner F, and Pleiss J (2010) Prediction and analysis of the modular structure of cytochrome P450 monooxygenases. *BMC Struct Biol* **10**:34.

Smith R V., and Rosazza JP (1975) Microbial systems for study of the biotransformations of drugs. *Biotechnol Bioeng* **17**:785–814.

Staudinger JL (2013) Disease, Drug Metabolism, and Transporter Interactions. *Pharm Res* **30**:2171–2173.

Stearns R, Chakravarty P, Chen R, and Chiu S (1995) Biotransformation of losartan to its active carboxylic acid metabolite in human liver microsomes. *Drug Metab Dispos* **23**:207–215.

Stroud ML, Stilgoe S, Stott VE, Alhabian O, and Salman K (2008) Vitamin D: A review. *Aust Fam Physician* **37**:1002–5.

Stupp R, Tosoni A, Bromberg JEC, Hau P, Campone M, Gijtenbeek J, Frenay M, Breimer L, Wiesinger H, Allgeier A, van den Bent MJ, Bogdahn U, van der Graaf W, Yun HJ, Gorlia T, Lacombe D, and Brandes AA (2011) Sagopilone (ZK-EPO, ZK 219477) for recurrent glioblastoma. A phase II multicenter trial by the European Organisation for Research and Treatment of Cancer (EORTC) Brain Tumor Group. *Ann Oncol* **22**:2144–2149.

Tamimi NAM, and Ellis P (2009) Drug Development: From Concept to Marketing! *Nephron Clin Pract* **113**:125–131.

Tang L (2000) Cloning and Heterologous Expression of the Epothilone Gene Cluster. *Science (80-)* **287**:640–642.

Tang L, Qiu R-G, Li Y, and Katz L (2003) Generation of novel epothilone analogs with cytotoxic activity by biotransformation. *J Antibiot (Tokyo)* **56**:16–23.

Taylor M, Lamb DC, Cannell R, Dawson M, and Kelly SL (1999) Cytochrome P450105D1 (CYP105D1) from Streptomyces griseus: heterologous expression, activity, and activation effects of multiple xenobiotics. *Biochem Biophys Res Commun* **263**:838–842.

Thompson D, and Oster G (1996) Use of terfenadine and contraindicated drugs. *JAMA* **275**:1339–1341.

Tixier C, Singer HP, Oellers S, and Müller SR (2003) Occurrence and Fate of Carbamazepine, Clofibric Acid, Diclofenac, Ibuprofen, Ketoprofen, and Naproxen in Surface Waters. *Environ Sci Technol* **37**:1061–1068.

Urlacher VB, and Girhard M (2012) Cytochrome P450 monooxygenases: An update on perspectives for synthetic application. *Trends Biotechnol* **30**:26–36.

Vail RB, Homann MJ, Hanna I, and Zaks A (2005) Preparative synthesis of drug metabolites using human cytochrome P450s 3A4, 2C9 and 1A2 with NADPH-P450 reductase expressed in Escherichia coli. *J Ind Microbiol Biotechnol* **32**:67–74.

Varon J, and Marik PE (2003) Clinical review: The management of hypertensive crises. *Crit Care* **7**:1–11.

Vogel G, and Vogel W (1995) *Drug Discovery and Evaluation*.

Wenzel SC, and Müller R (2009) Myxobacteria--'microbial factories' for the production of bioactive secondary metabolites. *Mol Biosyst* **5**:567–574.

Werck-Reichhart D, Bak S, and Paquette S (2002) Cytochromes P450. *Arab B* **1**:e0028, BioOne.

Weyler C, Bureik M, and Heinzle E (2015) Selective oxidation of UDP-glucose to UDP-glucuronic acid using permeabilized Schizosaccharomyces pombe expressing human UDP-glucose 6-dehydrogenase. *Biotechnol Lett* **38**(3):477-481.

Whitehouse CJC, Bell SG, and Wong L-L (2012) P450BM3 (CYP102A1): connecting the dots. *Chem Soc Rev* **41**:1218–1260, The Royal Society of Chemistry.

World Health Organization (2013) *Model List of Essential Medicines*.

Xu C, Li CY-T, and Kong A-NT (2005) Induction of phase I, II and III drug metabolism/t... [Arch Pharm Res. 2005] - PubMed result. *Arch Pharm Res* **28**:249–68.

Xu L-H, Ikeda H, Liu L, Arakawa T, Wakagi T, Shoun H, and Fushinobu S (2014) Structural basis for the 4′-hydroxylation of diclofenac by a microbial cytochrome P450 monooxygenase. *Appl Microbiol Biotechnol* **99**:3081–3091.

Yamazaki H, and Shimada T (1997) Progesterone and Testosterone Hydroxylation by Cytochromes P450 2C19, 2C9, and 3A4 in Human Liver Microsomes. *Arch Biochem Biophys* **346**:161–169.

Yang JK, Zhao L, Sun RC, Shen YM, Wang NQ, and Liu XL (2014) Purification of Epothilones A and B with Column Chromatography on a Sephadex LH-20. *Adv Mater Res* **904**:164–169.

Ye W, Zhang W, Chen Y, Li H, Li S, Pan Q, Tan G, and Liu T (2016) A new approach for improving epothilone B yield in Sorangium cellulosum by the introduction of vgb epoF genes. *J Ind Microbiol Biotechnol*, doi: 10.1007/s10295-016-1735-9.

Yin Y-C, Yu H-L, Luan Z-J, Li R-J, Ouyang P-F, Liu J, and Xu J-H (2014) Unusually Broad Substrate Profile of Self-Sufficient Cytochrome P450 Monooxygenase CYP116B4 from *Labrenzia aggregata*. *ChemBioChem* **15**:2443–2449.

Zanger UM, and Schwab M (2013) Cytochrome P450 enzymes in drug metabolism: Regulation of gene expression, enzyme activities, and impact of genetic variation. *Pharmacol Ther* **138**:103–141.

Zhang B, Carroll J, Trojanowski JQ, Yao Y, Iba M, Potuzak JS, Hogan a.-ML, Xie SX, Ballatore C, Smith a. B, Lee VM-Y, and Brunden KR (2012) The Microtubule-Stabilizing Agent, Epothilone D, Reduces Axonal Dysfunction, Neurotoxicity, Cognitive Deficits, and Alzheimer-Like Pathology in an Interventional Study with Aged Tau Transgenic Mice. *J Neurosci* **32**:3601–3611.

Zhang D, Freeman JP, Sutherland JB, Walker AE, Yang Y, and Cerniglia CE (1996) Biotransformation of chlorpromazine and methdilazine by Cunninghamella elegans. *Appl Environ Microbiol* **62**:798–803.

Zhang H, Wang K, Cheng X, Lu Y, and Zhang Q (2014) Synthesis and *In vitro* cytotoxicity of poly(ethylene glycol)-epothilone B conjugates. *J Appl Polym Sci* **131**:23.

Zhou Y, Zhong Z, Liu F, Sun M, Craig D, Eng S, Feng L, Sherrill M, Cropp GF, Yu K, Hannah AL, and Johnson RG (2005) KOS-1584: a rationally designed epothilone D analog with improved potency and pharmacokinetic (PK) properties. *Cancer Res* **65** :595.

Ziska A (2011) Study of CYP267B1 from So ce 56, Saarland University.